Scripps Institution of Oceanography

Marine Physical Laboratory Technical Memorandum #480

Cuvier's Beaked Whale (*Ziphius cavirostris*) Tissue Physical Properties: Measurements of Sound Speed/Attenuation, Density, CT numbers, Elasticity and Temperature Influences

Melissa S. Soldevilla [a], Megan F. McKenna [b], Sean M. Wiggins [a], Robert E. Shadwick [a], Ted W. Cranford [b], and John A. Hildebrand [a].

a) **Scripps Institution of Oceanography, University of California, San Diego, 9500 Gilman Drive, La Jolla California 92093-0205**

b) **San Diego State University, 5500 Campanile Drive, San Diego, CA 92182**

Contact first author at mhock@ucsd.edu.

Summary:

Physical properties of tissues from a Cuvier's beaked whale (*Ziphius cavirostris)* neonate are examined and compared to Computed Tomography (CT) X-ray imaging. Studied physical properties include longitudinal sound velocity and attenuation, density, and elasticity. Tissue samples were extracted throughout the body, although primarily from the head. These tissues were classified by type as follows: mandibular acoustic fat, mandibular blubber, melon, forehead blubber, body blubber, muscle, and connective tissue. Our results showed that each class of tissues had unique, co-varying physical properties. The mandibular acoustic fats had minimal values for sound speed (1350 ±10.6 m/s), sound attenuation (0.8 ±0.5 dB/mm), and mass density (890 ±23 kg/m^3). These values increased through mandibular blubber (1376 ±13 m/s, 0.8 ±0.2 dB/mm, 919 ±13 kg/m^3), melon (1382 ±23 m/s, 1.0 ±0.5 dB/mm, 937 ±17 kg/m^3), forehead blubber (1401 ±7.8 m/s, 1.1 ±0.4 dB/mm, 935 ±25 kg/m^3), and muscle (1517 ±46.8 m/s, 1.9 ±0.7 dB/mm, 993 ±58 kg/m^3). Connective tissue had the greatest average sound speed (1628 ±48.7 m/s), attenuation (2.6 ±0.7 dB/mm) and density (1087 ±41 kg/m^3). The melon formed a low density, low velocity core, supporting its function as a sound focusing organ. Hounsfield Unit (HU) numbers from Computed Tomography (CT) X-ray imaging are correlated with density, sound velocity, and sound attenuation allowing for HU numbers to be used as a proxy for these physical properties. Blubber and connective tissues have a higher elastic modulus than acoustic fats and melon, suggesting more collagen structure in blubber and connective tissues. Blubber tissue elastic modulus is non-linear with varying stress, becoming more incompressible as stress is increased. These data provide values needed to construct sound wave propagation models to better understand the generation of sound by *Ziphius cavirostris* as well as the interaction of anthropogenic sound with these animals.

Introduction:

Mass strandings of Cuvier's beaked whales (*Ziphius cavirostris)* have been associated with the use of high intensity anthropogenic sound, particularly mid-frequency (2-4 kHz) sonar (Evans and England, 2001; Frantzis, 1998, Simmonds and Lopez-Jurado, 1991). How the sound exposure is related to these strandings and subsequent deaths is unknown. Necropsies have shown hemorrhaging in the lungs, acoustic pathways, brain, spinal cord, kidneys, and eyes, congestion and bubbles in the brain, and embolisms in body fats (Evans and England, 2001). This has led researchers to speculate various causes including rectified diffusion of gas bubbles (Crum and Mao, 1996; Houser *et al.*, 2001) gas emboli formation in body fats (Jepson *et al.*, 2003), and bubble/lung resonance (Finneran, 2003). However, no study thus far has pinpointed the mechanisms leading to these stranding events and the phenomenon remains controversial.

Acoustic-structural modeling within a beaked whale's head and body may provide insight to possible acoustic-induced mechanisms affecting *Z. cavirostris* (*e.g.* Cheung *et al*., 2003; Nightingale *et al*., 2000). This type of model requires tissue physical property values. We present approximately 300 measurements for sound velocity and attenuation, density, X-ray Computed Tomography (CT) Hounsfield Unit (HU) numbers and elastic modulus for *Z. cavirostris* tissues that provide a base for an acoustic-structural model. These values suggest there is a predictable relationship between the Hounsfield units from CT scans and several other physical properties.

Background:

Cuvier's beaked whales are members of Ziphiidae, a family of toothed whales (Odontoceti) who have been studied primarily from occasional stranding data. Despite the scarcity of data, *Z. cavirostris* is one of the most abundant of the beaked whale species (Heyning, 1989b). They have a cosmopolitan distribution, occupying tropical, subtropical and temperate waters throughout the world's oceans (Heyning, 1989b). They are commonly found around oceanic islands and in enclosed seas, such as the Mediterranean and the Sea of Japan (Boutiba, 1994; Forney *et al.*, 1995; Houston, 1991; Marini *et al.*, 1996). *Ziphius cavirostris* inhabit deep, offshore waters and often occupy submarine canyons and the continental shelf edge (D'Amico *et al.*, 2003; Heyning, 1989b; Waring *et al.*, 2001). Stomach content studies indicate that their diet consists primarily of a wide range of squid species; fish and crustaceans are also a food source (Blanco and Raja, 2000; Fiscus, 1997; MacLeod *et al.*, 2003; Santos *et al.*, 2001). Squid typically inhabit the benthic region in the 200 to 2000 m depth range, so *Z. cavirostris* presumably dive to these depths (MacLeod *et al.*, 2003). *Ziphius cavirostris* are generally inconspicuous and rarely observed at sea due to their deep diving behavior, long dive times, and short time spent at the surface. (Heyning, 1989b; Barlow *et al.*, 1997; Baird *et al*., 2004). Studies of live specimens are rare.

Odontocetes, including beaked whales, have a well-adapted acoustic sensory system, including a unique sound generation system and enhanced reception capabilities (Au, 1993). All odontocetes, including *Ziphius cavirostris,* are thought to produce high intensity echolocation signals, although only a dozen have been tested using target detection experiments (Au 1993). However, comparative anatomic studies highlight homologous structures responsible for both the sound generation and sound reception associated with echolocation (Cranford *et al.*, 1996; Heyning, 1989a; Heyning and Mead, 1990; Lawrence and Schevill, 1956; Mead, 1975). Convincing evidence suggests that directional biosonar clicks are produced at a structural complex known as the monkey lips/dorsal bursae (MLDB) region (Cranford *et al.*, 1996). A sound beam is progressively focused by air spaces, connective tissue sheaths, and gradients within the melon. The melon is a complex connective tissue and lipid structure in the forehead region of all odontocetes (Cranford *et al.*, 1996). This fatty melon is present in all odontocetes, including *Z. cavirostris* (Fig. 1).

The specific structures in the forehead involved in sound production vary across odontocetes. The MLDB complex in beaked whales is describe as conspicuous and appears to be continuous with the melon on the right side (Heyning, 1989a). The right anterior and posterior bursae have been identified, however, the left side appears to be absent (Heyning, 1989a; Cranford *et al.*, 1996). This was also observed in the specimen analyzed in this study. The reflective surfaces in beaked whales consist of a concave skull basin and dense connective tissue theca that surrounds the dorsal and lateral sides of the posterior region of the melon in a mega-phone like fashion (Figs 1,2). A cross-section of the head in the posterior region highlights the geometry of these structures (Fig. 1A-C). In the anterior region of the forehead, the theca is absent and a layer of skin covers the dorsal surface of the melon (Fig. 1A,D-E). The musculature of the forehead is complex, and fibers of various groups invade the melon on the ventral and lateral sides. The lateral muscles fade at the anterior region of the forehead.

In addition to the complex topography of the forehead tissues, there exists variation in chemical composition within the fatty melon (Blomberg and Lindhom, 1976; Litchfield *et al.*, 1973; Varanasi *et al.*, 1982). This variation has lead to the melon being described as having inner, outer and under melon regions (Litchfield *et al.*, 1973). The composition not only varies across species of odontocetes, but recent evidence suggests that neonate melons exhibit less chemical differentiation than adults (Koopman, 2003b). These gradients and heterogeneity in chemical composition clearly influence the physical properties of tissue density, sound velocity, and sound attenuation that are the subjects of our investigation.

The second component of the acoustic system is sound reception. Although beaked whales have not been well studied in this area, the mechanisms are assumed to be similar to better-known odontocetes species based on homologous morphological structures (Au, 1993). The sound conduction pathway in odontocetes is unique among mammals. They lack external ears to guide the waves to the inner ear; instead sound waves are directed towards the inner ear complex through fat pads lining the lower jaw, thin translucent walls of the posterior mandible, and fat bodies within each mandible (Brill *et al*., 1988). The posterior region of the fat and bone structure has been termed the "acoustic window" (Norris, 1968). The fat bodies of the lower jaw also have distinct structure and composition like the fats of the forehead which may match the acoustic properties of the water and guide the wave towards the inner ear complex (Koopman *et al.*, 2003b). The fat bodies in the mandible connect to the bony tympanoperiotic complex on the lateral sides. The periotic bone is attached to the skull by ligaments. All odontocetes have an air sac surrounding the medial portion of the ear complex, the pterygoid sinuses (Fraser and Purves, 1960). These spaces are extremely large in both beaked and sperm whales, including the specimen investigated in this paper. The medial surface of the pterygoid sinus is attached to the ptergyoid bone, a large depression on the ventral side of the skull. The large cavity of the ptergyoid narrows posteriorly to form a layer of air that surrounds the medial and posterior surfaces of the ear complex. These air spaces are excellent acoustic reflectors and may function to shield the ear complex from internally produced sounds and isolate the ear complexes acoustically to facilitate directional hearing at depth (Norris, 1964). Understanding the highly derived structures of the middle ear is limited due the lack of experimental data and is beyond the scope of this paper. Although the external and middle ear components are sculptured to sound conduction in water from a terrestrial ear, the inner ear when the sense organ is located is remarkably conserved with several features unique to high frequency hearing (Hemila, et al, 1995). (Fig. 1).

In delphinoids, the melon has been shown to be a key component in the sound transmission pathway, playing a vital role in propagation and impedance matching, and the mandibular fats are part of the sound reception channels. As a consequence, sound velocity is an important physical property to characterize. Several studies have investigated sound velocity in the melon and spermaceti organ in odontocetes (Blomberg and Jensen, 1976; Blomberg and Lindhom, 1976; Flewellen and Morris, 1978; Goold *et al.*, 1996; Goold and Clarke, 2000; Litchfield *et al.*, 1973; Litchfield *et al*., 1979; Norris and Harvey, 1974; Varanasi *et al.*, 1982). However, most of these studies investigated melon oils, not tissues and only a few have presented detailed sound velocity or lipid composition topographical variation (Norris and Harvey, 1974; Litchfield *et al.*, 1973; Varanasi *et al.*, 1982). Understanding structural and compositional heterogeneity is invaluable information for building a model of the acoustic pathways in the head of the whale. Previous studies have mainly focused on the lipids of the forehead; consequently no data has been gathered for other forehead tissues or the mandibular fat tissues of the Cuvier's beaked whale. Also, no sound velocity studies have investigated specimens from Ziphiidae (beaked whales), which have a unique lipid composition compared to all other odontocetes (Litchfield *et al.*, 1976). Without known sound velocity profiles, accurate values are needed to model sound propagation in *Ziphius cavirostris*, hence this presentation of this study.

Physical properties other than sound velocity have not been studied extensively in odontocetes. One study reports the mass density of skin in a harbor porpoise, *Phocoena phocoena* (952 kg/m^3) and a bottlenosed dolphin, *Tursiops truncatus* (969 kg/m^3), (Kipps *et al.*, 2002). Another study reports elastic compliance of blubber in pilot whales, *Globicephala spp*., as 10 MPa^{-1} (Fitzgerald and Fitzgerald, 1995). Therefore, Young's elastic modulus, a measure of elastic stiffness that is the inverse of elastic compliance, is 0.1 MPa for pilot whale blubber tissue. To our knowledge there are no reports of CT scan Hounsfield units or sound attenuation values for odontocete tissues.

The main objective of this study was to measure the desired tissue properties in a neonate *Ziphius cavirostris.* The second objective was to examine the relationship between CT scan Hounsfield unit values and values from each of the other physical properties.

Methods:

Tissue physical property measurements require destructive sampling, and therefore, were done following opportunistic acquisition of a fresh stranded carcass. A Cuvier's beaked whale, *Ziphius cavirostris* (NMFS field number KXD0019), stranded on January 7, 2002 at Camp Pendleton in San Diego, California. The individual was a 314.9 cm long female neonate estimated to be about one month old at the time of death. Immediately after the body was recovered from the beach, it was frozen to -14^{o}C to prevent tissue decomposition. An unintentional thaw occurred prior to this study, followed by refreezing. In April 2002, the frozen specimen was cut across the long axis of the body into four manageable segments using an industrial band saw. The segments corresponded roughly to the head, thorax, abdomen, and tail. The segments were individually scanned, dissected, and cut into smaller pieces for further analysis.

CT Scans

Each segment was defrosted and subjected to CT scanning using a GE Light Speed Plus CT scanner. Axial scans, 5mm thick, were collected every 5 mm, to ensure the entire specimen was scanned. The scanner used a 50 cm diameter field of view scan region. Images were collected with 140 kV and 320 mA power setting whereas scouts were collected using 120 kV and 120 mA power setting. Image data were recorded directly to hard drive.

We analyzed the CT scan data to determine Hounsfield Units for the samples from the head. We used E-film, a specialized software package, to convert CT units of electron density into calibrated Hounsfield Units. Hounsfield Units are scaled from -1000 to >1000, where air is at -1000, water is at 0, and hard bone can be found near 1000+ (Robb, 1998). Mammalian soft tissues generally range between -100 and 100, with fatty tissues at the low end and denser connective tissues at the high end (Duck, 1990). Hounsfield units are standardized by defining water to zero and calibrated such that one unit is equal to the change in the density of 1 cc of water raised 1^{o}C at standard temperature and pressure. We referred to photos taken during the dissection to locate the position of dissected tissue samples in the CT scan images. We chose the CT image that corresponded to the center of each dissection slice by referring to landmarks such as the skull, eyes and ears. We developed a correction for samples at the outer edges to account for the mismatch of slice angle between the CT scans and the dissection slices. Samples were picked by visually correlating the CT image with the photo of each slice. HU values were measured using a 0.1 cm^2 circle tool that was placed at the approximate center of each sample, providing the average and standard deviation of HU values in the circular area.

Dissection

After each segment's CT scan, dissections were performed, with extra attention and finer scale sampling in the forehead and mandibular regions (see Table 1 for sample descriptions). The forehead was cut transversely into 2cm thick slices for a total of 15 slices (Fig. 3A,B). Each slice was further cut in a grid-like fashion into ~2cm cubes (Fig. 3C) so that we could obtain higher resolution topographical data than had previously been achieved. The left mandibular region was also cut transversely into 2 cm thick slices for a total of 12 slices. For each slice, one sample was taken from the blubber and the exterior mandibular fat and one to five samples were taken from the interior mandibular fat. Each cubic sample was numbered, notched on the anterior right dorsal corner, and stained on the anterior side with Basic Fuchsin to provide sample location and orientation reference during post-dissection evaluation. The dissections were recorded photographically with a 5 megapixel digital color camera (Sony Cyber-shot DSC-707).

Tissue samples were subjectively categorized by eye into the following broad categories: blubber; acoustic fats or melon; muscle; and connective tissue. All samples containing a mixture of these categories were discarded from further analysis because of their poorly quantified contribution of different tissue types. While accurate descriptions of tissue can only be determined by histological analysis, such an investigation was not within the scope of our analysis. The reader should interpret these subjective categories with appropriate caution.

Sound Velocity and Attenuation

Sound velocity was measured in each tissue sample using a Krautkramer Branson USD10 Ultrasonic Digital Flaw Detector and two Krautkramer Branson longitudinal acoustic transducers (Alpha series, 10 MHz, 0.25 mm) attached to Mitutoyo digital calipers (model no. CD-8”CS) (Fig. 4). The Krautkramer velocimeter and transducers were used at 10 MHz to measure the transmission time through tissue samples. The calipers were used to measure the sample thickness, and velocity was calculated by dividing the thickness by the travel time. Prior to measuring the samples, the velocimeter was calibrated using room-temperature (22.5^{o}C) distilled water, assuming a sound speed of 1490 m/s (Chen and Millero, 1977). We adjusted the gain for each sample such that the received signal was at 80% strength. We then calculated the relative transmission attenuation through the tissue as the difference in received signal gain in dB from the baseline signal gain divided by sample thickness (dB/mm). Each sample cube was measured along three directions (anterior-posterior, dorsal-ventral, lateral) to test for tissue anisotropy. Temperatures of the samples were recorded for later sound velocity normalization.

It should be noted that sound velocity and attenuation measurements were made at ultrasonic (10 MHz) frequencies, due to the need to measure small tissue samples. We do not expect sound velocity to be significantly dispersive, so our velocity measurements should apply at a broader range of frequencies, including mid-range (kHz) frequencies. On the other hand, acoustic attenuation depends on both scattering and absorption, and we expect that there will be significant differences as the frequency (and hence wavelength) are changed. The attenuation values are only applicable to the ultrasonic frequencies they were measured at; they cannot be directly applied for attenuation at mid- or low-frequencies.

Sound Velocity – Temperature Experiments

Temperature affects sound velocity in tissues, and we were interested in estimating *in vivo* (37^{o}C) sound velocity rather than room temperature (22^{o}C) sound velocity. A sample of each type of tissue was placed in a water bath at temperatures ranging from 0 – 35^{o}C until it reached equilibrium and then its sound velocity was measured.

Elasticity

Longitudinal compression tests of each sample were performed to measure the elastic modulus. This measure is similar to the linear Young's modulus, which is the ratio of stress to strain for a material. However, since tissue materials exhibit non-linear stress-strain curves, we determined the elastic modulus as the tangent to the non-linear curve at different stresses. A Mini Bionix 858 (MTS Corp) compressed each sample while force and displacement data were recorded to a computer running TestStar (Fig. 5). The instrument was set to run 10 low stress cycles at 2 cycles per second with 0.08 mm displacement followed by one high stress cycle at 0.5 cycles per second with a 2 mm displacement. The calipers that were used for the sound velocity measurements were also used to measure initial size of the cube to calculate length (i.e. distance between the compressing plates) and the area in contact with the plates. Each sample was placed in the instrument and the hydraulic arm was engaged to slightly compress the sample. This initial force was recorded and the displacement was zeroed prior to cycle loading the sample. We sampled force and displacement data at 100 samples per second. A customized MATLAB program created stress versus strain plots for each sample. We calculated the elastic modulus as the tangent to the stress-strain curve at several stresses (Fig. 6).

Density

Density was calculated using Archimedes' Principal. We measured volume by immersing each sample in distilled water and weighing the displaced water. Water temperature was monitored to get accurate volume measurements. Wet mass was determined by direct measurement with a Mettler PM 460 Delta Range mass balance. Density was calculated by dividing mass by volume.

Statistical Analysis

We used a paired Student's t-test to investigate sound velocity anisotropy among sample orientations within each tissue type (Hopkins *et al.*, 1987). We used an unpaired Student's t-test to compare values between tissue types for sound velocity, sound attenuation, density, Hounsfield Unit and elastic modulus. Linear regressions and a principal components analysis (PCA) were used to investigate the relationships between the various measures. First, we averaged the values from the three orientations for sound velocity, sound attenuation and elasticity. This enabled us to compare these measures to the density and HU measures which only had one value per sample. We used linear regressions to determine the relationship between Hounsfield Units and each of the other measures. We used PCA to determine the independence of the five physical property variables and to isolate the most important modes of variability in the data. PCA seeks linear combinations of variables that maximally explain the variance in the data (Jackson, 1991). The variance of a large dataset is concentrated into a small number of physically interpretable patterns of variability, the principal components. Patterns among the physical property variables are illustrated by loadings on the principal components (Jackson, 1991).

Results:

Sound Velocity vs. Temperature

Sound velocities were plotted versus temperature for forehead blubber, melon, muscle, mandibular blubber, mandibular acoustic fats, and connective tissue (Fig. 7). Sound velocities of all fatty tissues decreased with increasing temperature from 12^{o}C to 35^{o}C. Muscle and connective tissue sound velocities were nearly constant over the temperature range from 10^{o}C to 37^{o}C. For the remaining analyses, sound velocities were corrected to 37^{o}C by the following equation:

$$V_{37} = V_o + 37\text{-}T_o * m \qquad (1)$$

where V_o is the measured velocity, T_o is the measured temperature, and m is the slope from the empirical data for each tissue type (Table 2). This correction enabled us to compare sound velocities between samples, independent of temperature effects, as well as consider how this property may vary between tissue types *in vivo*. Melon, connective tissue and muscle tissues are at a temperature of 37^{o}C *in vivo*. However, we expect there is a temperature gradient in blubber ranging from ambient seawater temperature at the skin boundary to body temperature at the internal boundary.

Sound Velocity

Sound velocities within the forehead tissues of *Ziphius cavirostris* ranged between 1341 – 1708 m/s. Forehead sound velocity values corrected to 37^{o}C are plotted for each tissue type in Fig. 8A and presented in Table 3. There was a wide range in sound velocity values for connective tissue, and connective tissue values were significantly higher than values for the other three tissue types (Table 4). Muscle values were significantly higher than those of blubber and melon, and blubber tissue velocities were significantly higher than those of the melon tissues (Table 4). The average sound velocity of seawater is 1507 m/s at 15^{o}C, 1atm and a salinity of 35

(Chen and Millero, 1977). Fatty tissues in the melon and blubber exhibit sound velocities significantly lower than those of seawater (Table 5). Muscle tissues exhibit sound velocities that are not statistically different from seawater while connective tissue sound velocities were significantly higher (Table 5).

In the mandibular region, sound velocities ranged from 1331 – 1394 m/s. Values for sound velocity corrected to $37^{o}C$ are presented for each tissue type (Fig. 8B and Table 6). In the mandibular region, mean sound velocity values for blubber were significantly higher than those for acoustic fats (Table 7), while both these fatty tissues exhibit values significantly lower than that of seawater (Table 5). While the patterns between tissue types are similar, both blubber and acoustic fat tissues had significantly higher sound velocities in the forehead region than in the mandibular region (Table 8).

The organizational structure of the forehead has a strong effect on sound velocity. Laterally, velocities are lowest in the center of the forehead. However, in the posterior region, the low velocity center shifts toward the right (Fig. 9). This change in velocity is evident within the melon tissue as well as between tissue types. From anterior to posterior, the sound velocities are higher toward the rostrum where the melon fat grades into blubber. This change is also evident toward the front of the forehead in the dorsal-ventral direction. Overall, a low velocity core is present that converges posteriorally, exhibiting spatial asymmetry, and strong velocity gradients. Anteriorally, the core is broader in size/shape, spatially symmetric, and exhibits a low gradient toward the dorsal rostral side. Laterally, the gradient is sharp throughout the melon.

Anisotropy

To test for anisotropy of sound velocity values between the three orientations of each tissue cube, we performed paired Student's t-tests comparing velocities in each direction (Table 9, Fig. 10). Sound velocities throughout the head were significantly higher in the anterior-posterior (AP) direction than in the lateral (LR) direction (Table 9) and the dorsal-ventral (DV) direction (Table 9). Further analysis revealed that the AP-LR anisotropy was influenced by connective tissue in the forehead, while the AP-DV anisotropy was influenced by acoustic fats in the mandible. Additionally, we found that sound velocities in blubber were significantly higher in the lateral direction than the dorsal-ventral or anterior-posterior directions (Table 9, Fig. 10). This was especially evident in the mandibular tissues.

Sound Attenuation

Sound attenuation values in the *Ziphius cavirostris* forehead tissues ranged from 0.4 – 3.5 dB/mm at 10 MHz, greater than the 0.026 dB/mm for propagation in seawater at 15^{o}C and 1 atm (Francois and Garrison, 1982). Attenuation was significantly higher in connective tissues than in the fatty tissue types (Fig. 11A, Tables 3, 4). Muscle, blubber and melon values were not significantly different from one another (Table 4).

In the mandibular region, sound attenuation values were between 0.2 and 2.0 dB/mm. Sound attenuation values for acoustic fats and blubber were not significantly different from one another (Fig. 11B, Tables 6, 7). However, sound attenuation values of mandibular blubber and acoustic fats are significantly lower than those found in the forehead tissues (Table 8).

Mass Density

Forehead tissue densities ranged from 882 – 1175 kg/m^3. The range of values was small for fatty tissues, but high for both muscle and connective tissues (Fig. 12A, Table 3). Connective tissues were significantly denser than all three other tissue types, while muscle was significantly denser than blubber and melon (Table 4). Blubber and melon were not significantly different from one another (Table 4). Seawater with a salinity of 35, at 15^{o}C and 1atm has an average density of 1026 kg/m^3 (Pilson, 1998). Fatty tissues and muscle were significantly less dense than seawater, while connective tissue was significantly denser than seawater (Table 5).

Mandibular region tissue density values ranged from 854 – 941 kg/m^3. Acoustic fats were significantly less dense than blubber (Fig. 12B, Tables 6, 7). Acoustic fats in the melon were denser than the acoustic fats in the jaws (Table 8). Similar to the forehead tissues, fatty tissues were significantly less dense than water (Table 5).

Hounsfield Units

Hounsfield units in the forehead tissues ranged from -106.2 to 108.6 HU, with sampling standard deviations ranging from 0.9 – 29.1 HU. The fatty tissues, blubber and melon, had significantly lower HU values than connective tissue and muscle, but were not significantly different from each other (Fig. 13A, Tables 3, 4). Connective tissue had significantly higher HU values than muscle (Table 4) and a larger range of values. Blubber, melon and muscle values were significantly lower than those for water (Table 5). Connective tissue exhibited HU significantly higher than those of water (Table 5).

Hounsfield units in the mandibular tissues ranged from -106.5 to -29 HU, with sampling standard deviations ranging from 1.8 – 24.2 HU. Average blubber HU were significantly lower than those of acoustic fats (Fig. 13B, Tables 6, 7). Melon and acoustic fats HU values were significantly lower than those of water (Table 5). These results follow the same pattern seen in the forehead tissues, however mandibular blubber values are significantly lower than those of forehead blubber (Table 8).

Elastic Modulus

Stress-strain curves were plotted for each of the samples from the data collected in the biomechanical compression tests (Fig. 6). Since the stress-strain curves were non-linear, the elastic modulus was evaluated at a variety of stresses to investigate how the elastic modulus changed with stress. These were averaged by tissue type and plotted against stress in Figs 14, 15 for the forehead and mandible respectively. Muscle samples were discarded because myosin and actin connections, which are biologically important for retaining stiffness/structure, degrade with time after death (Schmidt-Nielsen, 1995).

Forehead elastic modulus averages for melon tissues ranged from 75 kPa to 910kPa between stresses of 2.5kPa and 50kPa (Table 10). Blubber sample averages ranged from 59 kPa to 1410 kPa, and connective tissue sample averages ranged from 124 to 1510 kPa. Across all stresses, melon samples had a lower elastic modulus for a given stress than connective tissue and blubber. Blubber exhibits a non-linear response, becoming less compressible with increasing stress.

Mandibular region elastic modulus averages for acoustic fat samples ranged from 78 kPa to 934 kPa between stresses of 2.5kPa and 50kPa (Table 10), and blubber sample averages ranged from 158 kPa to 1174 kPa. Similar to the forehead region, acoustic fat values were lower than blubber values at a given stress. Again, blubber exhibits a non-linear response, becoming less compressible with increasing stress

Correlations

Principal components analysis was undertaken to look for combinations of tissue properties that vary together systematically. The results show that the first principal component explained 73% of the variance, while the second component explained 18% (Fig. 16). Sound velocity, sound attenuation, density and Hounsfield unit were explained by the first principal component, and are therefore dependant measures (Fig. 17). Elasticity was an independent measure and is explained by the second component. The samples are distributed in a nonrandom pattern with similar tissues clumping together as shown in Fig. 18. The plot shows that the connective tissues, muscle and lipids separate out along the first component. On the other hand, melon and blubber can be distinguished by the second component.

Since sound velocity, sound attenuation, density and Hounsfield Unit are measuring a similar characteristic, we looked for the linear correlations between the measured values and determined r^2 values for Hounsfield Units versus density, sound velocity and sound attenuation. All three measures showed a strong positive relationship to Hounsfield unit (Fig. 19). The relationship between Hounsfield unit and sound velocity was the strongest ($r^2 = 0.85$), followed by density ($r^2 = 0.76$), while sound attenuation was less correlated ($r^2 = 0.63$).

Entire specimen

Results of physical property measurements for organs and tissues from each section of the *Z. cavirostris* body can be found in Table 11. Mean, standard deviation, minimum and maximum values are presented for sound velocity, sound attenuation and density. Blubber and muscle tissues were present throughout the body. Mean sound velocity values at 37^{o}C (1405±12 m/s) and mean densities (932 ± 25 kg/m^3) for twenty-seven blubber samples from the head, chest, abdomen and tail regions were similar to forehead sound velocity values, though higher than mandibular region values. Mean attenuation values for blubber (0.80 ±0.38 dB/mm) were similar to values in both the forehead and mandibular regions. Seventeen samples of muscle from the chest, abdomen and tail region had mean sound velocities at 37^{o}C (1595 ± 7 m/s) and mean densities (1060 ± 74 kg/m^3) that were higher than those found in the forehead. Mean attenuation values for muscle (0.83 ± 0.21 dB/mm) were lower than those found in the forehead muscle.

Specialized tissues, present in only a single section, that were measured include samples from the: diaphragm, esophagus, heart, liver, lungs, nasal plugs, thyroid cartilage, tongue, and trachea. Most values fell within the expected range for muscle and connective tissues. Nasal plugs exhibited the highest sound velocities of any *Z. cavirostris* tissues measured. A large difference exists between sound velocities for the left and right lungs. This discrepancy is likely due to the fact that the specimen settled on the left side prior to freezing resulting in the left lung being filled with fluids, while the right lung was not.

Discussion

Velocity

Several authors have discussed sound velocity variations in the melons of marine cetacea. Our measured sound velocities, ranging from 1412-1488 m/s at room temperature in the melon (Tables 2, 3), appear high compared to studies in other cetaceans where most room temperature values are around 1370 m/s (Apfel *et al.*, 1985; Blomberg and Jensen, 1976; Blomberg and Lindholm, 1976; Litchfield *et al.*, 1979; Norris and Harvey, 1974). The study by Norris and Harvey (1974) had the most comparable values, with sound velocities ranging from 1273-1481 m/s. These differences may be due to technique: most studies extracted the oils from the tissues to perform sound velocity tests, while our study and that of Norris and Harvey (1974) used the actual tissues. As Duck (1990) noted, water/lipid content significantly affects sound velocity of tissues, and this may be why velocities of pure lipids are so much less than those of intact tissues. Another important difference of our study is that the subject was a neonate. Koopman, (2003) as well as Lok and Folkersma (1979) have shown ontogenetic changes in beaked whale melon lipid composition, which may be reflected in changes of sound velocity and transmission properties.

Previous studies of sound velocity in the odontocete forehead have reported a low velocity inner core within the melon, consistent with the results of our study (Flewellen and

Morris, 1987; Litchfield *et al.*, 1979; Norris and Harvey, 1974). The presence of a low velocity core supports the hypothesis that the beaked whale melon helps to produce a directional sound beam. The structure of the forehead, involving different tissues components, may give rise to stages of directional sound beam formation. For example, air spaces, dense connective tissue layers, and boney regions can act as acoustically reflective surfaces that function to direct sound anteriorly. Another stage of beam formation results from the chemical topography in the melon that tends to focus the beam along the low velocity core.

The increase in sound velocity between melon and blubber may be important in impedance matching of the sound waves to the water to maximize the acoustic energy transfer out of the forehead. Impedance matching occurs when the acoustic impedances (the product of density and sound velocity) of two adjacent materials are similar, resulting in greater transmission of acoustic energy at the boundary between the two materials. Another factor influencing sound velocities, and thereby impedance matching, is the change in temperature from the interior to exterior boundaries of the blubber. At the interior, the 37^{o}C blubber has a sound velocity averaging 1401m/s, which increases to 1492m/s at the exterior blubber boundary in 15^{o}C water (Tables l and 2). These results support impedance matching as a proposed function for the Cuvier's beaked whale melon, as proposed for the bottlenose dolphin melon (Norris and Harvey, 1974). Sound velocity in the fats in the mandibular channel also exhibit low velocities compared to surrounding tissues. Again, the change in sound velocity from seawater to blubber to acoustic fat is probably important in impedance matching for sound reception, and the channeling of sound from seawater to the ear complexes.

The sound velocity values for *Z. cavirostris* fats are consistent with those reported in the literature for terrestrial mammal tissue fats. In our study, the sound velocities of beaked whale lipids, including blubber, melon, and jaw fats at 37^{o}C ranged from 1341 to 1442 m/s (Tables 3,6). Duck (1990) reviewed many studies that looked at sound velocities in mammalian tissue and found a similar range of values for fats (Human fat: 1436 – 1489m/s; Human and animal fat: 1412 – 1430 m/s; cow fat: 1430 – 1471m/s; dog fat: 1412 – 1459m/s; and pig fat: 1426 m/s). O'Brien (1977) had similar sound velocities for fat tissues, ranging from1410-1479 m/s. While these values may appear high compared to ours, these studies were conducted at room temperature. At room temperature, our sound velocities range from 1441-1489 m/s consistent with those found in land mammals.

The sound velocity values for *Z. cavirostris* muscle are similar to those reported in the literature for terrestrial mammal muscle, but do exhibit some noticeable differences. We show forehead muscle values ranging from 1460 to 1597 m/s at 37^{o}C, which show little change in value at room temperature (Tables 3, 6). The upper range of our values are consistent with those found in Duck's (1990) literature review for some terrestrial mammals (Human muscle: 1547 – 1580m/s; cow muscle: 1580 – 1604m/s; dog muscle: 1566-1629 m/s; pig muscle: 1579-1597m/s; and rabbit muscle: 1542 – 1610m/s), and O'Brien's (1977) values of 1545 – 1631 m/s. However, our values also extend quite a bit lower, particularly in the muscles found in the forehead region. The muscles in the forehead region appear to have higher lipid content than muscle tissues found throughout the body. Duck (1990) noted that an increase in fat content in tissues leads to a decrease in sound velocity. Our results for sound velocities for muscle in the chest, abdomen and tail sections range from 1571-1597 m/s which fit well with those from the literature.

The sound velocity values for *Z. cavirostris* connective tissue are similar to those reported in the literature for mammalian collagen fibers, which are a major component of connective tissue. Little data was available on connective tissues in the literature; however one study calculated the sound velocity for collagen at 1570 m/s (reviewed in Duck, 1990; Lees and Rollins, 1972). Our results for connective tissue show values ranging from 1531 to 1700 m/s at 37^{o}C, which have values of 1538 - 1708 at room temperature (Tables 3, 6). This large range is probably due to the high variability of tissue content in connective tissues which exhibit complex collagen structures. Duck (1990) noted that collagen content affects velocity significantly (from O'Brien, 1977) and that the range of measured velocity values may be associated with the relative proportions of water and collagen in the different skin samples measured. There may be a similar mechanism behind the results we see here.

The results of our temperature-sound velocity experiments are similar to those reported in the literature. Our study of fats shows a linear decrease in sound velocity with increasing temperature of about 4m/s/^{o}C, while muscle and connective tissue had a nearly constant slope. Duck (1990) shows that sound velocity in fats decreases linearly with increasing temperature, (at approximately -10m/s/^{o}C) until about 35^{o}C where it exhibits nonlinear behavior. By contrast, sound velocity in water, liver, blood and amniotic fluid increases gradually with increasing temperature. Studies have investigated sound velocity changes with temperature in forehead lipids in marine mammals. Lipids extracted from melon tissues decrease with increasing temperature, on the order of 1-13 m/s/^{o}C (Blomberg and Jensen, 1976; Goold *et al.*, 1996; Goold and Clarke, 2000; Litchfield *et al.*, 1979). These studies (except Litchfield *et al.*, 1979) have shown a non-linear effect due to the phase change of the oils near body temperature This is an important find since beaked whale melon/acoustic fats have a different lipid composition, particularly in neonates, yet the lipids exhibit the same pattern of properties. We were not able to investigate non-linear changes around body temperature since the lipids in our samples exhibited a phase change, and muscle and connective tissues were cooked. It would be important to study this effect in beaked whale tissues in the future to better understand how the melon functions for sound conduction.

Anisotropy

Sound velocity anisotropy indicates the structural orientation of fiber/strength components of the tissue. For example, sound will travel faster along fibers than transverse to them. Our data suggest a preferential anterior posterior (rostrum to tail) orientation for fibers of connective tissues and mandibular acoustic fats since the sound velocities are significantly higher in this direction. This suggests that the structural components preferentially run anterior to posterior, so that they stiffen the tissue in this direction, which contributes to a higher sound velocity along that axis. By contrast, sound velocity anisotropy data from blubber tissues suggest structural components are preferentially oriented in the lateral direction rather than anterior-posterior. In the mandibular region, a lateral preference was also apparent compared to the dorsal ventral. It is possible that this anisotropy is due to a preferential interior-exterior orientation of structural components, such that fibers are radially perpendicular to the long axis. This would not show up in our results for the forehead region due to our methods.   The blubber is radially symmetric around the anterior posterior axis, while our measurements were taken in a Cartesian plane. Therefore some of our interior-exterior measurements were in the dorsal-ventral orientation, and others were in the lateral orientation. An interior-exterior anisotropy would not be discernable from these measurements, while it would be apparent in the mandibular region where all lateral measurements were interior-exterior. An interior-exterior anisotropy could be caused by preferential orientation of the structural components in the blubber, or it could be a result of chemical/lipid compositional variation that have been found within the layers of odontocete blubber (Evans *et al.*, 2002; Koopman *et al.*, 2003). However, if this difference in anisotropy between the two regions is not an artifact, perhaps the sound velocity anisotropy contributes to filtering differentially in opposite mandibles, assisting in creating an asymmetric/ discernable sound field.

Attenuation

Almost nothing is known about acoustic attenuation in the tissues of marine mammals. However, some work has been done on other mammalian tissues. For example, O’Brien (1977) reports values of 0.44dB/mm, 0.76dB/mm and 1.4dB/mm for attenuation in fats at 1, 3 and 5 MHz, respectively. When these are extrapolated (linearly and quadratically) to 10MHz, attenuation coefficients of 2.55dB/mm and 4.4dB/mm are obtained, respectively. The linear extrapolation is similar to our maximum values, while the quadratic extrapolation is more than twice as high as the highest values that we obtained for lipids in this study. Our minimum value was 0.2dB/mm and our maximum value was 2.4dB/mm. O'Brien (1977) also provided data for striated muscle against the grain: low values were 0.64, 2.2, and 4.0dB/mm for attenuation at 1, 3 and 5 MHz, respectively. When these are extrapolated (linearly and quadratically) to 10MHz, attenuations of 8.16 dB/mm and 9.55 dB/mm are obtained, respectively, which are about 3 times higher than the maximum values of 2.9 dB/mm that we obtained for muscle. Linear extrapolation infers scattering is important, while a quadratic extrapolation suggests that absorption is dominating attenuation. The fact that our values are below, but close to the linear extrapolation suggests that scattering is more important than absorption in influencing attenuation. We expect that in the 10-200 kHz range where odontocetes vocalize, absorption would be even less important. In this frequency range, the wavelength ranges from 0.5 to 10 cm, so sound does not travel many wavelengths before passing into the ocean. Scattering is likely to be important at these wavelengths due to the presence of collagen fibers. For example, O'Brien (1977) noted that increasing collagen content in tissues increased attenuation. Additionally, it has been suggested that macro-molecular scale proteins are involved in a significant fraction of longitudinal wave attenuation in soft tissues (Madsen *et al.*, 1983), consistent with our results.

The differences in the attenuation values of the different tissue types in the head may be important for sound production and reception. For an organism to emit and receive the highest amplitude signal, it is important that the signal is not attenuated as it travels through the tissues. The acoustic fats in the mandible and the forehead exhibit the lowest sound attenuation of all the tissues (Fig. 11). This supports the sound production/ reception functions of these tissues. On the other hand, the higher attenuation values in the surrounding muscle and connective tissues of the forehead may be important in directionality of sound production. As more sound is scattered at the sides, a decreased signal will radiate out on side paths compared to a forward collimated beam. Therefore it may mute sounds that are traveling in a less desirable direction.

Sound attenuation within both blubber and acoustic fats were significantly lower in the mandibular region than they were in the forehead region. Perhaps higher sound velocities and attenuations result from more structural collagen fibers in forehead blubber than mandibular blubber. The beluga whale manipulates the shape of its melon during sound production (Perrin *et al.*, 2002), presumably affecting the directionality of its sound beam. If beaked whales manipulate the shape of their melon when vocalizing, then differential structure in forehead blubber and melon tissues could be used to change sound beam directionality. Histological analysis of blubber from different regions might provide some clues.

Mass Density

Mass densities of the *Z. cavirostris* tissue types are similar to those found in other mammals. Fatty tissues in this study ranged from 854 to 987 kg/m^3, averaging 922 kg/m^3. Duck (1990) has shown that the average density of pure mammalian fat is about 900 kg/m^3, while human breast fat ranges from 917 -939 kg/m^3, and the human breast including all tissues ranges from 990 – 1060 kg/m^3. The lower values that we found therefore correspond to pure fatty tissues, while the higher values include more structural tissues such as collagen in blubber. Duck (1990) showed that muscle densities range from 1038 to 1056 kg/m^3. *Z. cavirostris* values ranged from 909 to 1078 kg/m^3, which have a similar mean value but a greater range of values. While the results were not significantly different, possibly a result of the small sample size, muscle densities in the forehead were lower than muscle densities from other areas. The lower values for muscle in the forehead suggest the presence of lipids in forehead muscle tissues.

Note that the acoustic fats in the forehead were significantly denser than those in the mandibular region (Tables 3, 6). Sound velocity (v) is a function of density (rho) and the bulk modulus, a measure of stiffness (c) (Jensen et al.,1994),:

$$v = (c/rho)^{1/2} \qquad (2)$$

The difference in sound velocity and density between acoustic fats in the forehead and mandibular region suggests that stiffness is similar between the two tissues. This is consistent with our results on tissue elasticity, and sound attenuation. A possible reason for this difference may be related to the functional differences between the melon and the mandibles. Denser tissue may be easier to manipulate if the animal changes forehead shape to change the directionality of outgoing sound, as has been seen in beluga whales (Perrin *et al.*, 2002). On the other hand, shape changes that affect sound directionality in the mandibular region could be disruptive for discriminating incoming sounds.

Hounsfield Unit

Z. cavirostris fats, including acoustic fats and blubber had CT scan Hounsfield unit values ranging from -106.5 to -46.3. Robb (1998) found that mammalian fats typically lie between -100 and -70. Most of our samples lie within this range, however some blubber and melon fat samples from the forehead exhibited higher HU values than Robb found. This may be due to human error in matching the locations of the samples in the CT scan to their geometric space from dissection. It may also be indicate that changes are due to the unique lipid chemistry of odontocete blubber and acoustic fats compared to common mammal fats or the presence of collagen in the blubber. However, since these higher HU values were not found in the mandibular region, sample matching error seems the more plausible explanation. This is a topic which merits further investigation.

Muscle values typically fall between 25 and 60 HU (Robb, 1998). Our values ranged from -61 to 1.8. These are lower than those reported by Robb, particularly in the forehead region. This may be caused by lipid content in the muscle in forehead which would decrease the HU value. Goodpaster *et al.* (2000) found that human skeletal muscle containing high lipid concentrations exhibited lower HU values than muscle which contained low lipid concentrations. The differences in our values might also be due to the amount of postmortem time and consequent decomposition in muscle tissues, perhaps the most susceptible to these changes.

Hounsfield Units for blubber tissues were higher in the forehead than in the mandible. This may be related to the difference in sound attenuation and density for these regions. O'Brien (1977) suggests increased attenuation is due to increased collagen structure. If blubber tissues in the forehead contain more collagen fibers than those in the mandible, then they would be expected to have an increased HU value as well.

Elastic Modulus

Elastic modulus values for *Z cavirostris* tissues range between 0.1 and 1.4 MPa at stresses from 5 – 50 kPa. Connective tissue and blubber exhibit the full range of values above with elastic modulus increasing with increasing stress. Melon on the other hand, exhibits lower values, with a high of 0.95 MPa at 50 kPa. The higher values for blubber and connective tissue suggest that these tissues have greater structure than melon, which is reasonable since connective tissue and blubber are held together by collagen fibers. O'Brien (1977) notes that the elastic properties of soft tissue are determined primarily by the content of collagen and other structural proteins. Elastic moduli for tissues vary non-linearly with applied stress making comparisons with previously published values difficult as these measurements may have been carried out on different portions of the stress strain curve.

Correlations

The results of the principal component analysis show that connective tissue, muscle and lipids separate distinctly along the first principal component (Fig. 18), which represents sound velocity, sound attenuation, density and Hounsfield units (Fig. 17). This separation shows that sound velocity, sound attenuation, density or Hounsfield units can each be used to determine the type of tissue in a Cuvier's beaked whale, since each tissue type's physical properties are distinct. The high explanatory power of the first principal component (Fig. 16) illustrates that sound velocity, sound attenuation, density and Hounsfield units are measuring similar characteristics. This supports the notion that Hounsfield units can be used to model density, sound velocity and attenuation parameters needed for acoustic modeling, which is beneficial to modeling efforts since Hounsfield units can be collected throughout a whole specimen non-destructively. Hounsfield units cannot be used to predict elastic modulus values. Elasticity, primarily represented by the second principal component (Fig. 17), is the only measure that distinguishes between acoustic fats and blubber (Fig. 18). Elasticity is important for understanding the behavior of these tissues under high stress conditions.

The linear correlations between Hounsfield Units and sound velocity, sound attenuation, and density were high (0.85, 0.63, and 0.76 respectively). Attenuation shows the lowest r^2 value suggesting attenuation is less related to electron density than the other measures, or that the relationship is nonlinear. The linear relationships we found for these measures provide a model to determine the sound velocity, sound attenuation and density when only the Hounsfield Units from CT scanning are available (Fig. 19). Some of the noise in the data may be due to human error in correlating the samples to their location in the CT scans. Future studies should work to improve this method.

Limitations

One concern about the results of this study is possible differences between living and dead and/or frozen tissues. Several studies have attempted to quantify these effects for mammalian tissues. Van der Steen *et al.* (1991) found that formalin fixed and formalin fixed/frozen liver tissues exhibited similar sound velocities and sound attenuation coefficients to fresh tissues. Similarly, Dent *et al.* (2000) found that sound velocities between fresh and previously frozen myocardial samples were similar. However, their results showed that attenuation is lower in previously frozen samples compared to recently excised fresh samples. Foster *et al.* (1984) reported no change in ultrasonic parameters of human breast tissue that had been frozen when compared to fresh tissue. This suggests that our sound velocity and attenuation values should accurately reflect those of fresh *Ziphius cavirostris* tissues. Smeathers and Joanes (1988) and Woo *et al.* (1986) found that there were no significant changes in elasticity between fresh and frozen/thawed specimens of human intervertebral discs and rabbit ligaments respectively. Intervertebral discs and ligaments each have high collagen content, similar to connective tissues in the head of odontocetes, and collagen content also has a large effect on elastic properties (O'Brien, 1977). Therefore, we expect that elastic properties of collagenous odontocete connective tissue should be unaffected by freezing and thawing as was found for mammalian intervertebral discs and ligaments.

Significant changes in the elastic properties of muscles result from the postmortem and freezing process (Leitschuh *et al.*, 1996; Gottsauner-Wolf *et al.*, 1995; and Van Ee *et al.*, 2000). For this reason, we have discarded muscle from our analysis of elastic properties. Contrary to the other findings, Fitzgerald (1975) and Fitzgerald and Fitzgerald (1995) suggest there is a life to death transition in viscoelastic compliance for beef muscle, beef fat, porcine intervertebral disc, and whale blubber around 5-11 hours post-mortem. While other studies did not support this result, it suggests that caution should be taken when interpreting the results from previously frozen tissues.

Conclusion

This study provides new data on sound velocity, sound attenuation, mass density, CT scan Hounsfield units, and elasticity for *Z. cavirostris* tissues. This has been the first attempt at gathering this breadth of physical property data from beaked whale tissues. Evidence for a relationship between CT scan Hounsfield units and sound velocity, sound attenuation and mass density is presented. This may allow future studies to relate CT scan values from a *Z. cavirostris* to these physical properties without extracting tissue samples. While there are limitations to our methods and results, the data we present show promise for use in modeling sound propagation within a beaked whale.

Acknowledgements

We thank: Susan Chivers, NMFS, for providing access to the beaked whale specimen; Hubbs Sea-World for allowing us use of their dissection lab; Lisa Cooper and Liliana Fajardo for aiding in the dissection; Shultz Steel for allowing use of their band-saw to section the specimen; Mark Shaver at UCSD Medical Center for help with CT scanning; Dr Thomas Nelson for obtaining CT data and providing eFilm assistance; Dr. Richard Buxton allowing use of MR scanner; Cecelia Kemper for help with MR scanner; Graydon Armsworthy, Jeanine Donley, Chris Garsha, Scott Rappaport and Allan Sauter for all of their assistance throughout the study. This work was supported by the US Navy CNO-N45 with project management by Frank Stone and Ernie Young.

References

Apfel, R. E., Young, R. E., Varanasi, U., Maloney, J. R., and Malins, D. C. (1985). Sound velocity in lipids, oils, waxes, and their mixtures using an acoustic levitation technique. *Journal of the Acoustical Society of America* **78**, 868-870.

Au, W. W. L. (1993). The Sonar of Dolphins. Springer Verlag New York, Inc.: New York. 277pp.

Baird, R. W., McSweeney, D. J., Ligon, A. D., and Webster, D. L. (2004). Tagging feasibility and diving of Cuvier's beaked whales (*Ziphius cavirostris*) and Blainville's beaked whales (*Mesoplodon densirostris*) in Hawai'i**.** Report prepared under Order No. AB133F-03-SE-0986 to the Hawai'i Wildlife Fund, Volcano, HI, from the Southwest Fisheries Science Center, National Marine Fisheries Service, La Jolla, CA, 92037 USA.

Barlow, J., Forney, K., VonSaunder, A., and Urban-R, J. (1997). A report of cetacean acoustic detection and dive interval studies (CADDIS) conducted in the southern Gulf of California, 1995. NOAA Technical Memorandum NOAA-TM-NMFS-SWFSC-250.

Blanco, C., and Raga, J. A. (2000). Cephalopod prey of two *Ziphius cavirostris* (Cetacea) stranded on the western Mediterranean coast. *Journal of the Marine Biological Association of the United Kingdom* **80**, 381-382

Blomberg, J., and Jensen, B. N. (1976). Ultrasonic studies on the head oil of the North Atlantic pilot whale (*Globicephala melaena melaena*). *Journal of the Acoustical Society of America* **60**, 755-759.

Blomberg, J. and Lindholm, L. E. (1976). Variations in lipid composition and sound velocity in melon from the North Atlantic pilot whale, *Globicephala melaena melaena*. *Lipids* **11**, 153-156.

Boutiba, Z. (1994). A review of our knowledge on the presence of cetaceans off the Algerian coasts. *Mammalia* **58**, 613-622

Brill, R. L., Sevenich, M. L., Sullivan, T. J., Sustman, J. D., and Witt, R. E. (1988). Behavioral evidence for hearing through the lower jaw by an echolocating dolphin Tursiops truncatus. *Marine Mammal Science* **4**, 223-230.

Chen, C. T., and Millero, F. J. (1977). Speed of sound in seawater at high pressures. *J. Acoust. Soc. Am.*, **62**, 1129-1135.

Cheung, J. T. M., Zhang, M., Chow, D. H. K. (2003). Biomechanical responses of the intervertebral joints to static and vibrational loading: a finite element study. *Clinical Biomechanics* **18,** 790-799

Cranford, T. W., Amundin, M., and Norris, K. S. (1996). Functional morphology and homology in the odontocete nasal complex: Implications for sound generation. *Journal of Morphology* **228**, 223-285.

Crum, L. A. and Mao, Y. (1996). Acoustically enhanced bubble growth at low frequencies and its implications for human diver and marine mammal safety. *Journal of the Acoustical Society of America* **99,** 2898-2907.

D'Amico, A., Bergamasco, A., Zanasca, P., Carniel, S., Nacini, E., Portunato, N., Teloni, V., Mori, C., and Barbanti, R. (2003). Qualitative correlation of marine mammals with physical and biological parameters in the Ligurian Sea. *IEEE Journal of Oceanic Engineering* **28,** 29-43

Dent, C. L., Scott, M. J., Wickline, S. A., and Hall, C. S. (2000). High-frequency ultrasound for quantitative characterization of myocardial edema. *Ultrasound in Med. & Biol*. **26,** 375-384.

Duck, F. A. (1990). Physical Properties of Tissue: A Comprehensive Reference Book. Academic Press Ltd: San Diego. Pp 74-165

Evans, D. L., and England, G. R. (2001). Joint Interim Report Bahamas Marine Mammal Stranding Event of 14-16 March 2000.

Evans, K., Hindell, M. A., and Thiele, D. (2003). Body fat and condition in sperm whales, *Physeter macrocephalus,* from southern Australian waters. *Comparative Biochemistry and Physiology, Part A* **134**, 847-862.

Fiscus, C. H. (1997). Cephalopod beaks in a Cuvier's beaked whale (*Ziphius cavirostris*) from Amchitka Island, Alaska. *Marine Mammal Science* **13**, 481-486

Finneran, J.J. (2003). Whole-lung resonance in a bottlenose dolphin (*Tursiops truncatus*) and white whales (*Delphinapterus leucas*). *Journal of the Acoustical Society of America* **114,** 529-535.

Fitzgerald, E. R. (1975). Dynamic mechanical measurements during the life to death transition in animal tissues. *Biorheology* **12,** 397-408.

Fitzgerald, E. R., and Fitzgerald, J. W. (1995). Blubber and compliant coatings for drag reduction in water. I. Viscoelastic properties of blubber and compliant coating materials. *Materials Science and Engineering* **C2**, 209-214.

Flewellen, C. G., and Morris, R. J. (1978). Sound velocity measurements on samples from the spermaceti organ of the sperm whale (*Physeter catadon).* *Deep-Sea Research* **25**, 269-277.

Forney, K. A., Barlow, J., and Carretta, J. V. (1995). The abundance of cetaceans in California waters II. Aerial surveys in winter and spring of 1991 and 1992. *Fisheries Bulletin – NOAA* **93**, 15-26

Francois, R. E. and Garrison, G. R. (1982). Sound absorption based on ocean measurements. Part II: Boric acid contribution and equation for total absorption. *Journal of the Acoustical Society of America* **72**(6), 1879-1890.

Frantzis, A. (1998). Does acoustic testing strand whales? *Nature* **392**, 29.

Fraser, F. C. and Purves, P. E. (1960). Hearing in Cetaceans. Evolution of the accessory air sacs and the structure and function of the outer ear and middle ear in recent cetaceans. *Bulletin of the British Museum of Natural History Zoology* **7**, pp137

Goodpaster, B. H., Kelley, D. E., Thaete, F. L., He, J., and Ross, R. (2000). Skeletal muscle attenuation determined by computed tomography is associated with skeletal muscle lipid content. *Journal of Applied Physiology* **89**, 104-110.

Goold, J. C., Bennell, J. D. and Jones, S. E. (1996). Sound velocity measurements in spermaceti oil under the combined influences of temperature and pressure. *Deep-Sea Research I* **43**, 961-969.

Goold, J. C., and Clarke, M. R. (2000). Sound velocity in the head of the dwarf sperm whale, *Kogia sima*, with anatomical and functional discussion. *Journal of the Marine Biological Association of the United Kingdom* **80**, 535-542.

Gottsauner-Wolf, F., Grabowski, J. J., Chao, E. Y. S., and An, K. N. (1995). Effects of freeze/thaw conditioning on the tensile properties and failure mode of bone-muscle-bone units: a biomechanical and histological study in dogs. *J. Orthop. Res*. **13,** 90-95.

Hemila, S., Nummela, S., and Reuter, T. (1995). What middle ear parameters tell about impedance matching and high frequency hearing. Hearing Research 85, 31-44.

Heyning, J. E. (1989)a. Comparative facial anatomy of beaked whales (Ziphiidae) and a systematic revision among the families of extant Odontoceti. *Contributions in Science* **405,** 1-64N.

Heyning, J. E. (1989)b. Cuvier's beaked whale Ziphius cavirostris G. Cuvier 1823. *In* "Handbook of Marine Mammals. Volume 4: River Dolphins and the Larger Toothed Whales" (S.H. Ridgway and Sir R. Harrison, Eds.), pp289-308. Academic Press, New York.

Heyning, J. E., and Mead, J. G. (1990). Evolution of the Nasal Anatomy of Cetaceans. *In* "Sensory Abilities of Cetaceans" (J. Thomas and R. Kastelein, Eds.), pp. 67-79. Plenum Press, New York.

Hopkins, K. D., Glass, G. V., and Hopkins, B. R. (1987). Basic Statistics for the Behavioral Sciences, Second Edition. Allyn and Bacon: Boston. pp158-181.

Houser, D. S., Howard, R., Ridgway, S. (2001). Can diving-induced tissue nitrogen supersaturation increase the chance of acoustically driven bubble growth in marine mammals? *Journal of Theoretical Biology* **213**,183-195

Houston, J. (1991). Status of Cuvier beaked-whale, *Ziphius cavirostris*, in Canada. *Canadian Field Naturalist* **105**, 215-218

Jackson, J. E. (1991). A User's Guide to Principal Components. Eds V. Barnett *et al.*. John Wiley & Sons, Inc. New York.

Jensen, F. B., Kuperman, W. A., Porter, M. B. and Schmidt, H. (1994). Computational Ocean Acoustics. American Institute of Physics Press: New York. p71

Jepson, P. D., Arbelo, M., Deaville, R., Patterson, I. A. P., Castro, P., Baker, J. R., Degollada, E., Ross, H. M., Herraez, P., Pocknell, A.M., Rodriguez, F., Howie, F.E., Espinosa, A., Reid, R. J., Jaber, J. R., Martin, V., Cunningham, A. A., and Fernandez, A. (2003). Gas-bubble lesions in stranded cetaceans - Was sonar responsible for a spate of whale deaths after an Atlantic military exercise? *Nature* **425** (6958), 575-576

Kipps, E. K., McLellan ,W. A., Romme, S. A., and Pabst, D. A. (2002). Skin density and its influence on buoyancy in the manatee (*Trichechus manatus latirostris*), harbor porpoise (*Phocoena phocoena*), and bottlenose dolphin (*Tursiops truncatus*) *Marine Mammal Science* **18**, 765-778

Koopman, H. N., Budge, S. M., Ketten, D. R., and Iverson, S. J. (2003a). Sound reception by beaked whales and porpoises: Implications of variation in lipid composition of jaw fats. Abstract from the 17th Conference of the European Cetacean Society. Las Palmas de Gran Canaria. March 2003.

Koopman, H. N., Iverson, S. J., and Read, A. J. (2003b). High concentrations of isovaleric acid in the fats of odontocetes: variation and patterns of accumulation in blubber vs. stability in the melon. *Journal of Comparative Physiology Part B* **173**, 247-261

Lawrence, B., and Schevill, W. E. (1956). The functional anatomy of the Delphinid nose. *Bulletin of the Museum of Comparative Zoology* **114**.

Lees, S. and Rollins, F. R. (1972). Anisotropy in hard dental tissues. *J. Biomechanics* **5,** 557-566.

Leitschuh, P. H., Doherty, T. J., Taylor, D. C., Brooks, D. E., and Ryan, J. B. (1996). Effects of postmortem freezing on tensile failure properties of rabbit extensor digitorum longus muscle tendon complex. *Journal of Orthopaedic Research*. **14,** 830-833.

Litchfield, C., Greenberg, A. J., and Mead, J. G. (1976). The distinctive character of Ziphiidae head and blubber fats. *Cetology* **23**, 1-10.

Litchfield, C., Karol, R., and Greenberg, A. J. (1973). Compositional topography of melon lipids in the Altantic Bottlenosed dolphin *Tursiops truncatus*: Implications for echo-location. *Marine Biology* **23**, 165-169.

Litchfield, C., Karol, R., Mullen, M. E., Dilger, J. P. and Luthi, B. (1979). Physical factors influencing refraction of the echolocative sound beam in delphinid cetaceans. *Marine Biology* **52**, 285-290.

Lok, C. M., and Folkersma, B. (1979). Composition of wax esters and triacylglycerols in the melon and blubber fats of a young Sowerby's whale *Mesoplodon bidens*. *Lipids* **14**, 872-875.

MacLeod, C. D., Santos, M. B., and Pierce, G. J. (2003). Review of data on diets of beaked whales: evidence of niche separation and geographic segregation. *Journal of the Marine Biological Association of the United Kingdom* **83,** 651-665

Madsen, E. L, Sathoff, H. J., and Zagzebski, J. A. (1983). Ultrasonic shear wave properties of soft tissues and tissuelike materials. *Journal of the Acoustical Society of America* **74**, 1346-1355.

Marini L., Consiglio, C., Angradi, A. M., Catalano, B., Sanna, A., Valentini, T., Finoia, M. G., and Villetti, G. (1996). Distribution, abundance and seasonality of cetaceans sighted during scheduled ferry crossings in the central Tyrrhenian Sea: 1989-1992. *Italian Journal of Zoology* **63**, 381-388

Mead, J. (1975). Anatomy of the External Nasal Passages and Facial Complex in the Delphinidae (Mammalia: Cetacea). *Smithsonian Contributions to Zoology* **207**.

Nightingale, K.R., Nightingale, R.W., Palmeri, M.L., and Trahey, G.E. (2000). A finite element model of remote palpation of breast lesions using radiation force: Factors affecting tissue displacement. *Ultrasonic Imaging* **22,** 35-54

Norris, K. S. (1964). *In* “Marine Bioacoustics” (W. Tavolga ed.) Pergamom Press: New York

Norris, K. S. (1968). The evolution of acoustic mechanisms in odontocete cetaceans *In* “Evolution and Environment” (E. T. Drake ed.) pp297-324. Yale University Press, New Haven.

Norris, K. S., and Harvey, G. W. (1974). Sound transmission in the porpoise head. *Journal of the Acoustical Society of America* **56**, 659-664.

O’Brien, W. D. (1977). The relationship between collagen and ultrasonic attenuation and velocity in tissue. *Ultrasonics International* pp 194-205.

Perrin, W. F., Wursig, B., and Thewissen, J. G. M. (2002) Encyclopedia of Marine Mammals. Academic Press: San Diego. 1414pp

Pilson, M. E. Q. (1998). An Introduction to the Chemistry of the Sea. Prentice Hall: Upper Saddle River, NJ. p379.

Robb, R. A. (1998). Three-dimensional Biomedical Imaging: Principles and Practice. John Wiley & Sons, Inc., Publication (Wiley-Liss): New York. pp 42-48.

Santos, M. B., Pierce, G. J., Herman, J., Lopez, A., Guerra, A., Mente, E., and Clarke, M. R. (2001). Feeding ecology of Cuvier's beaked whale (*Ziphius cavirostris*): a review with new information on the diet of this species. *Journal of the Marine Biological Association of the United Kingdom* **81**, 687-694

Schmidt-Nielsen, K. (1995). Animal Physiology: Adaptation and Environment, Ed.4. Cambridge University Press: New York. pp 399-405.

Simmonds, M. P. and Lopez-Jurado, L. F. (1991). Whales and the military. *Nature* **351**, 448-448

Smeathers, J. E. and Joanes, D. N. (1988). Dynamic compressive properties of human lumbar intervertebral joints: A comparison between fresh and thawed specimens. *J. Biomechanics* **21,** 425-433.

Smith, J. A. and Ehman, R. L. (2000). Extraction of propagating waves in cine images from magnetic resonance elastography. *Materials Evaluation* **58**, 1395-1401

Van der Steen, A. F. W., Cuypers, M. H. M., Thijssen, J. M., and de Wilde, P. C. M. (1991). Influence of histochemical preparation on acoustic parameters of liver tissue: A 5-MHz study. *Ultrasound in Medicine and Biology* **17**, 879-891.

Van Ee, C. A., Chasse, A. L. and Meyers, B. S. (2000). Quantifying skeletal muscle properties in cadaveric test specimens: Effects of mechanical loading, postmortem time, and freezer storage. *J Biomech. Eng-T. Asme* **122,** 9-14.

Varanasi, U., Markey, D., and Malins, D. C. (1982). Role of isovaleroyl lipids in channeling of sound in the porpoise melon. *Chemistry and Physics of Lipids* **31**, 237-244.

Waring, G. T., Hamazaki, T., Sheehan, D., Wood, G., and Baker, S. (2001). Characterization of beaked whale (Ziphiidae) and sperm whale (*Physeter macrocephalus*) summer habitat in shelf-edge and deeper waters off the northeast US. *Marine Mammal Science* **17**, 703-717

Woo, S. L. Y., Orlando, C. A., Camp, J. F., and Akeson, W. H. (1986). Effects of postmortem storage by freezing on ligament tensile behavior. *J. Biomechanics* **19,** 399-404.

Tables

Table 1. List of samples used in the physical properties analysis of a *Ziphius cavirostris* neonate head.

Sample Name	Tissue Category	Slice Name	Samples / Slice
Left Dorsal Blubber	Blubber	A – B	1
Left Mandible Acoustic Blubber	Blubber	A – J	1
Left Mandible External Acoustic Fat	Acoustic Fat	A – L	1
Left Mandible Internal Acoustic Fat	Acoustic Fat	A	1
Left Mandible Internal Acoustic Fat	Acoustic Fat	B	2
Left Mandible Internal Acoustic Fat	Acoustic Fat	C	2
Left Mandible Internal Acoustic Fat	Acoustic Fat	D	2
Left Mandible Internal Acoustic Fat	Acoustic Fat	E	4
Left Mandible Internal Acoustic Fat	Acoustic Fat	F	5
Left Mandible Internal Acoustic Fat	Acoustic Fat	G	5
Left Mandible Internal Acoustic Fat	Acoustic Fat	H	6
Left Mandible Internal Acoustic Fat	Acoustic Fat	I	6
Left Mandible Internal Acoustic Fat	Acoustic Fat	J	5
Left Mandible Internal Acoustic Fat	Acoustic Fat	K	7
Forehead	Variable	A	3
Forehead	Variable	B	6
Forehead	Variable	C	9
Forehead	Variable	D	11
Forehead	Variable	E	13
Forehead	Variable	F	17
Forehead	Variable	G	17
Forehead	Variable	H	20
Forehead	Variable	I	23
Forehead	Variable	J	16
Forehead	Variable	K	31
Forehead	Variable	L	20
Forehead	Variable	M	14
Forehead	Variable	N/O	3
Left Nasal Plug	Muscle	O	1
Right Nasal Plug	Muscle	O	2
Tongue	Muscle	A – B	1

Table 2. Results of sound velocity – temperature analysis for various tissue types from the head of a *Ziphius cavirostris* neonate. Slopes and r^2 values of the best fit line are presented.

	Acoustic fat	Blubber - Forehead	Blubber - Mandible	Connective tissue	Melon	Muscle
Slope (m)	-7.113	-4.1655	-4.8081	0.4842	-4.4225	-0.116
r^2	0.946	0.932	0.953	-	0.979	0.080

Table 3. Physical property measurements of *Ziphius cavirostris* forehead tissues by tissue types. Means, standard deviations, minimum and maximum values are presented for sound velocity at 21°C, calculated sound velocity at 37°C, sound attenuation, density and CT scan Hounsfield units.

	Blubber N = 36	Melon N = 66	Muscle N = 13	Connective Tissue N = 30
Sound Velocity at 37°C (m/s)				
Mean	1401	1382	1517	1628
St Dev.	± 7.8	± 23.0	± 46.8	± 48.7
Min	1382	1341	1460	1538
Max	1422	1409	1592	1708
Sound Velocity at 21°C (m/s)				
Mean	1465	1450	1522	1620
St Dev.	± 8.3	± 17.6	± 47.2	± 48.7
Min	1446	1412	1461	1531
Max	1489	1483	1594	1700
Sound Attenuation (dB/mm) at 10 MHz				
Mean	1.1	1.0	1.9	2.6
St Dev.	± 0.4	± 0.5	± 0.7	± 0.7
Min	0.5	0.4	0.7	0.4
Max	2.1	2.4	2.9	3.5
Density (kg/m^3)				
Mean	935	937	993	1087
St Dev.	± 25	± 17	± 58	± 41
Min	882	908	909	1007
Max	986	987	1066	1175
Hounsfield Unit				
Mean	-83.7	-81.0	-33.3	44.8
St Dev.	± 15	± 12	± 23	± 45
Min	-106.2	-96.2	-61.3	-35.6
Max	-46.3	-47.2	1.8	108.6

Table 4. Results of Student's t-tests examining differences between physical properties of tissue types in the forehead of a *Ziphius cavirostris* neonate. * significantly different at alpha - 0.05
**** significantly different for alpha = 0.1**

	Blubber/ Connective Tissue	Blubber/ Melon	Blubber/ Muscle	Connective Tissue / Melon	Connective Tissue/ Muscle	Melon/ Muscle
Velocity						
t	-27.62 *	4.59 *	-14.58 *	33.65 *	6.74 *	-15.44 *
n1	36	36	36	30	30	66
n2	30	66	12	66	12	12
Attenuation						
t	-2.01 **	0.09	-0.81	2.44 *	0.71	-0.93
n1	36	36	36	30	30	66
n2	30	66	13	66	13	13
Density						
t	-18.50 *	-0.66	-5.00 *	24.69 *	6.04 *	-6.52 *
n1	36	36	36	30	30	62
n2	30	62	13	62	13	13
Hounsfield						
t	-15.50 *	-1.09	-8.70 *	21.05 *	5.83 *	-11.11 *
n1	34	34	34	29	29	66
n2	29	66	13	66	13	13
YM 2500						
t	-2.50 *	-0.24	-0.67	2.62 *	0.83	-0.54
n1	17	17	17	18	18	21
n2	18	21	3	21	3	3
YM 5000						
t	3.28 *	5.25 *	3.73 *	0.61	1.72	1.89 **
n1	36	36	36	30	30	65
n2	30	65	13	65	13	13
YM 10000						
t	4.98 *	11.82 *	8.88 *	4.53 *	4.72 *	2.69 *
n1	36	36	36	30	30	65
n2	30	65	13	65	13	13
YM 20000						
t	2.15 *	9.71 *	6.02 *	6.27 *	4.14 *	0.72
n1	36	36	36	29	29	65
n2	29	65	12	65	12	12
YM 30000						
t	0.60	8.42 *	7.64 *	6.92 *	6.52 *	2.38 *
n1	36	36	36	29	29	60
n2	29	60	12	60	12	12
YM 40000						
t	-1.27	8.61 *	6.84 *	7.91 *	5.09 *	1.60
n1	36	36	36	28	28	56
n2	28	56	8	56	8	8
YM 50000						
t	-1.32	7.11 *	3.78 *	7.02 *	3.32 *	0.45
n1	28	56	8	56	8	8
n2	26	50	6	50	6	6

**Table 5. Results of single-sample t-tests examining differences between physical property values of tissue types and water. Physical property values of water were: 1) sound velocity - 1507 m/s; 2) density - 1026 kg/cm3; 3) Hounsfield units - 0. * significantly different at alpha = 0.05
** significantly different at alpha = 0.1**

	Forehead Tissues								Mandibular Tissues			
	Melon		Blubber		Muscle		Connective Tissue		Acoustic Fat		Blubber	
Velocity												
n	66		36		12		30		44		11	
t	-44.05	*	-81.86	*	0.72		13.59	*	-98.81	*	-33.36	*
Density												
n	62		36		13		30		43		10	
t	-40.77	*	-21.79	*	-2.03	**	8.13	*	-38.31	*	-26.41	*
Hounsfield Unit												
n	66		34		13		29		45		11	
t	-56.81	*	-32.13	*	-5.15	*	5.30	*	-19.32	*	-96.23	*

Table 6. Physical property measurements of *Ziphius cavirostris* mandibular region tissues by tissue types. Means, standard deviations, minimum and maximum values are presented for sound velocity at 21°C and 37°C, sound attenuation, density and CT scan Hounsfield units.

	Blubber N = 11	**Acoustic Fats N = 44**
Sound Velocity at 37°C (m/s)		
Mean	1376	1350
St Dev.	± 13.0	± 10.6
Min	1345	1331
Max	1394	1378
Sound Velocity at 21°C (m/s)		
Mean	1453	1460
St Dev.	± 8.8	± 10.6
Min	1441	1442
Max	1468	1488
Sound Attenuation (DB/mm) at 10 MHz		
Mean	0.8	0.8
St Dev.	± 0.5	± 0.2
Min	0.2	0.5
Max	2.0	1.1
Density (kg/m^3)		
Mean	919	890
St Dev.	± 13	± 23
Min	901	854
Max	937	941
Hounsfield Unit		
Mean	-101.9	-77.7
St Dev.	± 3	± 27
Min	-106.5	-106.2
Max	-95.2	-65.3

Table 7. Results of Student's t-tests examining differences between physical properties of tissue types in the mandibular region of a *Ziphius cavirostris* neonate. * significantly different at alpha - 0.05.

	Acoustic fat/ Blubber	
Velocity		
t	-7.03	*
n1	44	
n2	11	
Attenuation		
t	-0.11	
n1	44	
n2	9	
Density		
t	-3.81	*
n1	43	
n2	10	
Hounsfield		
t	2.95	*
n1	45	
n2	11	
YM 2500		
t	-1.57	
n1	7	
n2	3	
YM 5000		
t	-0.19	
n1	40	
n2	11	
YM 10000		
t	-2.48	*
n1	44	
n2	11	
YM 20000		
t	-4.99	*
n1	44	
n2	11	
YM 30000		
t	-4.76	*
n1	41	
n2	11	
YM 40000		
t	-3.53	*
n1	37	
n2	11	
YM 50000		
t	-2.68	*
n1	29	
n2	11	

Table 8. Results of paired t-tests testing for differences between forehead and mandibular regions. * significant at alpha = 0.05.

	Blubber		Melon/acoustic fat	
Velocity				
t	0.03		-0.05	
n1	36		66	
n2	11		44	
Attenuation				
t	2.44	*	2.73	*
n1	36		66	
n2	9		44	
Density				
t	1.85		12.02	*
n1	36		62	
n2	10		43	
Hounsfield				
t	3.92	*	-0.82	
n1	34		66	
n2	11		45	
YM 2500				
t	-2.84		0.08	
n1	17		21	
n2	3		7	
YM 5000				
t	0.26		-4.14	*
n1	36		65	
n2	11		40	
YM 10000				
t	0.65		-3.98	*
n1	36		65	
n2	11		44	
YM 20000				
t	1.45		0.64	
n1	36		65	
n2	11		44	
YM 30000				
t	1.39		1.46	
n1	36		60	
n2	11		41	
YM 40000				
t	3.11	*	0.93	
n1	36		56	
n2	11		37	
YM 50000				
t	2.34	*	0.13	
n1	35		50	
n2	11		29	

Table 9. T-values from paired t-tests testing for anisotropy in sound velocity between orientations for *Ziphius cavirostris* tissues. * significant at alpha = 0.05 ** significant at alpha = 0.1 Orientations: AP = Anterior – Posterior, DV = Dorsal – Ventral, LR = Left – Right

	AP-DV		AP - LR		DV-LR	
All Tissues n = 196	1.77	*	2.59	**	0.66	
Forehead Tissues n = 141	1.20		2.58	*	1.01	
Mandibular Tissues n = 54	2.71	*	0.45		-1.71	**
All Acoustic Fats/Melon n = 105	2.40	*	1.33		-0.41	
Acoustic Fat n = 41	2.45	*	1.53		-0.47	
Melon n = 64	0.82		0.36		-0.13	
All Blubber n = 45	-0.08		-2.60	*	-2.26	*
Forehead Blubber n = 35	-0.69		-1.71	**	-1.08	
Mandibular Blubber n = 10	1.18		-2.16	*	-2.50	*
Connective Tissue n = 30	1.19		3.47	*	1.27	
Muscle n = 15	0.34		-0.37		-0.45	

Table 10. Elastic modulus (kPa) at selected stresses in the various tissue types of the forehead and mandible of a *Ziphius cavirostris* neonate.

	Forehead Tissues			Mandible Tissues	
Stress (kPa)	Blubber	Melon	Connective Tissue	Blubber	Acoustic Fat
5	208	153	149	220	215
10	411	212	279	400	303
20	712	412	618	650	420
30	1006	626	1030	913	587
40	1200	739	1295	991	726
50	1410	910	1510	1174	934

Table 11. Results of physical property measurements for tissue samples from a *Ziphius cavirostris* neonate. Means and standard deviations are presented for sound velocity at 22°C, calculated sound velocity at 37°C, sound attenuation and density. For each sample type, n=1 unless otherwise noted.

			Sound Velocity at 22°C (m/s)		Sound Velocity at 37°C (m/s)		Sound Attenuation (dB/mm)		Density (kg/m^3)	
Section	Sample type		Mean	St. Dev.	Mean	St. Dev.	Mean	St. Dev.	Mean	St. Dev.
Head										
	Blubber	n=3	1463	20.1	1401	±20.1	0.9	0.8	940	±48
	Left Nasal Plug		1648	-	-	-	0.9	-	1119	-
	Right Nasal Plug	n=2	1652	±10.6	-	-	1.5	0.4	1117	±13
	Thyroid cartilage		1578	-	-	-	3.8	-	1088	-
	Tongue		1592	-	-	-	0.6	-	-	-
Chest										
	Blubber	n=6	1462	3.7	1399	±3.7	0.8	0.2	927	±8
	Muscle	n=3	1591	±1.8	1589	±1.6	1.0	0.3	1108	±39
	Diaphram		1585	-	-	-	1.1	-	1175	-
	Esophagus		1613	-	-	-	1.1	-	1087	-
	Heart - Atrium		1578	-	-	-	1.6	-	1079	-
	Heart - Ventrical		1561	-	-	-	1.1	-	1087	-
	Lung - left		1612	-	-	-	0.6	-	1147	-
	Lung - right		1552	-	-	-	11.9	-	963	-
	Liver		1585	-	-	-	1.5	-	1064	-
	Trachea		1629	-	-	-	2.7	-	1097	-
Abdomen										
	Blubber	n=3	1480	3.3	1418	±3.3	0.8	0.1	917	-
	Muscle	n=4	1596	±5.0	1592	±3.0	0.5	0.2	1068	-
Tail										
	Blubber	n=12	1469	12.0	1407	±12.0	0.8	0.4	933	±25
	Muscle	n=10	1600	±7.5	1598	±7.4	0.9	0.2	1046	±78

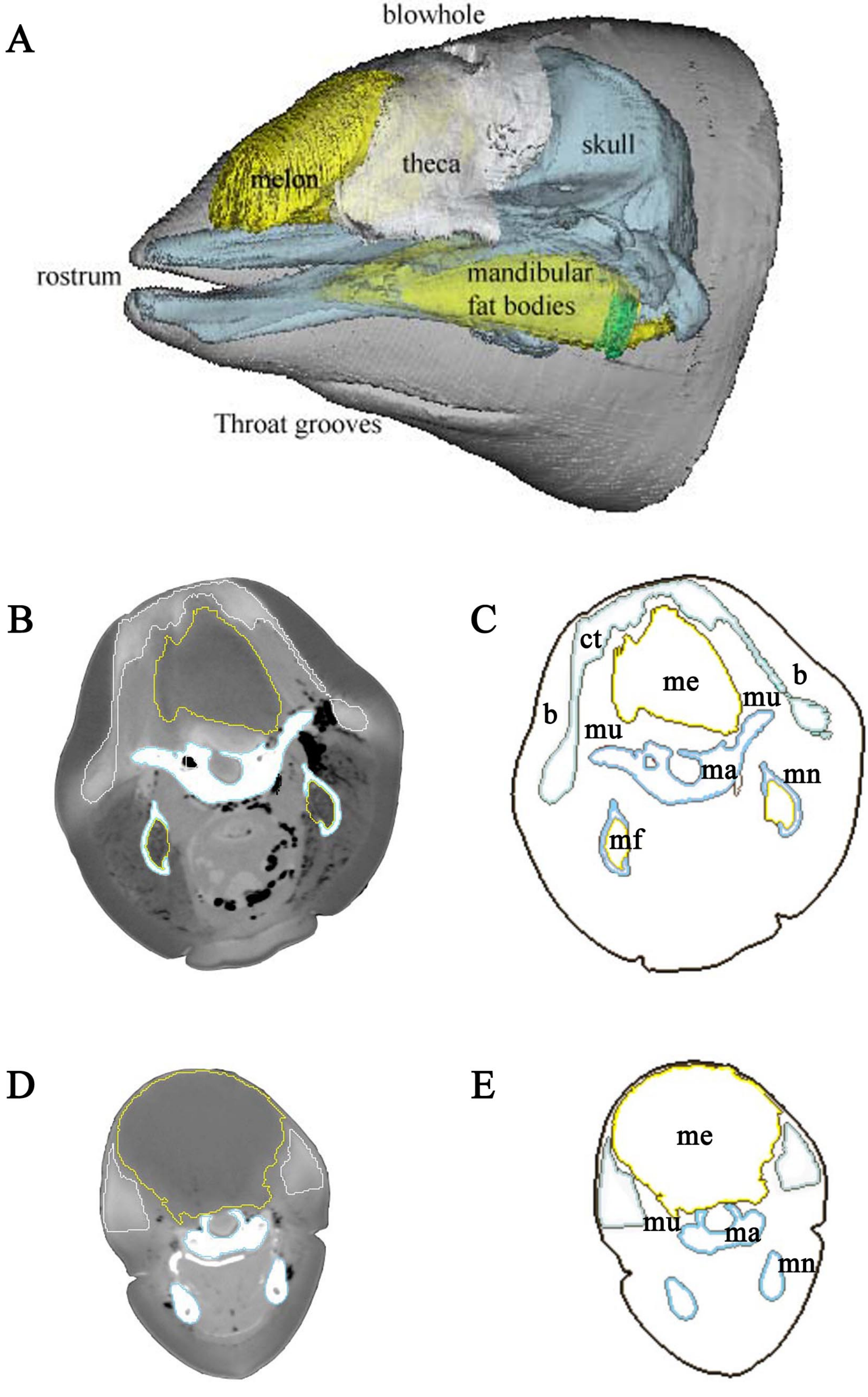
A
blowhole
skull
theca
melon
rostrum
mandibular
fat bodies
Throat grooves
B
C
ct
me
b
mu
b
mu
ma
mn
mf
D
E
me
mu
ma
mn

Figure 1. A) Reconstructed computer image of a neonate *Z. cavirostris* head. Dark grey areas show the outer skin layer. The light blue region is bone, i.e. the skull and mandible. The white area is the connective tissue theca that encompasses the melon, seen in yellow. Mandibular fat bodies are also shown in yellow. Colorized CT scans of transverse slices through B) a posterior region and D) an anterior region of the head. C) and E) represent line drawings of the scans to diagram body parts. b is blubber; ct is connective tissue; me is melon; mu is muscle; ma is the maxilla; mn is the mandibular bones; mf is mandibular fat. Only interior mandibular fat is represented in these images.

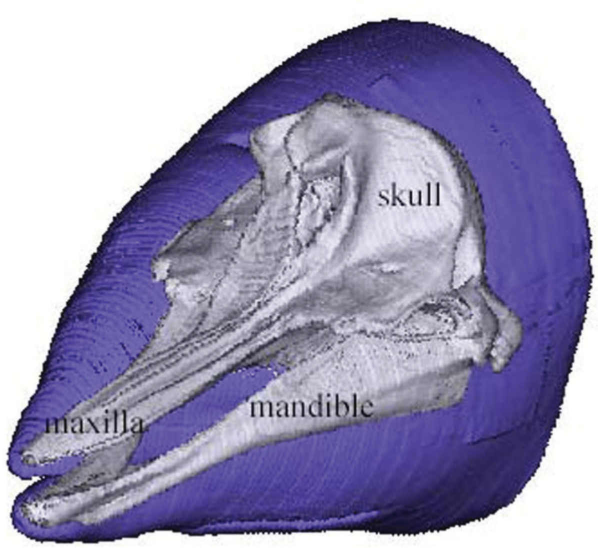

Figure 2. *Ziphius cavirostris* skull. The concave skull basin where the melon is located is readily apparent. The hollowed mandibles which house the acoustic fats that are important in sound reception are also noted.

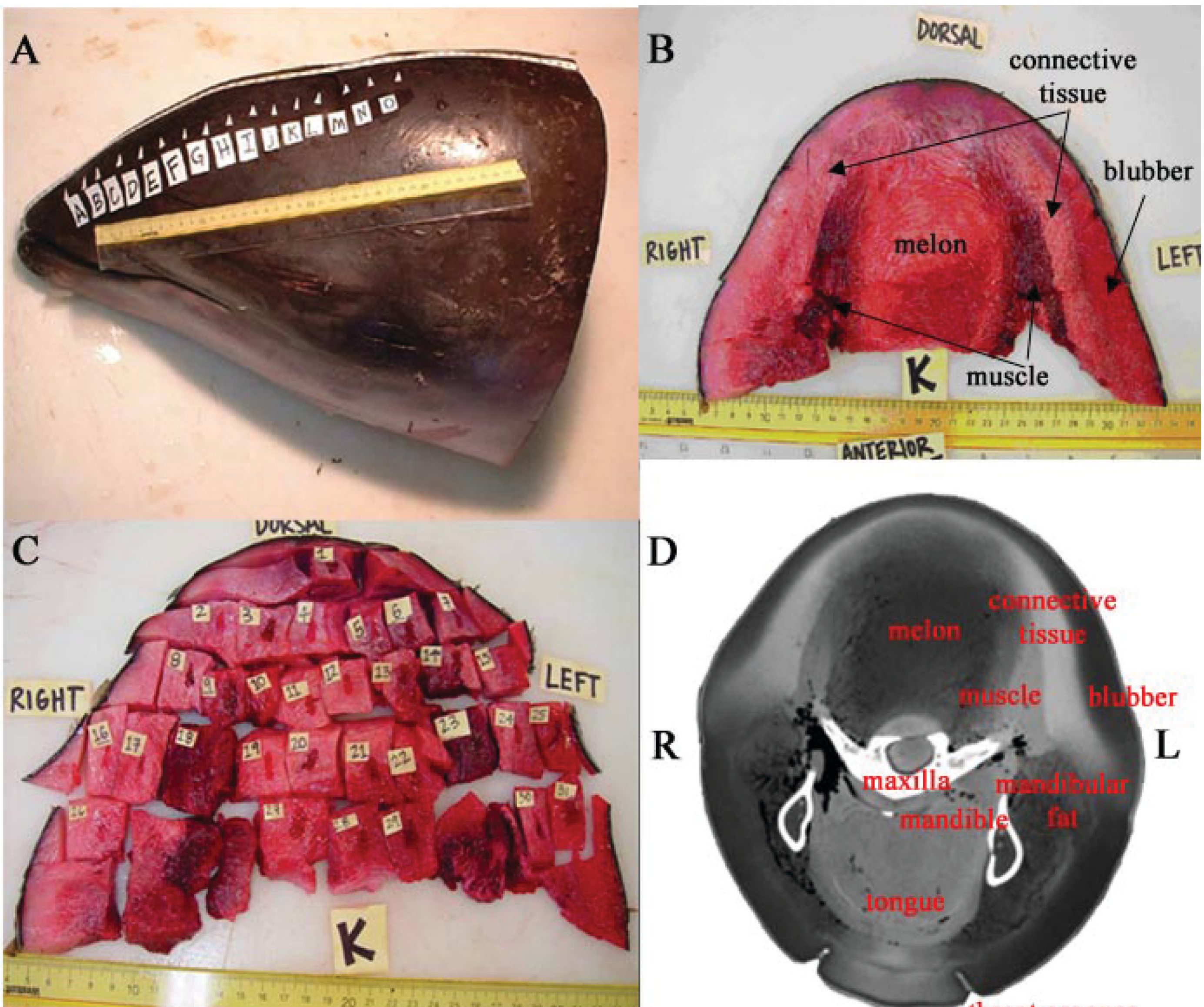

Figure 3. A) Head of a neonate *Z. cavirostris*. Arrows point to transverse slices that were taken through the melon B) Anterior side of a transverse slice through the melon, which corresponds to slice K, from previous picture. Skin, blubber, connective tissue, muscle and melon tissues are noted. C) Transverse melon slice K showing grid like sampling of tissues into cubes for further analysis. D) Transverse CT image of slice K. Maxillary and mandibular bones are visible as bright white areas. Between these is the tongue. A blubber sheath can be seen surrounding the animal. The connective tissue, muscle and melon fats can be discerned in the upper portion of the figure. Interior and exterior mandibular fats can be seen inside of and around the mandibular bones. Throat grooves are also visible.

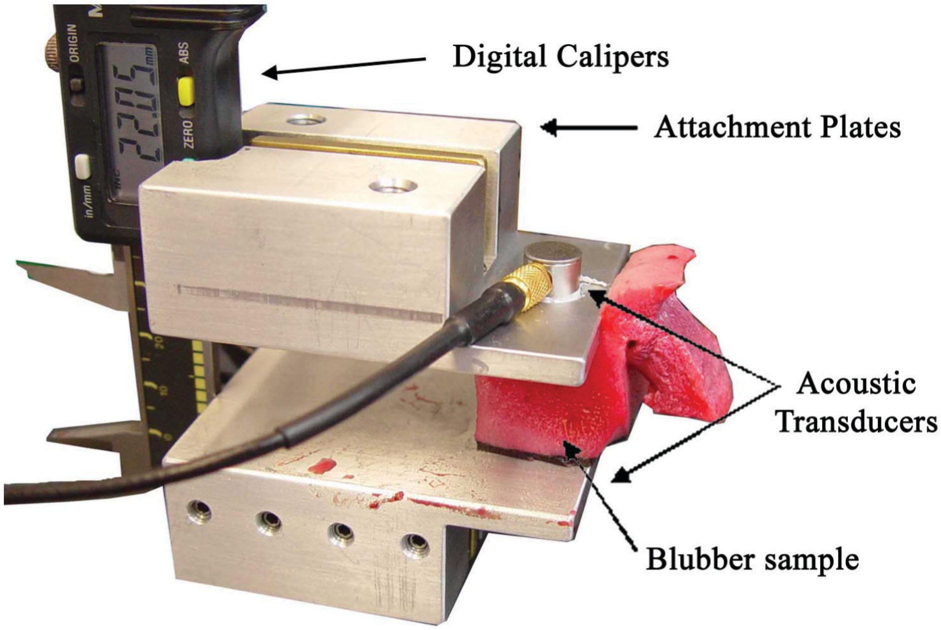

Figure 4. Photo of instrument combining digital calipers with metal plates enclosing the acoustic transducers that were used for the sound velocity and attenuation measurements of *Z. cavirostris* tissues. A sample of blubber can be seen in the instrument.

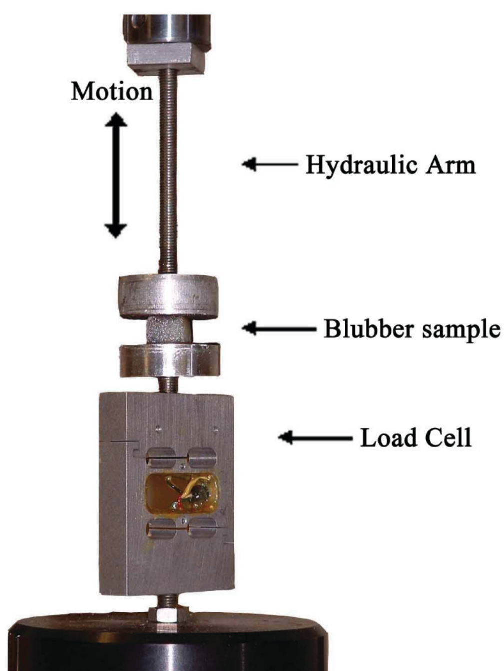

Figure 5. Instrument used for biomechanical compression. Hydraulic arm is visible on top, with a blubber sample centered in middle. Load cell below measures force.

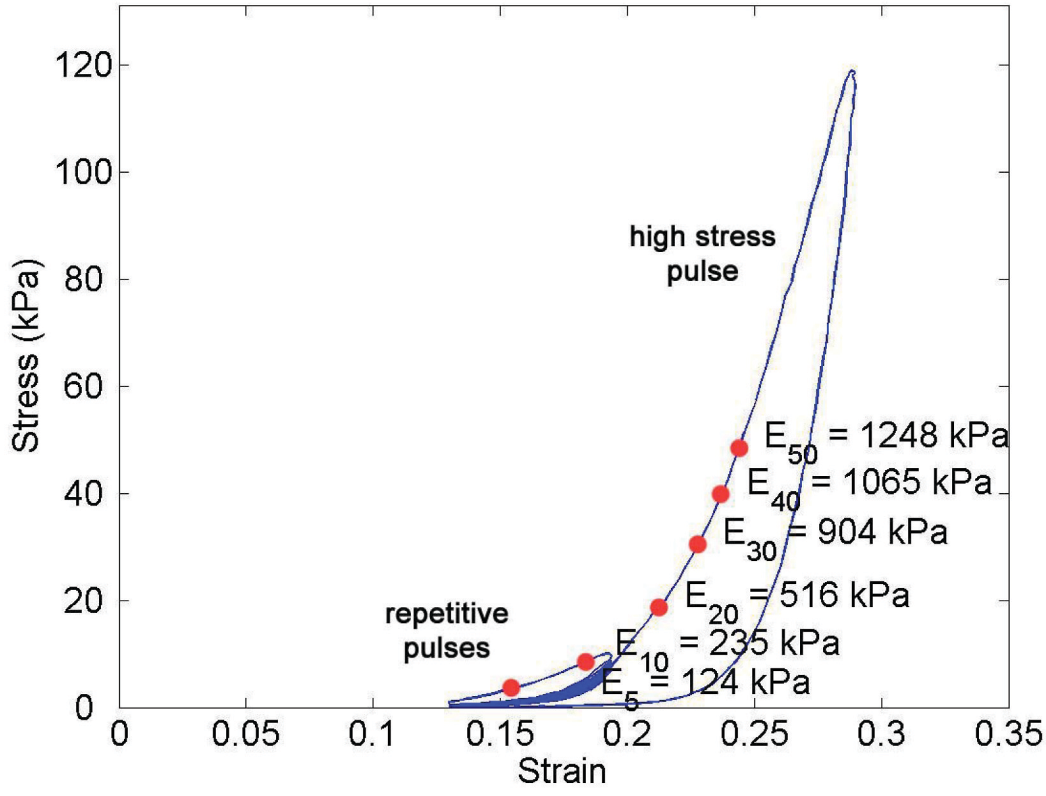

Figure 6. Stress-Strain curve for a sample of *Ziphius cavirostris* forehead blubber. The ten low stress pulses are visible at the low end of the curve, while larger curve represents the single high stress pulse.

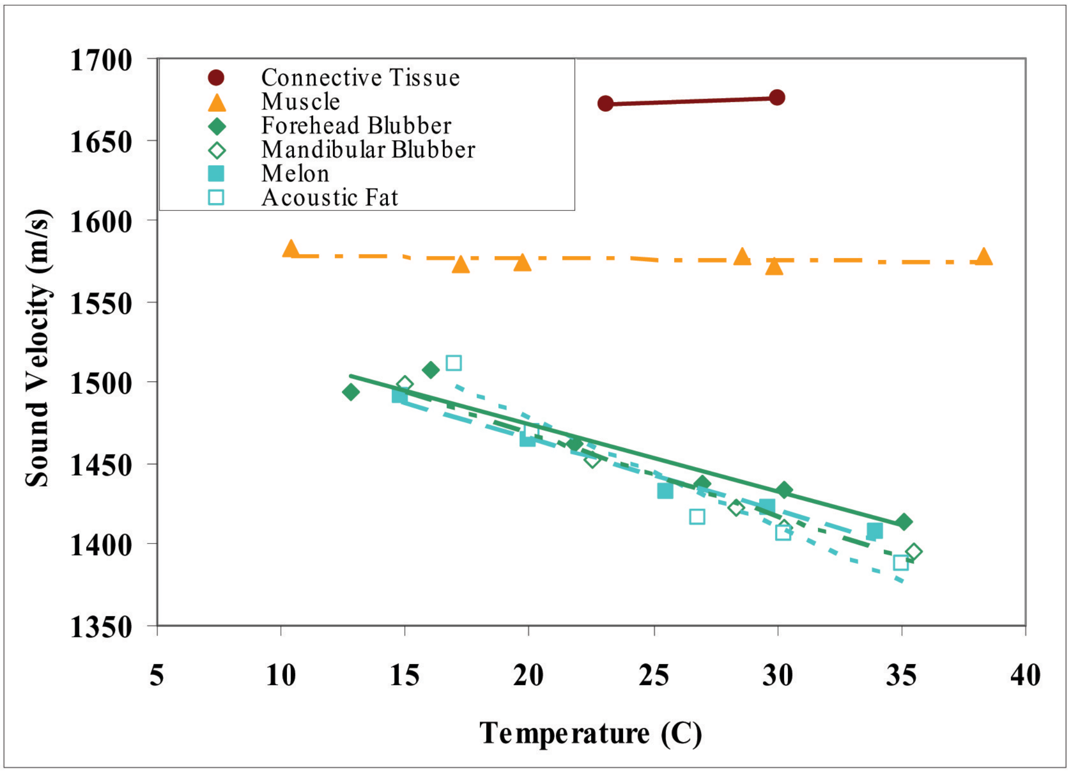

Figure 7. Sound velocity versus temperature from *Ziphius cavirostris* head tissues.

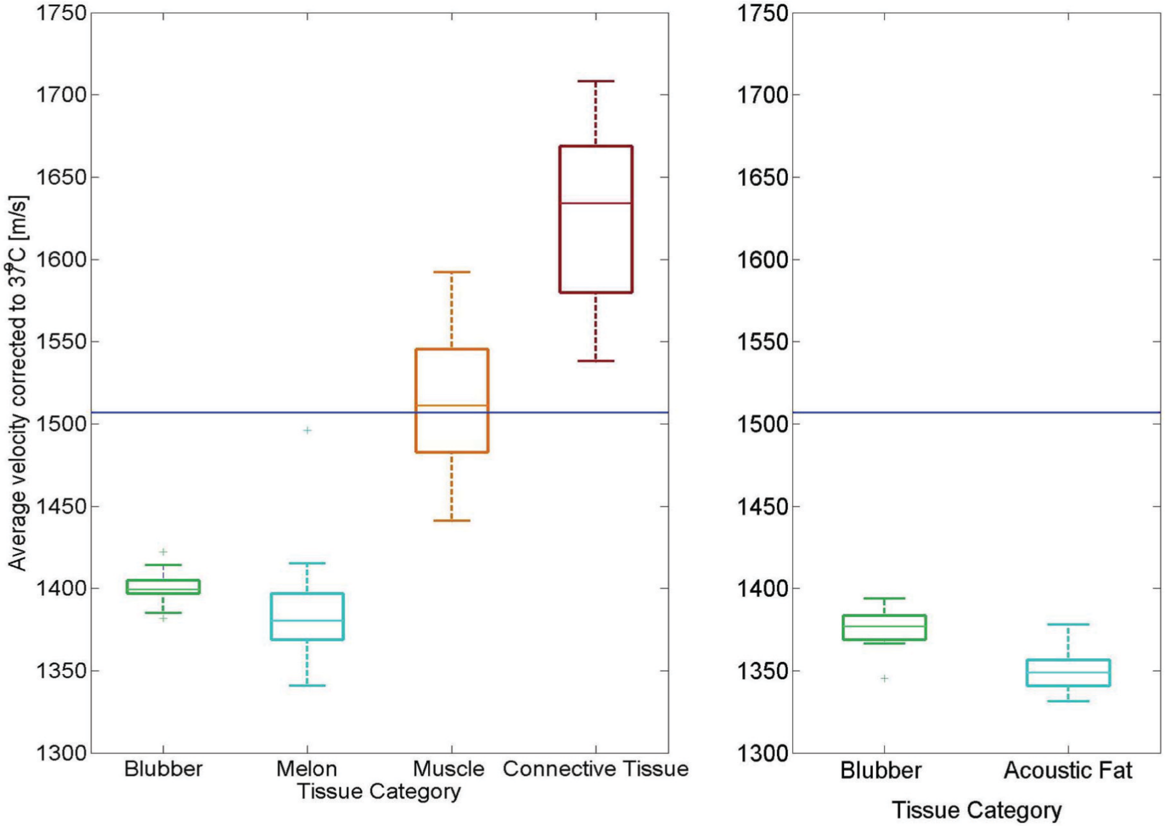

Figure 8. Box and whisker plots of sound velocity corrected to 37°C for various tissue types in the (a) forehead and (b) mandible. The lines of the boxes represent the lower quartile, median, and upper quartile values. The whiskers extending from each end of the box show the extent of the rest of the data. Outliers are represented by +'s beyond the whiskers. The dark blue line at 1507 m/s represents the sound velocity of seawater at 15°C and 1atm.

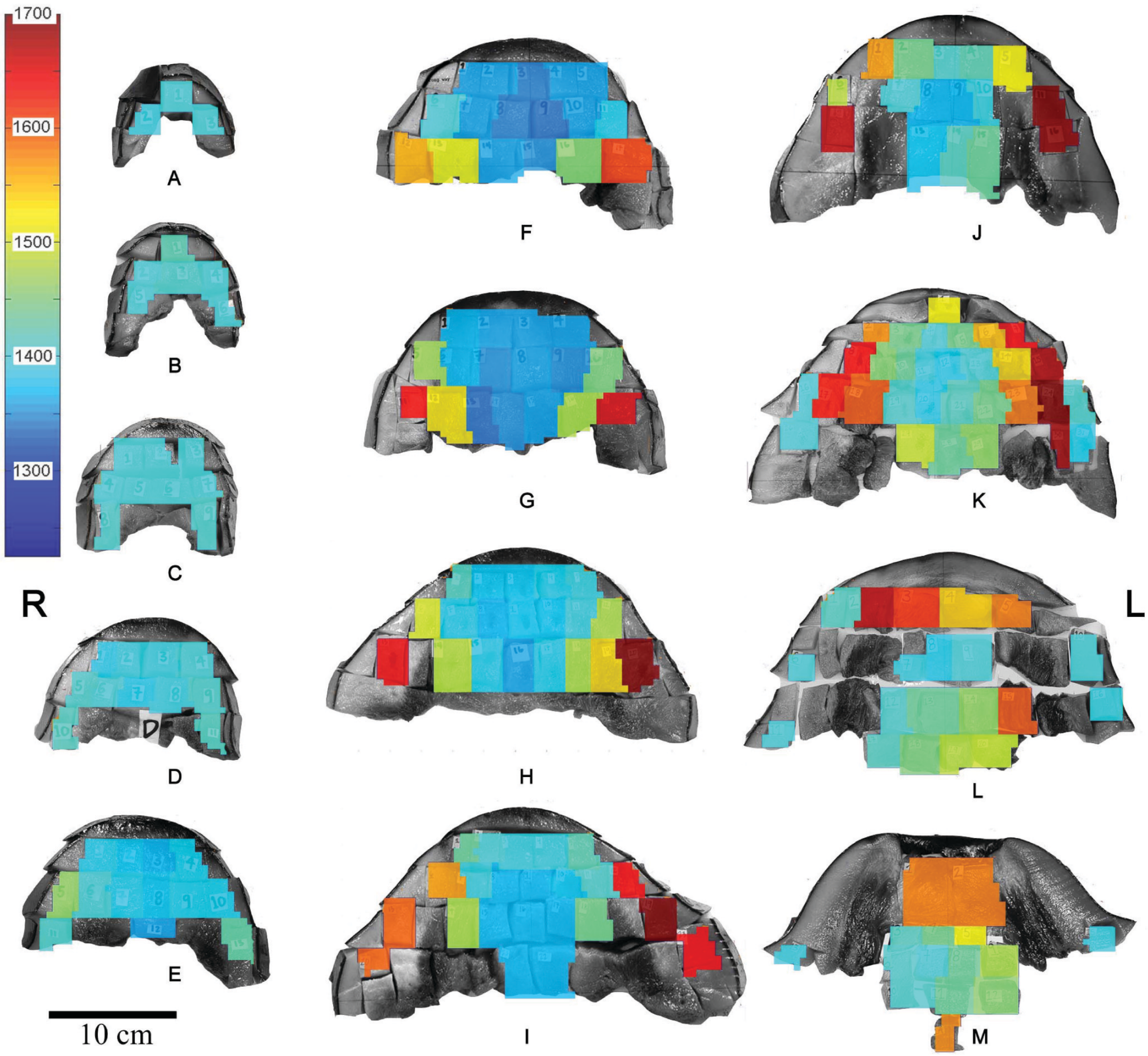

Figure 9. Sound velocity changes through 13 transverse slices of *Ziphius cavirostris* melon. Slices N and O are not shown in this analysis since they encompass the nasal plugs. The figures show the anterior face with dorsal side up. The animal's right and left are as shown in figure. The color bar scale shows sound velocity values (m/s) for each color.

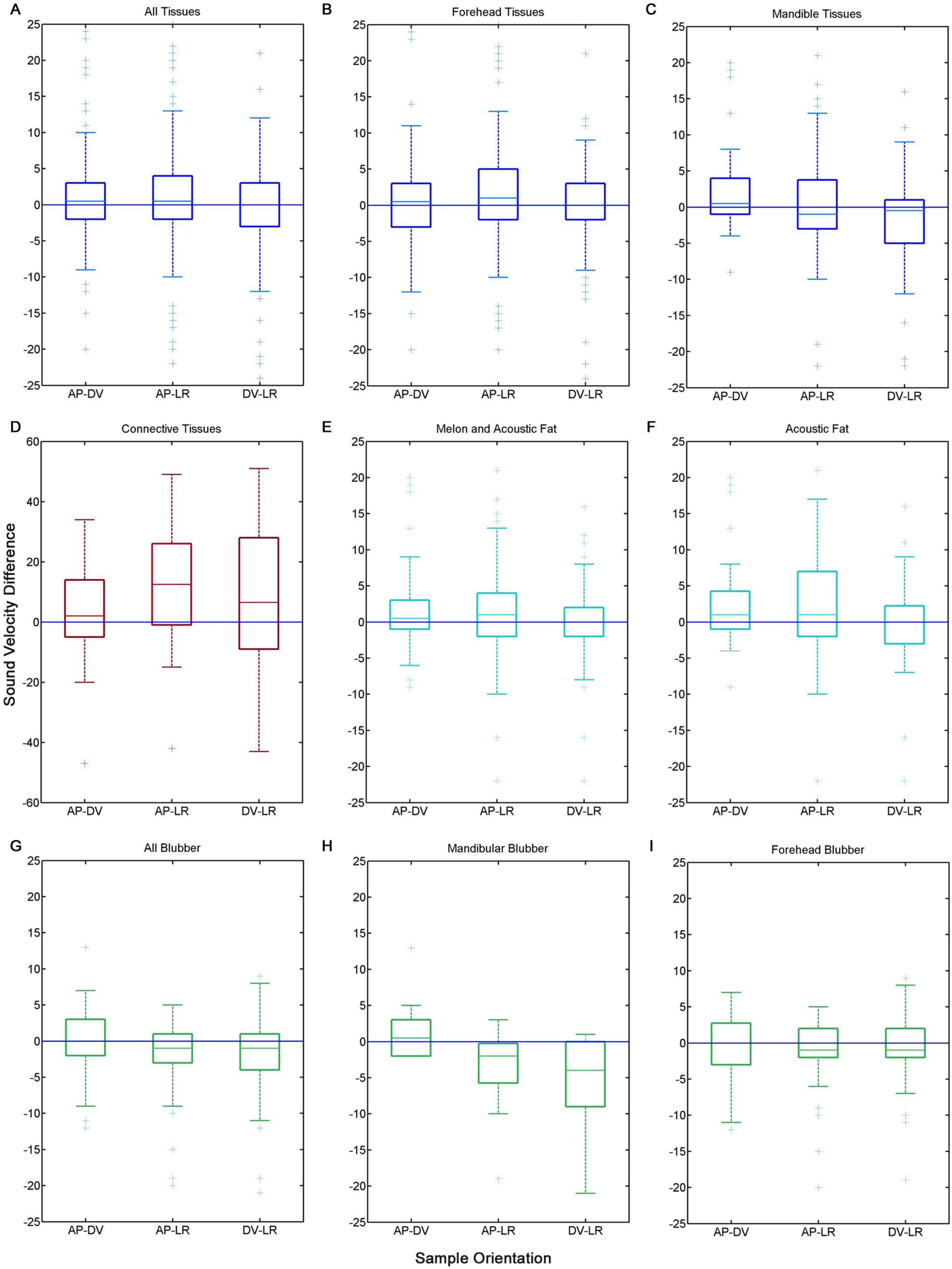
A
All Tissues
B
Forehead Tissues
C
Mandible Tissues
D
Connective Tissues
E
Melon and Acoustic Fat
F
Acoustic Fat
G
All Blubber
H
Mandibular Blubber
I
Forehead Blubber
AP-DV
AP-LR
DV-LR
Sound Velocity Difference
Sample Orientation

Figure 10. Box and whisker plots of sound velocity anisotropy for different groups of tissue types. a) All tissues, b) All Forehead tissues, c) All Mandibular tissues, d) Connective tissues, e) Acoustic fats and Melon, f) Mandibular acoustic fats, g) All blubber tissues, h) Mandibular blubber tissues, i) Forehead blubber tissues. Note the difference in scale for connective tissues.

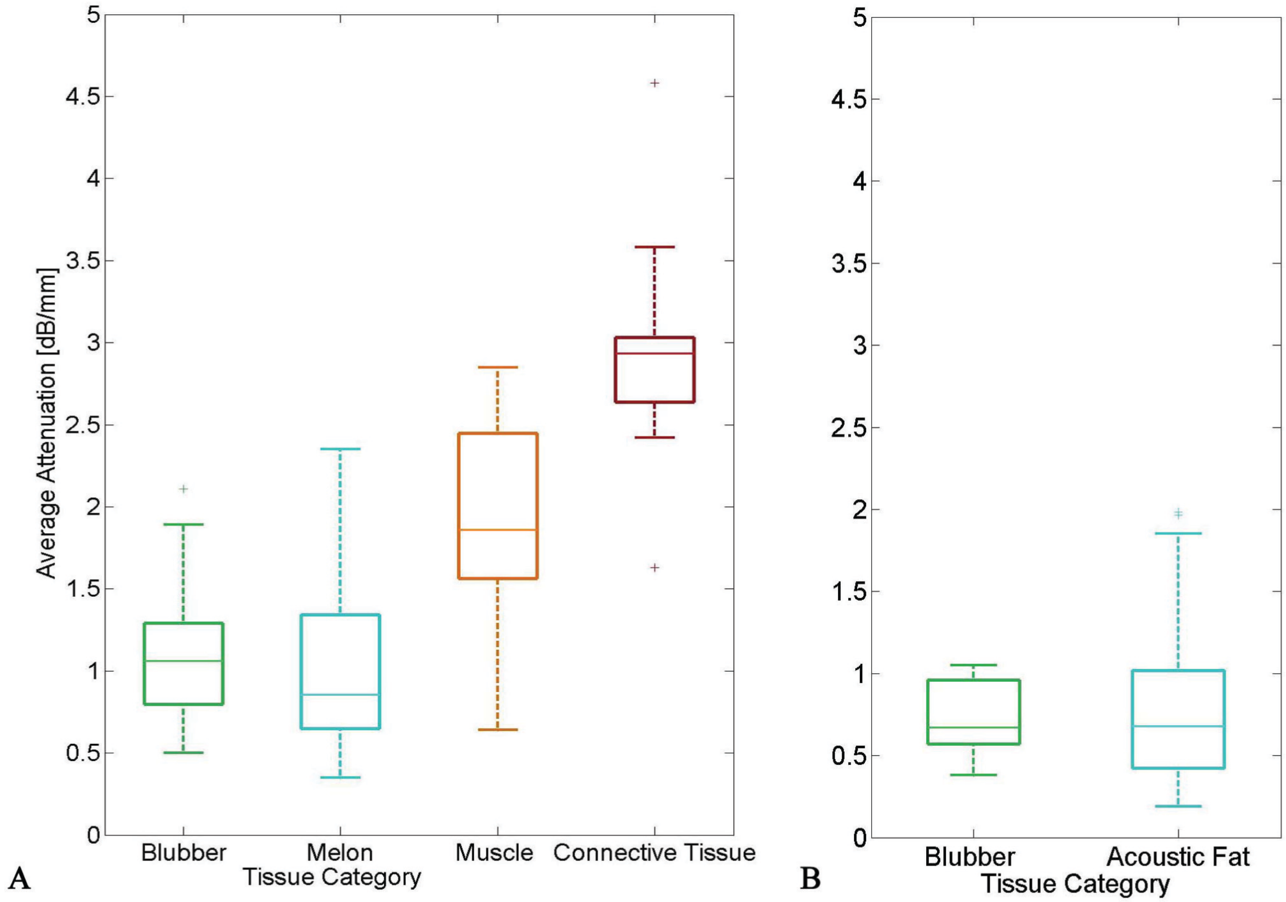

Figure 11. Box and whisker plots of sound attenuation for various tissue types in the (a) forehead and (b) mandible. The lines of the boxes represent the lower quartile, median, and upper quartile values. The whiskers extending from each end of the box show the extent of the rest of the data. Outliers are represented by +'s beyond the whiskers.

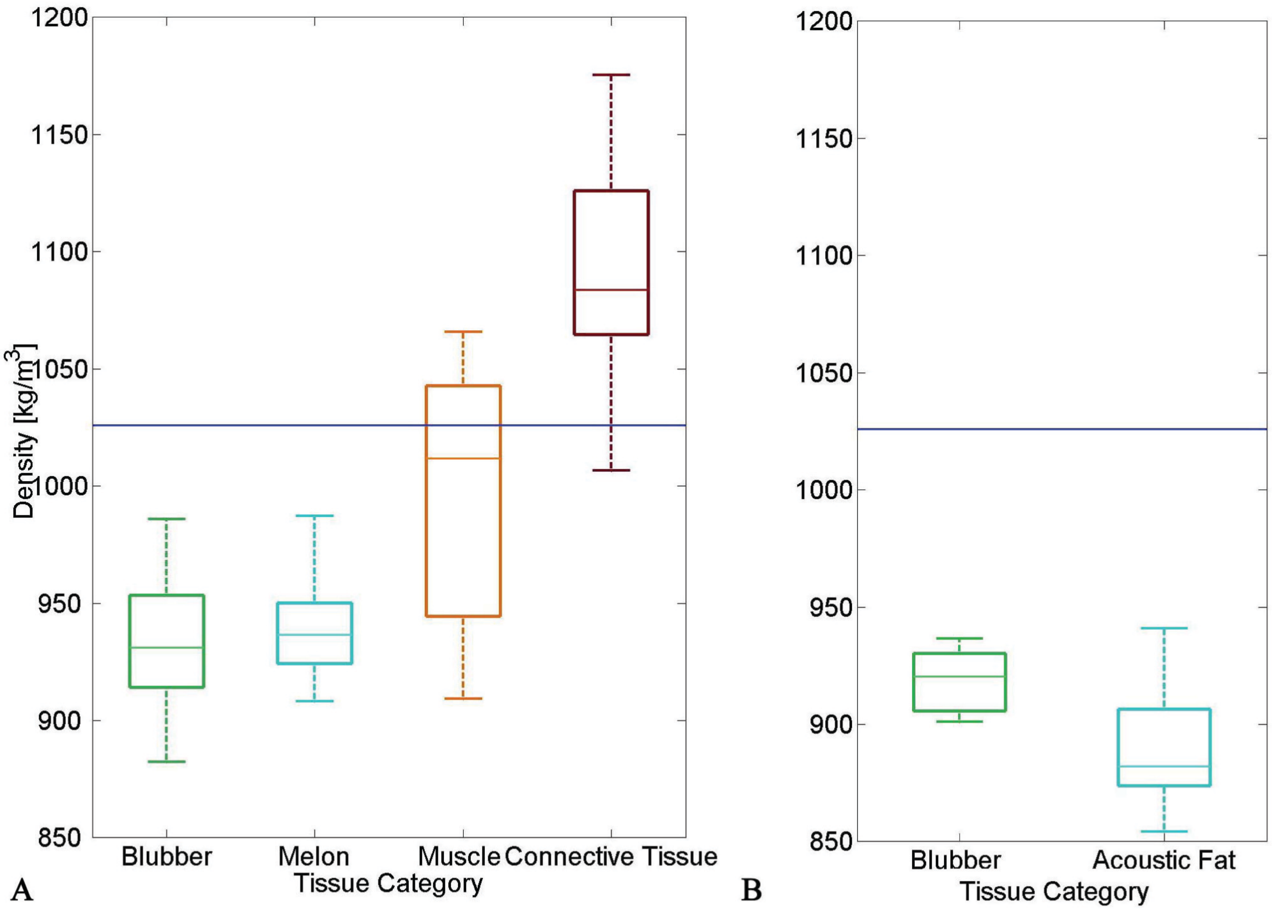

Figure 12. Box and whisker plots of mass density for various tissue types in the (a) forehead and (b) mandible. The lines of the boxes represent the lower quartile, median, and upper quartile values. The whiskers extending from each end of the box show the extent of the rest of the data. Outliers are represented by +'s beyond the whiskers. The dark blue line at 1026 kg/m^3 represents the density of seawater at 15^{o}C and 1atm.

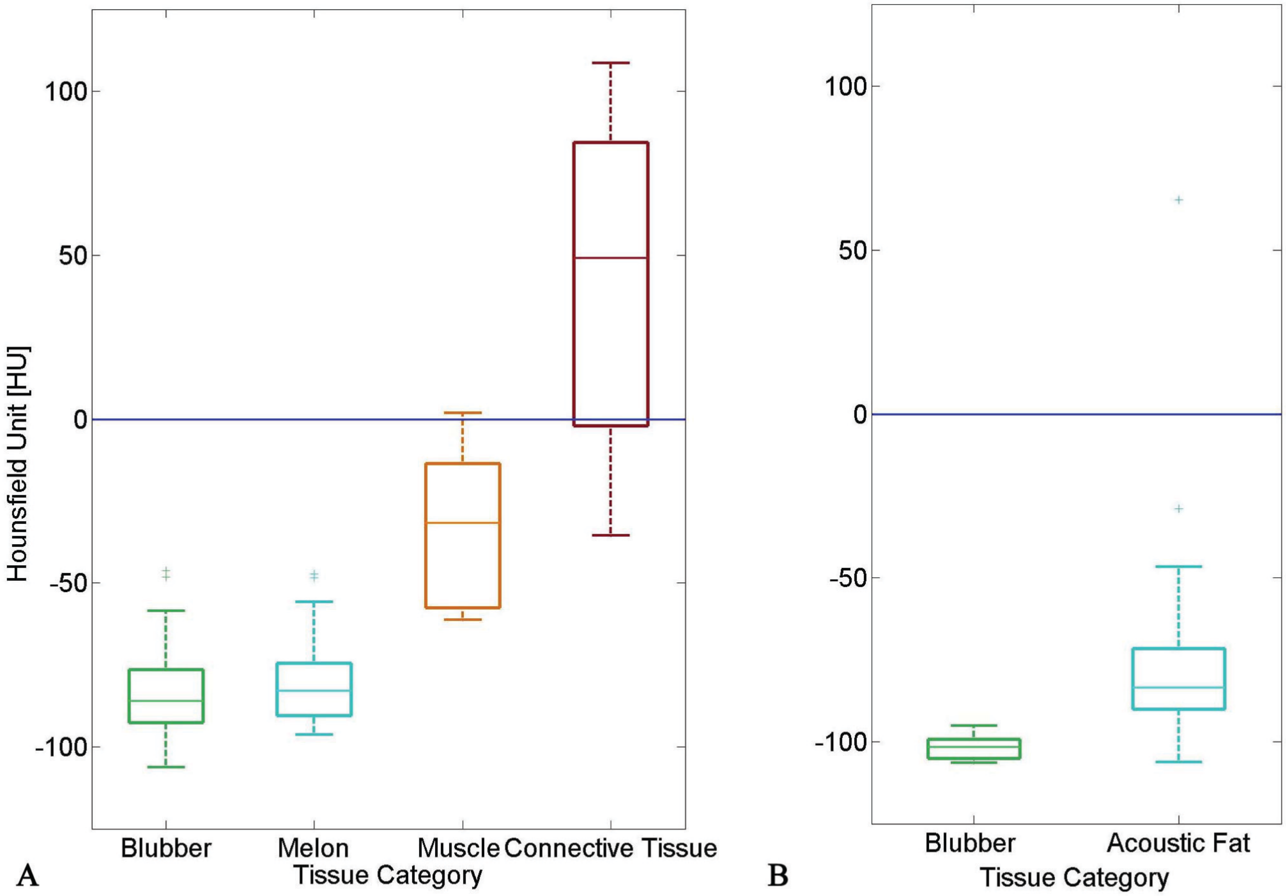

Figure 13. Box and whisker plots of CT scan Hounsfield Units for various tissue types in the (a) forehead and (b) mandible. The lines of the boxes represent the lower quartile, median, and upper quartile values. The whiskers extending from each end of the box show the extent of the rest of the data. Outliers are represented by +'s beyond the whiskers. The dark blue line at 0 represents the value of water.

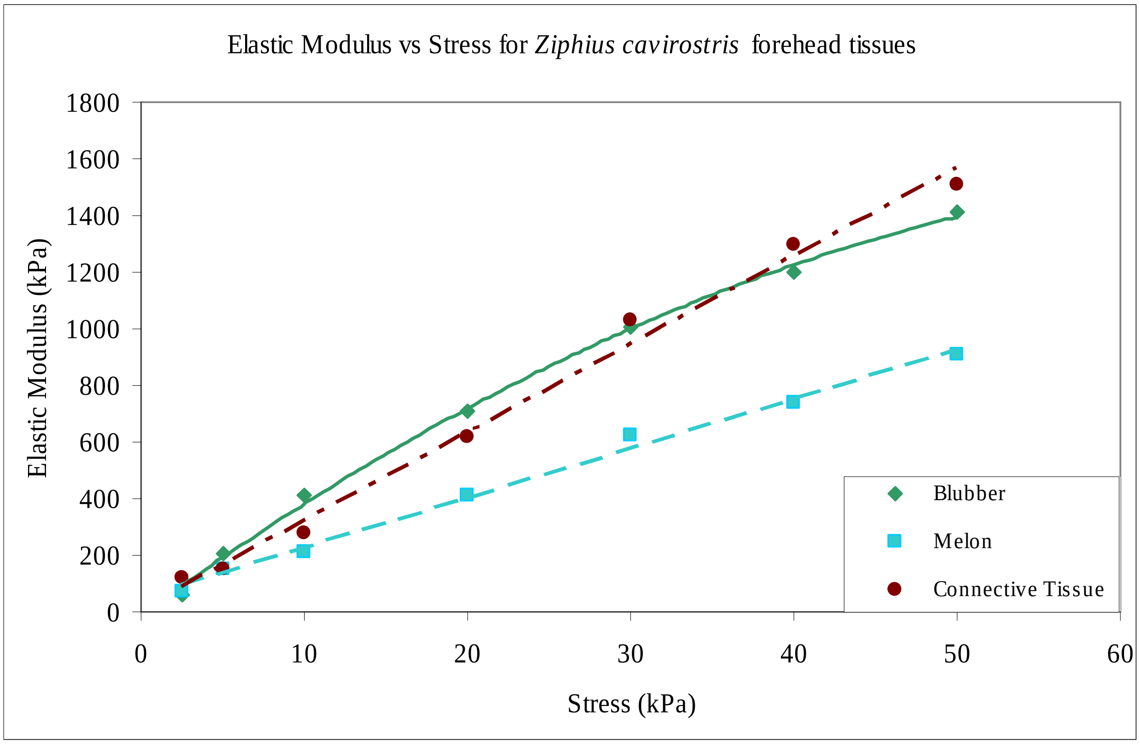

Figure 14. Elastic modulus versus stress for tissues from a *Ziphius cavirostris* forehead. Blubber, melon and connective tissues are plotted. Note that values have been averaged across three orientations (anterior-posterior, dorsal-ventral, lateral).

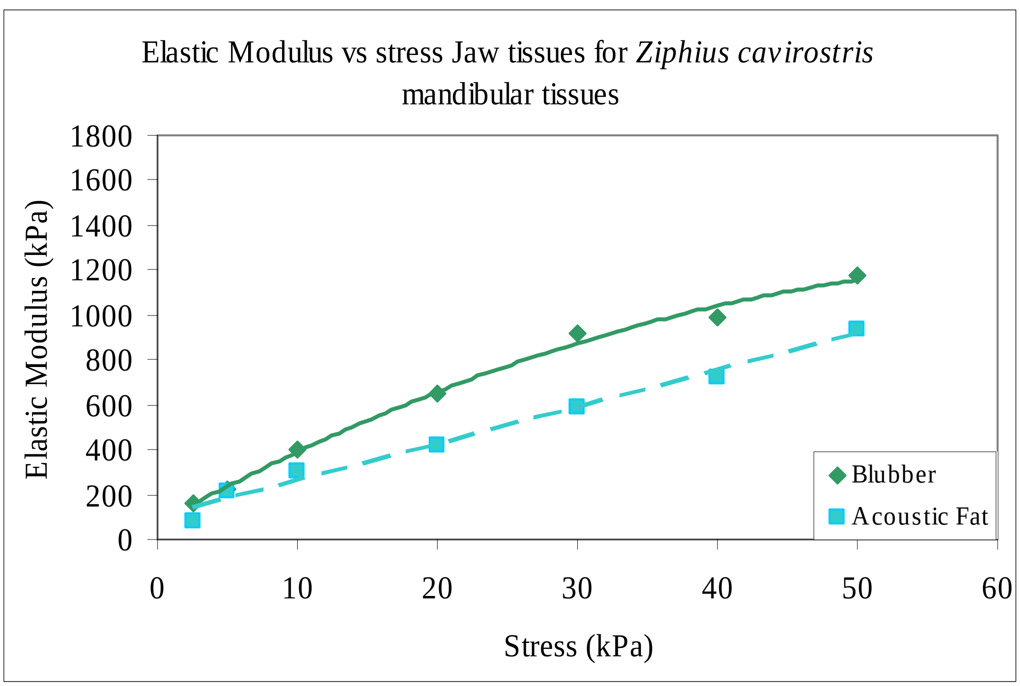

Figure 15. Elastic modulus versus stress for tissues from a *Ziphius cavirostris* mandible. Blubber and melon tissues are plotted. Note that the values have been averaged across three orientations (anterior-posterior, dorsal-ventral, lateral).

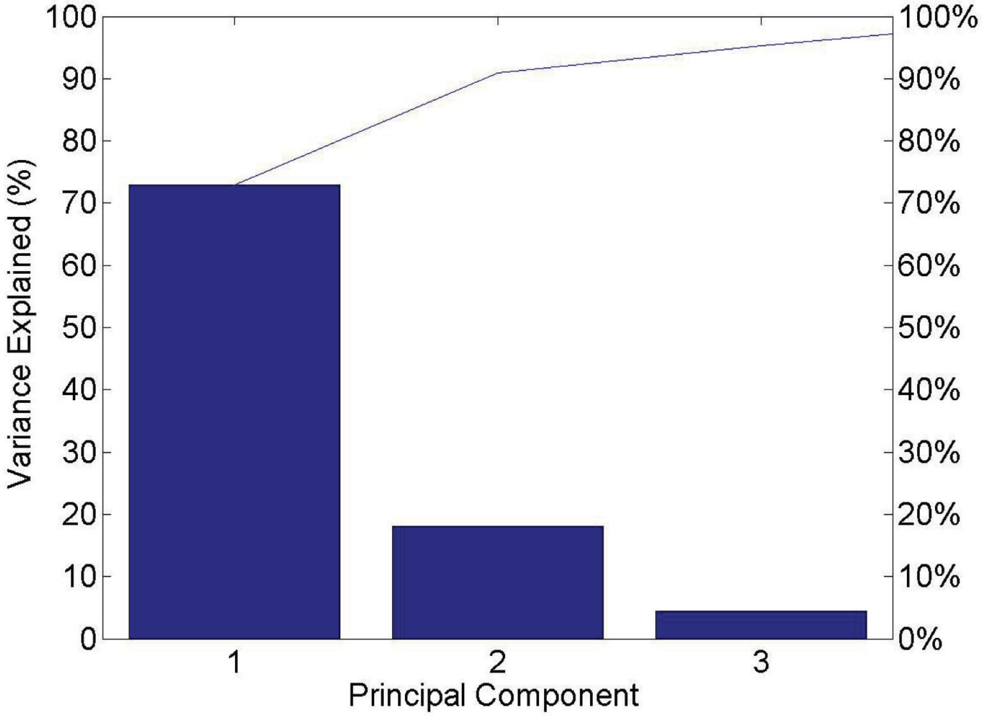

Figure 16. Percent of Variance explained by each of the principal components.

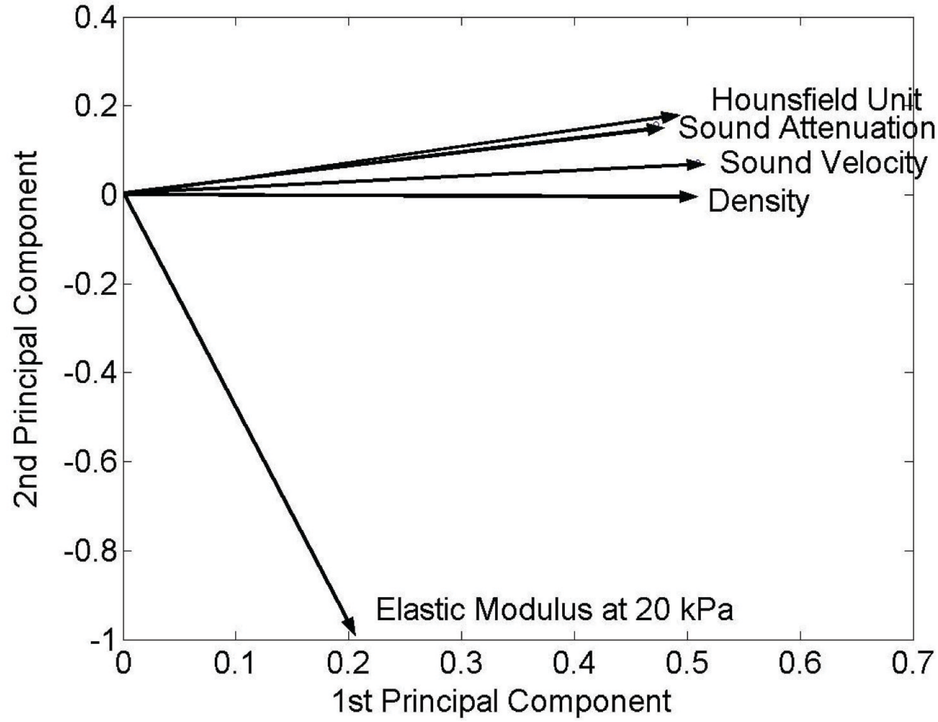

Figure 17. Results of a Principal Components Analysis showing the strength of each variable for the first two principal components. Density, Hounsfield Unit, Sound Attenuation and Sound Velocity are all described by the 1st principal component primarily, while elastic modulus is described by the 2nd principal component.

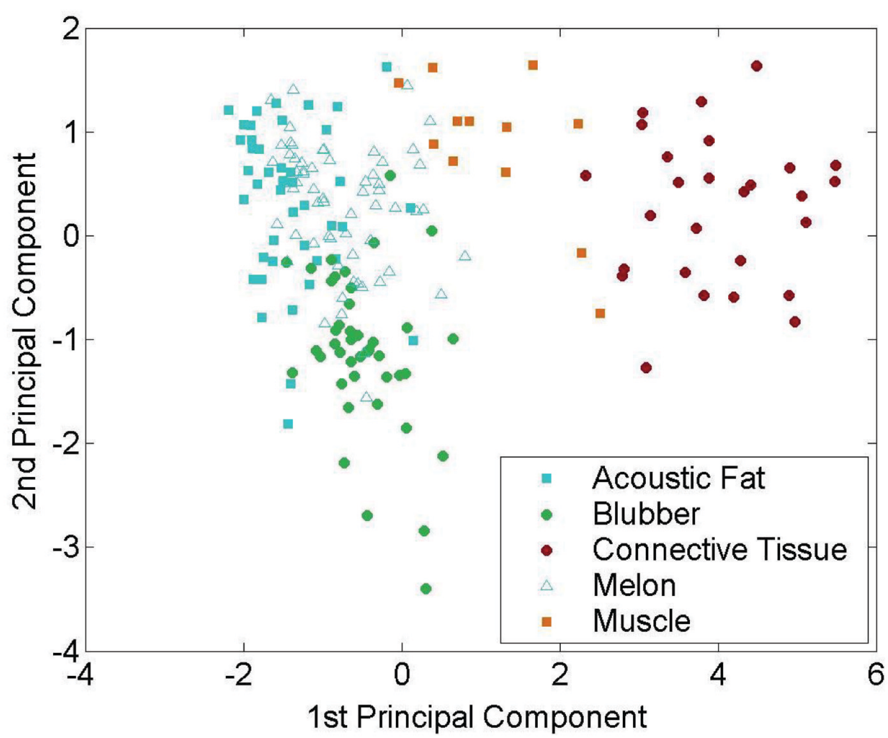

Figure 18. Scatter plot of each sample of *Ziphius cavirostris* tissues as they are described by the 1st and 2nd principal components. Lipids, Muscle and Connective Tissue are distinguished between by the first component, while Acoustic fats and melon are distinguished from Blubber by the second component.

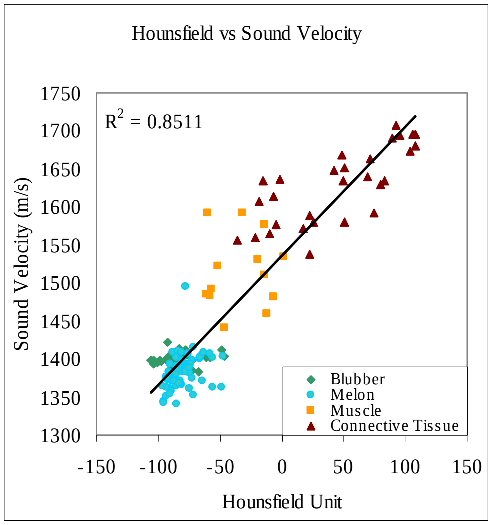

A.

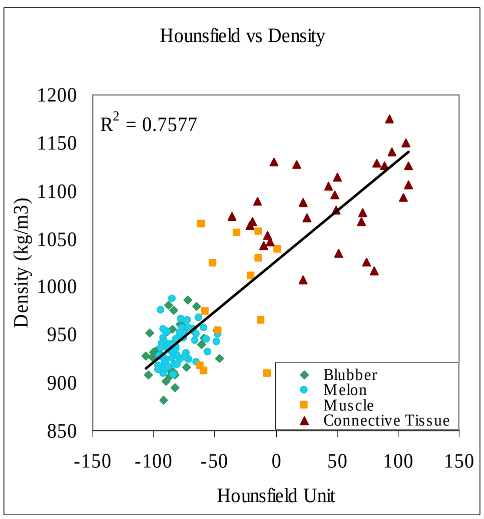

B.

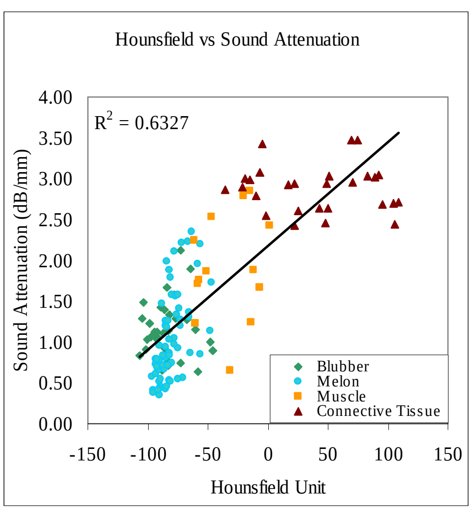

C.

Figure 19. Regression analysis of Hounsfield units versus a) sound velocity, b) density and c) sound attenuation for tissues from a *Ziphius cavirostris*. Best fit lines are represented by the following equations: Sound Velocity = 1.6889HU + 1535.9; Density = 0.001HU + 1.0265; Sound Attenuation = 0.0127HU + 2.1743.

Appendix: Physical property data collected from *Ziphius cavirostris* specimen

Sample #	Tissue Category	Temp. (^{o}C)	Thickness (mm) AP	Thickness (mm) DV	Thickness (mm) LR	Velocity (m/s) AP	Velocity (m/s) DV	Velocity (m/s) LR	Attenuation (dB/mm) AP	Attenuation (dB/mm) DV	Attenuation (dB/mm) LR	Density (kg/m3)	Hounsfield Units
1-DLB-A	conn tiss/blub	21.6	10.25	11.52	10.93	1483	1502	1478	4.04	4.15	3.51	995.1	-92.3
1-DLB-B	blubber	22.0	11.82	11.35	11.20	1453	1455	1454	2.40	2.50	2.63	920.0	-95.2
1-EMB-A	blubber	23.0	10.22	12.70	11.54	1457	1444	1453	3.48	2.65	2.91	932.5	-98.5
1-EMB-B	blubber	22.3	11.43	10.02	9.68	1444	1446	1446	2.50	3.05	2.95	920.9	-101.3
1-EMB-C	blubber	21.8	9.66	10.10	8.07	1438	1440	1441	3.06	2.83	3.30	930.3	-105.4
1-EMB-D	blubber	22.4	12.60	12.11	11.54	1436	1370	1441	2.19	2.28	2.48	901.9	-98.6
1-EMB-E	blubber	22.0	10.70	12.74	11.80	1436	1438	1443	2.39	2.56	2.81	901.2	-106.5
1-EMB-F	blubber	22.5	15.72	17.86	14.83	1453	1450	1454	2.52	2.16	2.60	n/a	-104.1
1-EMB-G	blubber	22.6	10.59	11.45	10.14	1448	1443	1449	3.03	2.80	2.87	916.6	-101.5
1-EMB-H	blubber	23.1	11.28	14.00	14.61	1449	1446	1467	2.68	2.15	2.59	936.5	-101.0
1-EMB-I	blubber	22.6	12.89	13.39	14.88	1461	1458	1470	2.68	2.49	2.78	926.5	-105.9
1-EMF-A	acoustic fat	25.8	7.60	9.27	7.35	1460	1455	1457	4.46	3.44	3.80	905.0	-61.3
1-EMF-B	acoustic fat	22.9	8.91	8.95	8.78	1448	1446	1448	2.91	2.78	2.95	924.7	-71.1
1-EMF-C	acoustic fat	23.3	8.08	12.65	9.53	1439	1437	1437	3.21	2.05	2.51	897.6	-87.2
1-EMF-D	acoustic fat	22.6	12.76	9.20	10.71	1435	1433	1434	2.03	2.60	2.32	883.0	-91.5
1-EMF-E	acoustic fat	23.3	10.60	11.93	10.99	1436	1435	1437	2.35	2.09	2.36	887.4	-85.3
1-EMF-F	acoustic fat	20.1	12.97	14.32	14.39	1469	1469	1471	3.05	2.77	0.74	n/a	-89.8
1-EMF-G	acoustic fat	22.9	8.29	8.11	8.51	1439	1441	1440	2.76	3.07	2.93	867.6	-88.4
1-EMF-H	acoustic fat	23.7	7.25	7.69	8.76	1443	1441	1442	3.30	3.11	2.84	885.2	-89.9
1-EMF-I	acoustic fat	23.1	8.59	8.01	9.52	1442	1440	1438	2.78	2.98	2.55	880.8	-92.0
1-EMF-J	acoustic fat	23.2	10.17	10.36	9.78	1477	1480	1469	4.59	4.20	3.75	940.8	-46.6
1-EMF-K	acoustic fat	23.2	7.00	8.33	8.08	1472	1452	1457	4.09	4.63	4.16	938.9	-29.0
1-IMF-A	acoustic fat	22.9	6.47	11.73	8.65	1443	1443	1465	3.54	2.46	4.27	929.4	-59.3
1-IMF-B1	acoustic fat	22.9	8.29	7.84	5.73	1440	1441	1437	2.88	3.18	4.52	901.5	-77.5
1-IMF-B2	acoustic fat	n/a	n/a	n/a	n/a	n/a	n/a	n/a	n/a	n/a	n/a	n/a	-53.5
1-IMF-C1	acoustic fat	23.0	7.45	7.52	7.44	1437	1441	1437	3.74	3.44	3.21	896.8	-70.3
1-IMF-C2	acoustic fat	23.1	10.20	14.93	6.06	1501	1493	1501	4.08	3.12	4.22	895.2	-80.5
1-IMF-D1	acoustic fat	23.2	9.16	8.81	8.91	1435	1436	1436	2.61	2.83	2.68	875.7	-76.2
1-IMF-D2	acoustic fat	23.5	8.00	11.88	5.15	1509	1513	1511	5.70	4.51	5.94	883.4	-77.5
1-IMF-E1	acoustic fat	24.1	10.67	10.35	12.71	1448	1449	1448	3.46	3.18	3.45	915.9	-67.4
1-IMF-E2	acoustic fat	25.0	14.90	13.61	13.53	1441	1442	1443	2.21	2.34	2.43	904.8	-83.5
1-IMF-E2	muscle	n/a	n/a	n/a	n/a	n/a	n/a	n/a	n/a	n/a	n/a	n/a	-21.6
1-IMF-E3	acoustic fat	23.6	8.77	13.12	10.26	1441	1442	1449	3.18	2.43	3.30	876.2	-74.5
1-IMF-E4	acoustic fat	23.8	11.33	10.12	15.42	1460	1460	1444	3.35	3.96	2.86	898.5	-53.5
1-IMF-F1	ac fat/muscle	23.3	9.19	9.20	9.45	1462	1448	1455	4.04	3.71	3.82	911.8	-47.2
1-IMF-F2	acoustic fat	22.7	6.90	9.57	9.57	1434	1436	1436	3.35	2.62	2.62	882.0	-84.1
1-IMF-F3	acoustic fat	25.0	7.85	11.86	11.99	1431	1431	1437	3.64	2.83	3.30	873.2	-79.8
1-IMF-F4	acoustic fat	21.3	4.02	n/a	n/a	1480	n/a	n/a	9.10	n/a	n/a	n/a	-78.1
1-IMF-F5	acoustic fat	23.7	3.81	4.17	6.14	1061	1474	1488	6.98	6.86	5.80	869.8	-68.2
1-IMF-G1	ac fat/muscle	23.3	12.30	11.50	11.96	1481	1479	1485	3.95	3.70	3.81	952.6	-26.1
1-IMF-G2	acoustic fat	23.6	11.86	11.93	12.26	1439	1440	1437	2.24	2.40	2.17	904.6	-98.8
1-IMF-G3	acoustic fat	23.7	10.91	10.82	9.33	1438	1435	1435	2.62	2.37	2.85	854.2	-88.0
1-IMF-G4	acoustic fat	23.9	8.46	10.64	9.22	1454	1448	1446	3.26	2.59	2.99	859.9	-90.9
1-IMF-G5	acoustic fat	23.3	9.57	11.10	11.03	1446	1447	1450	2.99	2.67	2.68	875.9	-90.2
1-IMF-H1	ac fat/muscle	25.1	8.98	8.09	8.01	1558	1542	1553	4.44	4.81	4.64	1020.7	-51.7
1-IMF-H2	acoustic fat	22.8	7.90	8.05	9.74	1453	1462	1457	3.48	3.57	2.95	907.9	-68.5
1-IMF-H3	acoustic fat	22.5	14.16	10.67	12.28	1457	1458	1448	2.47	2.71	2.21	878.9	-86.9
1-IMF-H4	acoustic fat	22.0	11.27	11.37	14.65	1469	1462	1462	2.93	3.01	2.56	865.7	-71.8
1-IMF-H5	acoustic fat	23.0	10.50	11.13	9.66	1463	1456	1456	3.35	2.66	3.06	907.2	-99.4
1-IMF-H6	muscle	n/a	n/a	n/a	n/a	n/a	n/a	n/a	n/a	n/a	n/a	n/a	47.8
1-IMF-I1	ac fat/muscle	23.8	7.27	7.09	7.96	1566	1561	1565	4.77	4.61	4.48	1024.3	-2.8
1-IMF-I2	ac fat/muscle	23.0	10.34	5.61	13.19	1466	1501	1461	4.13	5.19	3.27	950.2	-94.9
1-IMF-I3	acoustic fat	23.2	13.05	13.89	10.19	1441	1438	1442	2.15	2.02	2.66	870.1	-78.5
1-IMF-I4	acoustic fat	23.8	10.55	11.87	12.57	1452	1453	1453	3.14	2.79	2.32	877.1	-81.6
1-IMF-I5	acoustic fat	22.7	13.19	11.24	9.99	1446	1447	1444	2.36	2.68	2.91	867.1	-89.4
1-IMF-I6	acoustic fat	23.4	9.41	6.60	10.00	1451	1453	1455	3.41	4.26	3.27	911.1	-102.3
1-IMF-J1	muscle	24.3	9.26	10.37	10.41	1572	1564	1576	4.83	4.10	4.85	1035.1	19.9
1-IMF-J2	acoustic fat	22.9	12.29	13.14	13.72	1435	1439	1445	2.16	2.17	2.66	877.7	-105.9

Appendix: Physical property data collected from *Ziphius cavirostris* specimen

Sample #	Tissue Category	Temp. (^oC)	Thickness (mm) AP	Thickness (mm) DV	Thickness (mm) LR	Velocity (m/s) AP	Velocity (m/s) DV	Velocity (m/s) LR	Attenuation (dB/mm) AP	Attenuation (dB/mm) DV	Attenuation (dB/mm) LR	Density (kg/m3)	Hounsfield Units
1-IMF-J3	acoustic fat	23.6	8.01	8.90	9.49	1470	1457	1449	5.18	4.52	3.53	859.1	-82.2
1-IMF-J4	acoustic fat	24.0	8.72	12.54	11.78	1452	1448	1445	3.12	2.65	2.73	860.7	-87.8
1-IMF-J5	acoustic fat	25.6	7.61	11.50	11.83	1446	1444	1442	3.44	2.71	2.38	881.8	-106.2
1-IMF-K1	acoustic fat	23.2	5.95	6.14	8.00	1442	1435	1451	4.74	3.94	5.28	917.9	-76.8
1-IMF-K2	acoustic fat	23.7	13.67	8.63	11.82	1434	1431	1431	2.21	3.34	4.50	865.1	65.3
1-IMF-K3	acoustic fat	24.2	5.25	8.07	14.66	1455	1437	1441	4.99	3.25	2.67	934.3	-96.2
1-IMF-K4	acoustic fat	23.6	6.20	11.47	11.91	1446	1427	1434	6.81	2.84	3.75	876.1	-73.1
1-IMF-K5	conn tiss/muscle	n/a	n/a	n/a	n/a	n/a	n/a	n/a	n/a	n/a	n/a	n/a	80.3
1-IMF-K6	conn tiss/muscle	n/a	n/a	n/a	n/a	n/a	n/a	n/a	n/a	n/a	n/a	n/a	43.9
1-IMF-K7	conn tiss/muscle	n/a	n/a	n/a	n/a	n/a	n/a	n/a	n/a	n/a	n/a	n/a	61.5
1-LNP-1	conn tiss/muscle	21.6	6.39	5.59	8.49	1653	1647	1646	4.65	4.78	3.38	1119.3	89.4
1-LNP-1	conn tiss/muscle	22.7	5.79	5.20	7.44	1659	1653	1666	5.82	4.75	4.26	1126.5	81.6
1-RNP-2	conn tiss/muscle	22.6	9.26	7.17	13.34	1629	1653	1650	3.75	4.98	3.80	1108.3	73.8
1-Thyroid-1	cartilage	22.9	5.46	n/a	12.37	1566	n/a	1590	9.47	n/a	4.02	1088.0	61.9
1-Thyroid-2	cartilage	n/a	n/a	n/a	n/a	n/a	n/a	n/a	n/a	n/a	n/a	n/a	59.8
1-Thyroid-3	cartilage	n/a	n/a	n/a	n/a	n/a	n/a	n/a	n/a	n/a	n/a	n/a	60.2
1-Tongue-1A	muscle	23.2	7.16	8.05	16.58	1596	1597	1599	3.06	3.59	2.23	1078.1	29.7
1-Tongue-2P	muscle	24.1	9.53	13.37	8.23	1585	1589	1585	3.03	2.56	3.03	1076.6	21.7
1-VCB-1	blubber	21.8	11.39	14.81	13.65	1449	1451	1449	2.41	1.85	2.01	905.7	-102.5
1-Hyoid-1	cartilage	n/a	n/a	n/a	n/a	n/a	n/a	n/a	n/a	n/a	n/a	n/a	144.2
1-Hyoid-2	cartilage	n/a	n/a	n/a	n/a	n/a	n/a	n/a	n/a	n/a	n/a	n/a	148.4
1-Hyoid-3	cartilage	n/a	n/a	n/a	n/a	n/a	n/a	n/a	n/a	n/a	n/a	n/a	171.3
1-Hyoid-4	cartilage	n/a	n/a	n/a	n/a	n/a	n/a	n/a	n/a	n/a	n/a	n/a	202.3
1-Hyoid-5	cartilage	n/a	n/a	n/a	n/a	n/a	n/a	n/a	n/a	n/a	n/a	n/a	175.1
1-Hyoid-6	cartilage	n/a	n/a	n/a	n/a	n/a	n/a	n/a	n/a	n/a	n/a	n/a	185.6
1-F-A1	blubber	23.1	12.50	13.01	12.49	1456	1457	1454	2.78	2.74	2.86	931.8	-100.2
1-F-A2	blubber	21.9	10.90	11.80	14.51	1457	1450	1461	3.28	3.03	3.08	908.1	-104.3
1-F-A3	blubber	22.0	12.05	13.95	12.24	1465	1459	1460	3.05	3.06	3.65	951.8	-103.6
1-F-B1	blubber	25.4	10.19	14.83	10.44	1471	1471	1469	3.27	2.58	3.09	882.2	-92.0
1-F-B2	blubber	20.2	10.43	11.59	10.91	1468	1462	1466	3.03	2.87	2.95	926.3	-101.3
1-F-B3	melon	20.2	11.00	12.42	10.56	1483	1489	1478	3.29	3.25	3.83	953.5	-88.6
1-F-B4	blubber	19.3	9.55	12.94	19.87	1473	1473	n/a	3.25	2.78	1.66	927.4	-106.2
1-F-B5	blubber	20.3	10.66	10.72	10.54	1466	1468	1467	3.10	3.17	3.23	933.7	-97.8
1-F-B6	blubber	20.2	11.73	11.97	13.48	1470	1470	1467	3.13	3.07	2.95	925.3	-98.8
1-F-C1	blubber	21.2	11.36	12.84	12.59	1467	1465	1466	2.88	2.73	2.64	933.2	-85.6
1-F-C2	melon	20.6	10.30	10.52	11.02	1476	1476	1472	3.35	3.47	3.31	741.8	-84.7
1-F-C3	blubber	19.5	10.28	12.41	10.54	1470	1472	1471	3.26	2.94	3.27	929.2	-93.9
1-F-C4	blubber	20.7	11.55	11.63	11.23	1471	1471	1468	3.07	3.00	3.11	913.4	-87.1
1-F-C5	melon	19.6	10.13	11.98	10.34	1480	1473	1476	3.45	3.19	3.69	944.0	-65.9
1-F-C6	melon	20.0	10.05	10.49	9.66	1476	1475	1470	3.30	3.26	3.95	965.4	-72.2
1-F-C7	blubber	19.5	10.59	11.50	10.11	1474	1471	1472	3.14	3.10	3.41	912.5	-92.1
1-F-C8	blubber	20.0	11.82	12.12	12.31	1480	1475	1476	3.28	3.30	3.25	952.4	-89.2
1-F-C9	blubber	19.6	9.36	12.19	10.04	1479	1478	1478	3.74	3.12	3.78	907.4	-86.5
1-F-D1	blubber	19.5	8.16	9.62	9.09	1461	1460	1459	3.31	3.01	3.19	980.7	-87.8
1-F-D2	melon	20.5	10.40	12.48	10.70	1466	1465	1464	3.17	2.88	3.14	923.8	-77.9
1-F-D3	melon	21.4	7.96	11.83	10.18	1462	1465	1462	3.35	3.02	3.41	936.7	-90.1
1-F-D4	blubber	21.4	12.25	12.51	10.83	1469	1467	1466	2.91	2.85	3.11	942.7	-92.5
1-F-D5	blubber	20.1	8.87	11.34	8.55	1477	1475	1477	3.80	3.24	3.94	959.2	-76.5
1-F-D6	melon	21.6	8.70	9.67	12.67	1477	1470	1467	3.69	3.70	3.16	950.5	-65.2
1-F-D7	melon	20.1	9.64	11.22	13.90	1461	1460	1459	3.02	2.86	2.63	943.3	-82.0
1-F-D8	melon	19.8	10.30	12.65	12.45	1474	1470	1466	3.38	3.16	3.21	946.4	-75.4
1-F-D9	blubber	20.0	11.80	12.36	10.96	1477	1475	1473	3.22	3.16	3.38	945.7	-81.7
1-F-D10	blubber	20.1	11.01	11.13	11.29	1479	1488	1481	3.63	3.68	3.45	961.0	-77.9
1-F-D11	blubber	19.7	11.08	12.90	13.71	1487	1480	1490	3.79	3.26	3.36	975.0	-83.6
1-F-E1	musc/blub	19.3	9.39	11.78	11.21	1458	1457	1457	3.09	2.63	2.77	952.0	-86.6
1-F-E2	melon	20.0	7.97	10.51	11.26	1458	1452	1453	3.51	2.95	2.75	946.1	-91.7
1-F-E3	melon	19.9	9.71	13.53	12.15	1452	1448	1446	2.91	2.46	2.50	926.0	-92.6
1-F-E4	musc/blub	19.5	11.94	13.35	12.31	1461	1459	1460	2.91	2.67	2.90	931.5	-90.3

Appendix: Physical property data collected from *Ziphius cavirostris* specimen

Sample #	Tissue Category	Temp. (^oC)	Thickness (mm) AP	Thickness (mm) DV	Thickness (mm) LR	Velocity (m/s) AP	Velocity (m/s) DV	Velocity (m/s) LR	Attenuation (dB/mm) AP	Attenuation (dB/mm) DV	Attenuation (dB/mm) LR	Density (kg/m3)	Hounsfield Units
1-F-E5	conn tiss/blub	19.8	9.48	11.22	9.21	1500	1499	1490	4.72	4.07	4.74	984.3	-77.2
1-F-E6	musc/blub	19.6	10.20	13.83	10.47	1476	1471	1474	3.60	2.94	3.70	966.0	-72.2
1-F-E7	melon	20.6	10.53	10.75	10.65	1460	1451	1451	2.92	2.86	2.88	942.0	-90.7
1-F-E8	melon	24.0	10.22	12.09	12.03	1435	1437	1433	2.59	2.19	2.16	918.6	-90.6
1-F-E9	melon	22.1	10.73	12.08	10.31	1448	1452	1443	3.36	2.81	2.72	951.9	-74.5
1-F-E10	blubber	19.7	12.02	14.30	13.62	1453	1457	1454	3.08	2.94	2.86	954.8	-67.6
1-F-E11	blubber	21.7	9.29	10.92	9.54	1467	1478	1469	4.41	3.94	4.13	979.1	-64.8
1-F-E12	melon	21.3	11.17	8.98	11.81	1430	1430	1434	2.96	3.69	3.14	942.3	-48.4
1-F-E13	musc/blub	20.4	8.09	11.08	11.30	1495	1507	1507	5.82	4.61	4.88	1035.1	-79.5
1-F-F1	musc/blub	21.6	11.42	12.01	10.40	1428	1430	1426	2.49	2.42	2.69	923.2	-85.8
1-F-F2	musc/blub	20.2	11.80	13.78	10.64	1433	1435	1425	2.63	2.47	2.85	928.0	-91.4
1-F-F3	melon	20.5	9.98	12.21	11.36	1422	1425	1423	3.09	2.52	2.79	939.8	-93.2
1-F-F4	musc/blub	21.5	13.12	13.11	13.67	1433	1432	1431	2.51	2.43	2.33	235.0	-94.2
1-F-F5	musc/blub	20.0	11.97	14.39	12.83	1434	1436	1432	2.83	2.43	2.56	930.2	-97.1
1-F-F6	blubber	20.2	11.95	13.87	11.97	1466	1461	1480	4.01	3.53	4.17	985.9	-72.2
1-F-F7	musc/blub	20.4	11.61	10.71	11.30	1434	1429	1430	2.89	3.04	2.94	935.8	-81.8
1-F-F8	melon	20.7	10.99	12.30	12.17	1416	1417	1418	2.41	2.25	2.28	917.2	-95.7
1-F-F9	melon	20.5	9.10	10.22	10.16	1414	1416	1419	2.82	2.62	2.53	927.7	-95.5
1-F-F10	musc/blub	21.9	10.27	11.96	10.89	1432	1431	1427	2.89	2.73	2.85	930.4	-86.4
1-F-F11	musc/blub	20.3	9.89	12.73	10.67	1462	1463	1455	4.35	3.61	3.94	975.0	-42.6
1-F-F12	connective tissue	19.6	9.56	12.54	11.13	1536	1556	1550	5.75	4.09	4.89	1073.7	-35.6
1-F-F13	muscle	21.4	10.82	8.79	9.90	1511	1503	1526	4.94	5.62	4.89	1029.6	-14.5
1-F-F14	melon	20.8	10.51	10.37	13.59	1432	1431	1440	2.70	3.03	2.75	931.7	-55.8
1-F-F15	melon	20.2	9.26	13.41	13.59	1422	1430	1429	2.85	2.34	2.24	923.8	-71.1
1-F-F16	muscle	20.7	9.94	12.28	10.35	1462	1461	1461	4.06	3.62	4.19	964.9	-11.9
1-F-F17	connective tissue	20.1	10.50	14.72	15.08	1604	1610	1583	5.56	4.21	4.38	1067.4	-18.7
1-F-G1	musc/blub	21.8	11.03	13.15	12.26	1435	1437	1442	2.90	2.66	2.69	934.1	-84.0
1-F-G2	melon	20.8	8.50	11.89	11.26	1430	1433	1434	3.24	2.58	2.73	954.7	-90.4
1-F-G3	melon	20.4	11.29	12.11	12.25	1435	1434	1437	2.72	2.62	2.51	936.3	-93.5
1-F-G4	musc/blub	19.0	11.97	15.14	14.24	1441	1442	1441	2.90	2.49	2.58	929.1	-91.1
1-F-G5	conn tiss/blub	19.0	9.24	11.88	11.75	1501	1495	1521	5.60	4.60	4.57	1031.1	-75.8
1-F-G6	musc/blub	19.2	9.76	11.64	11.58	1445	1444	1448	3.56	3.15	3.17	918.0	-84.2
1-F-G7	melon	21.1	11.23	11.47	12.47	1428	1427	1429	2.47	2.33	2.30	924.3	-89.6
1-F-G8	melon	21.8	11.90	11.81	11.89	1431	1430	1432	2.50	2.35	2.54	913.9	-96.2
1-F-G9	musc/blub	19.5	11.45	14.04	10.99	1434	1433	1430	2.44	2.34	2.63	926.6	-93.2
1-F-G10	conn tiss/blub	19.0	9.25	13.10	11.19	1484	1488	1493	5.07	4.19	4.37	987.9	-25.9
1-F-G11	connective tissue	19.5	11.91	10.01	7.83	1631	1629	1621	4.44	4.59	5.61	1129.7	-1.3
1-F-G12	muscle	20.2	11.43	12.13	13.72	1518	1522	1535	3.75	3.78	3.49	1024.2	-51.5
1-F-G13	melon	20.1	11.36	12.27	10.08	1447	1447	1352	3.07	3.09	3.43	933.0	-85.3
1-F-G14	melon	19.9	10.67	12.49	11.28	1429	1434	1429	2.60	2.22	2.36	911.5	-90.7
1-F-G15	melon	20.4	10.04	10.93	11.05	1436	1433	1435	2.65	2.62	2.68	926.2	-74.7
1-F-G16	muscle	20.3	13.31	14.55	12.14	1491	1480	1480	3.28	3.62	3.18	909.2	-6.9
1-F-G17	connective tissue	20.4	12.39	11.65	12.50	1654	1645	1634	4.49	4.77	4.17	1114.2	50.2
1-F-H1	musc/blub	24.5	10.85	11.96	11.92	1465	1462	1466	3.38	2.91	2.23	957.6	-78.1
1-F-H2	melon	20.0	12.23	11.63	9.97	1457	1454	1455	2.66	2.79	2.96	939.6	-84.7
1-F-H3	melon	20.6	9.22	8.49	9.73	1450	1450	1450	2.94	3.46	2.92	913.1	-91.1
1-F-H4	melon	21.5	10.98	10.80	10.80	1453	1450	1451	2.68	2.72	2.89	955.1	-91.8
1-F-H5	musc/blub	20.7	11.56	11.82	11.45	1460	1462	1456	2.90	2.92	2.93	945.6	-88.8
1-F-H6	conn tiss/blub	24.8	10.44	10.90	12.40	1512	1535	1538	5.02	5.50	4.46	1033.1	-68.7
1-F-H7	musc/blub	19.9	11.39	9.11	10.84	1461	1458	1463	3.10	3.66	3.44	947.9	-80.5
1-F-H8	melon	21.1	8.67	10.25	9.91	1441	1443	1443	2.79	3.46	2.77	939.9	-86.5
1-F-H9	melon	22.2	10.61	12.70	9.00	1442	1438	1440	2.59	2.17	2.83	926.9	-91.5
1-F-H10	melon	22.6	11.83	12.02	12.89	1443	1440	1440	2.49	2.37	2.44	975.9	-93.5
1-F-H11	musc/blub	21.2	14.47	12.24	12.66	1460	1452	1458	2.66	2.93	2.99	944.1	-82.8
1-F-H12	conn tiss/blub	20.7	10.07	10.86	12.02	1503	1507	1528	4.46	4.78	4.23	1037.3	-6.6
1-F-H13	connective tissue	21.0	9.02	10.18	10.24	1639	1654	1627	5.64	4.47	4.66	1104.7	42.8
1-F-H14	muscle	20.2	11.47	12.96	12.52	1488	1492	1502	3.64	3.76	3.33	974.1	-57.3
1-F-H15	melon	22.1	14.52	8.84	9.22	1452	1444	1449	2.80	3.02	2.90	928.4	-80.2

Appendix: Physical property data collected from *Ziphius cavirostris* specimen

Sample #	Tissue Category	Temp. (^oC)	Thickness (mm) AP	Thickness (mm) DV	Thickness (mm) LR	Velocity (m/s) AP	Velocity (m/s) DV	Velocity (m/s) LR	Attenuation (dB/mm) AP	Attenuation (dB/mm) DV	Attenuation (dB/mm) LR	Density (kg/m3)	Hounsfield Units
1-F-H16	melon	20.4	12.11	13.35	14.92	1439	1437	1439	2.20	2.08	2.00	933.2	-84.7
1-F-H17	melon	23.5	9.12	11.72	13.38	1443	1440	1441	2.83	2.54	2.23	923.3	-90.7
1-F-H18	muscle	21.0	9.46	13.79	12.37	1486	1485	1484	3.68	3.47	3.78	912.6	-58.5
1-F-H19	muscle	19.9	9.06	12.30	10.24	1535	1540	1536	4.61	4.62	4.50	1038.3	1.8
1-F-H20	connective tissue	21.5	10.80	11.54	11.82	1693	1689	1680	5.30	4.09	4.59	1140.6	95.2
1-F-I1	musc/blub	23.9	9.84	12.07	11.08	1486	1492	1500	4.30	3.60	4.16	998.8	-72.8
1-F-I2	musc/blub	21.7	11.23	13.76	11.99	1468	1470	1461	3.30	3.06	2.93	949.8	-83.7
1-F-I3	melon	21.4	13.03	11.08	12.34	1458	1460	1458	2.62	2.99	2.76	755.7	-85.1
1-F-I4	melon	21.5	12.79	12.45	12.64	1463	1460	1460	2.74	2.82	2.86	939.4	-82.2
1-F-I5	musc/blub	21.4	10.36	12.96	13.36	1483	1493	1483	3.77	3.56	3.38	984.8	-77.8
1-F-I6	connective tissue	20.4	10.99	12.61	10.39	1549	1546	1558	4.90	4.91	4.85	1064.5	-21.3
1-F-I7	musc/blub	20.1	12.12	9.10	10.71	1466	1466	1466	3.25	3.76	2.36	983.0	-78.5
1-F-I8	melon	20.1	9.57	11.87	11.72	1444	1443	1444	2.74	2.46	2.32	908.2	-83.7
1-F-I9	melon	20.3	11.82	12.04	11.92	1445	1446	1445	2.39	2.51	2.40	919.4	-89.6
1-F-I10	melon	20.5	9.79	11.36	11.51	1449	1446	1446	3.06	2.64	2.88	909.4	-92.2
1-F-I11	musc/blub	20.0	11.55	11.01	10.20	1484	1476	1483	3.39	4.01	4.43	978.1	-82.2
1-F-I12	connective tissue	20.3	11.12	12.67	11.87	1639	1625	1613	5.14	4.99	4.49	1088.8	-14.7
1-F-I13	connective tissue	19.2	9.65	10.78	11.58	1630	1538	1581	6.65	5.31	4.79	1025.9	74.5
1-F-I14	muscle	20.7	11.89	15.00	10.67	1485	1491	1483	3.99	3.97	4.26	916.7	-61.3
1-F-I15	melon	20.4	11.77	12.61	16.32	1443	1443	1446	2.42	2.39	1.81	919.1	-82.4
1-F-I16	melon	20.6	11.73	12.07	14.56	1439	1441	1439	2.43	2.28	2.16	919.2	-80.6
1-F-I17	melon	20.7	11.66	11.39	10.82	1444	1443	1445	2.70	2.68	2.73	934.1	-87.4
1-F-I18	muscle	20.4	10.09	11.54	11.71	1375	1478	1476	4.71	4.55	4.40	953.7	-46.8
1-F-I19	connective tissue	20.0	13.71	13.51	11.35	1689	1685	1689	3.90	4.40	4.27	1150.3	106.0
1-F-I20	connective tissue	20.4	10.91	10.04	11.02	1593	1565	1587	5.55	4.85	4.75	1087.8	22.2
1-F-I21	melon	20.6	11.01	15.65	18.00	1443	1442	1447	2.66	2.38	2.18	915.8	-87.2
1-F-I22	melon	20.2	12.80	13.31	16.08	1445	1446	1446	2.45	2.42	2.57	921.8	-64.8
1-F-I23	connective tissue	20.5	12.69	10.09	11.01	1664	1548	1669	5.15	5.58	4.39	1128.6	82.8
1-F-J1	connective tissue	22.8	11.33	13.99	12.01	1574	1550	1549	5.27	3.84	4.70	1043.3	-9.8
1-F-J2	musc/blub	20.7	10.77	10.58	10.18	1516	1515	1506	4.87	4.76	4.57	1029.8	-73.8
1-F-J3	melon	22.1	7.70	10.78	10.62	1483	1478	1467	4.40	4.63	4.04	987.2	-84.5
1-F-J4	musc/blub	20.7	12.57	14.76	12.80	1492	1490	1488	3.41	3.86	3.98	978.8	-63.5
1-F-J5	conn tiss/blub	20.3	12.23	12.71	12.43	1538	1553	1549	4.24	4.40	4.66	1053.8	44.3
1-F-J6	conn tiss/blub	20.2	11.15	11.50	10.37	1509	1506	1542	4.80	4.48	4.87	1024.1	77.2
1-F-J7	melon	21.2	12.36	13.47	9.12	1464	1470	1466	3.11	3.75	3.78	946.5	-79.8
1-F-J8	melon	20.1	12.70	11.28	12.28	1446	1442	1442	2.40	2.88	2.81	934.1	-81.7
1-F-J9	melon	20.9	10.70	12.15	9.14	1443	1440	1436	2.85	2.76	2.90	727.3	-82.7
1-F-J10	musc/blub	20.7	10.18	8.65	7.79	1467	1460	1457	3.49	4.80	4.30	971.8	-68.9
1-F-J11	connective tissue	20.3	7.64	10.33	10.77	1711	1688	1701	6.35	5.28	4.69	1175.4	92.7
1-F-J12	connective tissue	20.2	11.80	13.62	10.85	1659	1667	1638	5.13	4.37	4.97	1077.3	71.1
1-F-J13	melon	20.2	9.42	15.22	12.18	1448	1450	1451	3.60	2.56	3.11	924.7	-72.5
1-F-J14	musc/melon	20.8	12.42	12.41	12.24	1454	1449	1446	2.81	2.65	3.01	933.0	-68.1
1-F-J15	musc/melon	19.8	12.63	13.01	14.27	1469	1469	1474	3.43	3.36	3.16	954.4	-79.2
1-F-J16	connective tissue	21.2	10.06	12.47	12.31	1683	1681	1685	5.18	4.82	4.88	1126.1	89.2
1-F-K1	conn tiss/blub	24.9	11.76	11.27	10.61	1547	1537	1544	4.17	4.97	5.37	1015.2	-12.4
1-F-K2	connective tissue	22.2	9.32	16.04	13.93	1549	1553	1592	6.33	3.74	4.12	1126.9	16.9
1-F-K3	musc/blub	23.0	8.92	10.30	14.68	1501	1507	1501	4.64	5.20	3.94	980.6	-52.8
1-F-K4	melon	23.3	8.74	14.90	14.62	1465	1468	1456	4.90	3.28	4.02	945.3	-56.3
1-F-K5	musc/blub	23.2	8.73	15.79	11.01	1510	1494	1502	5.82	4.10	5.52	977.6	-34.5
1-F-K6	conn tiss/blub	23.6	10.75	11.36	11.97	1568	1567	1586	5.56	5.35	5.17	1049.0	17.5
1-F-K7	connective tissue	20.5	9.15	13.79	14.13	1649	1615	1615	6.22	4.13	4.15	1079.9	49.2
1-F-K8	connective tissue	23.0	8.46	9.95	10.50	1649	1651	1600	6.42	6.06	4.98	1068.1	69.8
1-F-K9	musc/blub	23.8	7.08	11.85	9.83	1519	1511	1526	6.12	4.35	4.36	1006.2	-39.0
1-F-K10	musc/blub	23.6	10.59	13.98	8.16	1507	1487	1483	4.33	3.57	4.28	983.0	-70.9
1-F-K11	melon	20.0	12.11	12.46	13.57	1467	1462	1466	2.44	3.34	3.29	n/a	-83.1
1-F-K12	melon	23.2	10.19	9.67	10.73	1450	1449	1444	3.52	3.30	3.35	925.4	-84.5
1-F-K13	melon	23.0	8.86	10.71	11.90	1457	1461	1462	4.86	3.74	3.27	937.4	-81.1
1-F-K14	muscle	24.0	10.38	14.39	9.79	1535	1528	1533	4.56	4.47	5.34	1011.7	-19.8

Appendix: Physical property data collected from *Ziphius cavirostris* specimen

Sample #	Tissue Category	Temp. (°C)	Thickness (mm) AP	Thickness (mm) DV	Thickness (mm) LR	Velocity (m/s) AP	Velocity (m/s) DV	Velocity (m/s) LR	Attenuation (dB/mm) AP	Attenuation (dB/mm) DV	Attenuation (dB/mm) LR	Density (kg/m3)	Hounsfield Units
1-F-K15	connective tissue	22.9	7.92	9.42	10.26	1681	1680	1641	5.64	5.38	4.45	1093.4	104.2
1-F-K16	blubber	22.9	8.84	9.28	8.56	1458	1461	1461	3.13	2.98	3.35	946.9	-58.5
1-F-K17	connective tissue	22.0	4.81	7.87	8.36	1633	1681	1553	11.58	6.57	5.77	1016.8	80.4
1-F-K18	muscle	23.8	6.85	6.54	9.48	1595	1594	1593	3.68	4.16	3.15	1056.1	-31.7
1-F-K19	melon	22.6	6.27	7.07	6.99	1473	1470	1467	4.29	5.84	4.48	956.8	-76.3
1-F-K20	melon	23.2	7.76	7.88	9.79	1445	1447	1439	3.65	3.59	3.71	951.4	-78.1
1-F-K21	musc/melon	23.7	9.54	9.36	9.59	1447	1441	1434	3.18	3.77	3.68	926.0	-76.5
1-F-K22	musc/melon	23.7	6.78	9.12	11.49	1473	1472	1473	4.54	4.18	3.40	987.4	-73.8
1-F-K23	muscle	22.4	11.52	12.72	12.67	1585	1590	1560	2.96	3.59	2.66	1057.5	-14.2
1-F-K24	connective tissue	24.6	10.10	10.24	10.28	1692	1700	1678	5.18	5.11	4.42	1106.7	108.6
1-F-K25	blubber	22.7	8.36	9.31	9.57	1460	1465	1470	3.52	3.05	3.42	956.0	-84.5
1-F-K26	blubber	23.0	9.64	10.20	9.70	1461	1462	1462	3.28	3.10	3.15	925.8	-46.3
1-F-K27	melon	22.9	8.87	9.65	12.18	1696	1489	1489	4.46	4.62	3.91	966.6	-77.7
1-F-K28	musc/melon	22.6	9.17	7.44	11.69	1475	1469	1461	3.74	5.16	4.09	949.8	-60.5
1-F-K29	musc/melon	22.2	9.99	9.81	11.42	1498	1496	1495	4.38	5.28	4.21	978.1	-34.4
1-F-K30	connective tissue	23.2	6.30	9.56	11.49	1686	1686	1647	8.29	5.67	4.63	1126.1	108.1
1-F-K31	blubber	21.1	6.24	9.22	9.59	1448	1451	1454	4.04	3.38	3.15	916.5	-73.1
1-F-L1	blubber	24.5	11.33	10.67	13.51	1454	1467	1474	2.75	3.22	2.77	954.4	-48.1
1-F-L2	connective tissue	21.5	12.32	14.81	18.07	1659	1663	1662	4.28	4.06	3.60	1096.3	48.1
1-F-L3	connective tissue	23.9	11.03	14.18	16.38	1608	1607	1609	5.03	4.83	4.37	1053.7	-6.3
1-F-L4	connective tissue	22.5	12.23	12.86	16.87	1516	1580	1497	4.37	4.24	3.54	1006.7	22.2
1-F-L5	connective tissue	23.7	12.17	9.97	12.72	1575	1568	1577	4.54	5.54	4.86	1034.7	51.0
1-F-L6	blubber	22.1	10.15	18.46	13.80	1460	1459	1461	3.03	1.82	2.34	910.8	-83.5
1-F-L7	melon	24.2	12.44	11.45	12.26	1451	1449	1450	3.01	3.27	3.54	931.0	-73.3
1-F-L8	melon	21.1	11.93	14.60	12.43	1456	1456	1463	3.39	2.84	3.73	927.1	-74.3
1-F-L9	melon	21.8	10.79	14.15	15.44	1467	1470	1472	4.41	4.00	3.38	955.7	-66.6
1-F-L10	blubber	22.1	13.07	19.46	11.12	1458	1460	1463	2.85	2.01	3.44	894.8	-82.7
1-F-L11	blubber	22.5	8.11	14.77	15.88	1456	1465	1465	3.85	2.72	2.59	939.6	-60.7
1-F-L12	melon	21.9	11.51	12.22	10.30	1467	1462	1496	3.41	3.71	4.50	944.8	-81.5
1-F-L13	musc/melon	24.6	9.37	22.45	18.48	1472	1465	1452	3.71	2.66	2.80	957.3	-56.8
1-F-L14	musc/melon	25.6	8.84	12.71	16.70	1498	1490	1491	5.29	4.63	3.22	979.7	-35.1
1-F-L15	muscle	22.7	11.30	16.62	11.22	1592	1592	1595	3.17	2.61	3.24	1065.7	-60.6
1-F-L16	blubber	22.6	11.29	12.61	14.60	1455	1454	1456	2.71	2.57	2.22	914.8	-90.8
1-F-L17	melon	24.2	9.33	9.84	12.98	1467	1472	1476	4.54	4.61	3.88	957.5	-71.3
1-F-L18	musc/melon	23.7	11.98	12.44	16.01	1486	1487	1478	4.82	4.47	3.35	1000.9	-8.0
1-F-L19	musc/melon	22.8	11.15	15.40	14.68	1509	1532	1508	4.73	3.68	3.93	1014.1	65.2
1-F-L20	musc/blub	25.7	13.82	10.96	13.29	1538	1545	1554	4.56	5.75	4.82	1010.9	-20.0
1-F-M1	connective tissue	22.4	16.23	12.80	13.09	1582	1558	1570	5.15	5.04	4.93	1047.4	-4.6
1-F-M2	connective tissue	19.8	15.20	14.44	15.54	1607	1597	1512	4.25	4.13	3.90	1071.3	25.5
1-F-M3	musc/blub	20.7	12.09	14.22	14.59	1481	1486	1493	5.27	4.19	4.39	988.7	-66.1
1-F-M4	musc/blub	26.0	13.14	12.92	15.01	1493	1505	1486	4.03	4.16	4.13	980.7	-55.6
1-F-M5	melon	23.1	13.56	12.80	13.33	1588	1571	1575	4.20	4.14	3.68	1062.2	-24.2
1-F-M6	melon	21.5	16.81	11.99	12.22	1468	1477	1484	3.40	4.25	4.42	967.6	-62.9
1-F-M7	melon	23.0	14.14	13.21	14.01	1465	1465	1465	3.27	3.42	3.37	950.1	-47.2
1-F-M8	musc/melon	22.9	13.03	10.73	16.20	1469	1475	1465	3.62	4.40	3.10	960.6	-32.4
1-F-M9	musc/melon	22.3	15.79	12.07	12.11	1514	1510	1504	3.41	4.28	4.37	963.1	-10.7
1-F-M10	melon	22.1	17.64	14.17	9.54	1469	1474	1475	3.40	3.59	4.08	957.2	-58.2
1-F-M11	musc/melon	21.7	15.63	15.90	17.52	1465	1465	1466	3.22	3.03	2.88	918.5	-12.5
1-F-M12	musc/melon	23.0	13.35	16.12	16.79	1485	1491	1495	3.48	3.13	3.06	955.9	36.8
1-F-M13	blubber	23.5	16.49	16.38	12.96	1450	1455	1450	2.09	2.16	2.50	907.8	-82.5
1-F-M14	musc/melon	21.6	14.58	15.29	14.14	1616	1579	1614	3.35	3.30	3.07	1074.6	50.5
1-F-M15	blubber	22.7	15.07	16.85	15.75	1452	1455	1453	2.12	2.02	2.22	900.5	-90.3
1-F-O1	connective tissue	22.8	10.36	10.70	10.73	1619	1623	1617	3.54	4.08	3.62	1079.2	n/a
1-F-O2	blubber	23.8	16.16	14.07	17.62	1451	1451	1451	2.09	2.35	2.07	930.5	n/a
1-F-O3	blubber	27.0	12.82	12.31	15.40	1447	1444	1446	2.22	2.27	2.04	927.0	n/a
2-DLB-A1	blubber	19.0	15.19	14.77	19.93	1478	1476	1474	2.32	2.06	1.78	929.4	
2-DLB-B1	blubber	19.7	10.95	15.21	15.38	1463	1467	1469	2.69	2.14	2.11	934.4	
2-DLB-C1	blubber	20.4	16.74	11.96	13.90	1468	1466	1466	2.00	3.43	2.28	936.0	

Appendix: Physical property data collected from *Ziphius cavirostris* specimen

Sample #	Tissue Category	Temp. (°C)	Thickness (mm) AP	Thickness (mm) DV	Thickness (mm) LR	Velocity (m/s) AP	Velocity (m/s) DV	Velocity (m/s) LR	Attenuation (dB/mm) AP	Attenuation (dB/mm) DV	Attenuation (dB/mm) LR	Density (kg/m3)	Hounsfield Units
2-DLB-D1	blubber	21.4	12.85	12.63	14.76	1466	1463	1466	2.39	2.35	2.08	926.2	
2-DLB-E1	blubber	19.2	14.87	11.27	13.13	1474	1472	1470	2.47	2.64	2.34	916.8	
2-DLB-F1	blubber	21.2	17.69	18.77	12.02	1474	1470	1468	2.39	2.16	2.66	917.9	
2-Diaphram	diaphram	20.3	3.77	n/a	n/a	1585	n/a	n/a	7.08	n/a	n/a	1174.8	
2-EM-A1	muscle	20.6	15.25	9.91	17.48	1590	1589	1591	2.20	3.73	1.73	1152.9	
2-EM-C1	muscle	21.0	12.91	14.40	12.03	1591	1588	1592	2.53	3.03	2.14	1080.1	
2-EM-F1	muscle	18.1	16.05	13.80	16.03	1588	1592	1600	2.16	3.31	2.85	1090.1	
3-DLB-A	blubber	n/a	10.22	11.76	11.72	1473	1474	1471	3.06	2.45	2.72	916.5	
3-DLB-B	blubber	25.9	12.69	14.94	13.42	1461	1462	1459	2.52	2.14	2.46	n/a	
3-DLB-C	blubber	26.4	18.01	15.65	13.03	1462	1463	1459	1.90	2.04	2.69	n/a	
3-DLB-D	blubber	n/a	14.12	10.99	12.91	1449	1445	1446	2.36	2.64	2.58	n/a	
3-DLB-E	blubber	n/a	15.32	13.29	15.10	1456	1455	1453	2.19	2.29	2.19	n/a	
3-DLB-F	blubber	26.0	12.51	13.53	11.32	1445	1741	1215	2.62	2.57	2.90	n/a	
3-EM-A	muscle	n/a	18.69	11.71	19.68	1602	1610	1604	1.87	2.47	1.52	1067.6	
3-EM-B	muscle	24.5	9.87	10.70	7.93	1607	1591	1594	2.84	2.62	4.04	n/a	
3-EM-C	muscle	24.8	13.01	11.30	8.69	1593	1595	1593	2.15	2.48	2.99	n/a	
3-EM-D	muscle	n/a	8.70	10.81	9.16	1596	1591	1598	2.60	2.34	2.61	n/a	
3-EM-E	muscle	23.3	10.62	8.78	9.33	1595	1594	1594	2.76	3.12	3.03	n/a	
3-EM-F	muscle	24.1	10.95	13.82	14.31	1591	1590	1589	2.77	2.16	1.96	n/a	
4-DLB-A1	blubber	24.0	10.99	14.78	14.49	1465	1468	1472	2.61	2.14	2.33	930.8	
4-DLB-B1	blubber	19.2	13.89	14.88	13.98	1471	1473	1471	2.21	2.13	2.20	928.4	
4-DLB-B2	blubber	19.0	15.35	14.46	11.39	1466	1467	1465	2.00	1.85	2.34	909.8	
4-DLB-C1	blubber	19.1	13.54	12.12	12.14	1471	1474	1475	2.42	2.29	2.53	930.7	
4-DLB-D1	blubber	19.9	14.04	15.11	14.06	1468	1466	1465	2.19	2.16	2.11	906.4	
4-DLB-E1	blubber	25.0	13.69	15.01	16.24	1465	1463	1468	2.62	2.45	3.50	905.7	
4-DLB-F1	blubber	24.3	14.11	14.18	14.15	1469	1467	1467	2.16	2.14	2.16	981.3	
4-DLB-G1	blubber	21.3	14.77	14.21	16.62	1471	1473	1471	2.17	2.17	2.00	918.7	
4-DLB-G2	blubber	18.9	13.63	13.39	12.95	1471	1467	1467	2.62	2.21	2.29	977.0	
4-DLB-H1	blubber	24.9	14.23	16.41	15.76	1466	1470	1467	2.23	2.00	2.02	918.7	
4-DLB-I1	blubber	21.3	17.56	14.46	16.01	1471	1472	1472	2.10	2.41	2.11	932.5	
4-DLB-J1	blubber	23.0	12.18	12.70	16.33	1487	1488	1491	3.92	3.37	3.23	952.4	
4-EM-A1	muscle	20.5	12.37	14.80	11.66	1604	1607	1606	2.32	2.14	2.80	1053.9	
4-EM-B1	muscle	20.4	17.94	13.86	13.15	1603	1615	1603	1.93	2.86	2.56	1072.7	
4-EM-B2	muscle	20.8	12.31	16.22	11.31	1604	1606	1605	2.41	2.02	3.24	1078.0	
4-EM-C1	muscle	20.5	11.81	10.70	12.34	1618	1606	1602	2.68	3.43	2.41	827.7	
4-EM-D1	muscle	21.0	13.47	15.11	13.94	1601	1615	1603	3.17	2.69	2.06	1073.0	
4-EM-E1	muscle	20.5	12.57	16.07	11.04	1598	1601	1599	2.40	2.22	2.49	1046.6	
4-EM-F1	muscle	21.9	12.58	12.87	11.41	1595	1600	1592	3.38	2.28	3.16	1082.4	
4-EM-G1	muscle	22.6	8.68	10.50	9.14	1594	1594	1597	3.35	3.37	2.98	1071.0	
4-EM-G2	muscle	21.8	11.16	14.27	16.54	1597	1588	1597	2.92	1.93	2.94	1079.5	
4-EM-H1	muscle	22.0	14.37	10.02	11.28	1585	1584	1588	2.49	2.57	3.00	1074.4	
2-atrium	heart	11.0	15.42	n/a	n/a	1576	n/a	n/a	2.19	n/a	n/a	1079.3	
2-atrium	heart	11.0	15.81	n/a	n/a	1581	n/a	n/a	3.81	n/a	n/a	1079.3	
2-esphagus	esphagus	14.9	6.92	n/a	n/a	1613	n/a	n/a	4.29	n/a	n/a	1087.2	
2-left lung-1	lung	15.8	9.58	n/a	n/a	1621	n/a	n/a	3.20	n/a	n/a	1146.8	
2-left lung-2	lung	15.8	10.68	n/a	n/a	1603	n/a	n/a	2.41	n/a	n/a	1146.8	
2-right lung	lung	13.2	4.90	n/a	n/a	1552	n/a	n/a	16.47	n/a	n/a	963.5	
2-trachaea	cartilage	18.8	3.76	n/a	n/a	1629	n/a	n/a	8.70	n/a	n/a	1096.8	
2-ventrical-1	heart	5.6	10.14	n/a	n/a	1552	n/a	n/a	2.93	n/a	n/a	1087.2	
2-ventrical-2	heart	5.6	15.23	n/a	n/a	1569	n/a	n/a	2.93	n/a	n/a	1087.2	
2-liver	liver	13.7	13.00	n/a	n/a	1585	n/a	n/a	3.21	n/a	n/a	1064.4	

Appendix: Physical property data collected from *Ziphius cavirostris* specimen

Sample #	Elastic Modulus at 5 kPa AP	Elastic Modulus at 10 kPa AP	Elastic Modulus at 20 kPa AP	Elastic Modulus at 30 kPa AP	Elastic Modulus at 40 kPa AP	Elastic Modulus at 50 kPa AP	Elastic Modulus at 5 kPa DV	Elastic Modulus at 10 kPa DV	Elastic Modulus at 2 0kPa DV	Elastic Modulus at 30 kPa DV	Elastic Modulus at 40 kPa DV	Elastic Modulus at 50 kPa DV
1-DLB-A	162200	440300	563600	873900	1772700	1645200	160700	255700	622100	1556000	1089200	1527700
1-DLB-B	158700	280400	858000	793500	877800	793500	268900	497600	719900	663400	1103300	1237300
1-EMB-A	252900	414800	703400	927500	839400	n/a	288000	448100	592100	726100	1214600	1566200
1-EMB-B	299500	441200	642800	808400	1283900	1313500	171800	388800	581400	1104200	956700	1211300
1-EMB-C	213600	349400	621500	530200	1025500	1068900	n/a	612300	617600	1186200	1013400	1184500
1-EMB-D	273400	404000	630000	587600	980600	1138600	184200	309600	678900	928900	965000	1132400
1-EMB-E	223500	360400	524700	877300	707000	739300	163000	307200	431600	n/a	n/a	n/a
1-EMB-F	217600	262800	615800	712200	676000	782700	n/a	426800	598900	1291400	1340700	1158700
1-EMB-G	249400	432800	478300	896800	868800	570600	115000	271200	515000	1006400	1041900	n/a
1-EMB-H	165200	301700	884900	642400	595200	576800	197500	317600	635100	737800	607100	732200
1-EMB-I	333800	673300	828700	795700	1400000	2109800	278500	380900	597900	1380100	1270200	1194500
1-EMF-A	268600	515700	525700	698400	483500	1557900	209800	298300	305500	626700	839300	731100
1-EMF-B	265000	307400	410300	829100	718900	697700	256300	337800	473700	178600	862000	885300
1-EMF-C	554300	458200	932400	808100	893100	772100	270800	731600	856300	972000	1030500	2235000
1-EMF-D	336100	466800	575100	631500	1008400	1020800	140600	244200	763300	878800	959400	1102900
1-EMF-E	278500	340300	462200	1082900	966700	983100	216300	402600	467800	848700	782200	1124000
1-EMF-F	346200	516100	493100	256300	1374300	898700	n/a	523100	589000	674500	1108700	1283000
1-EMF-G	303100	421900	559300	671300	735300	1157100	333400	622300	491600	578100	596400	n/a
1-EMF-H	561800	825800	1363200	1564800	1667800	1409200	292500	352300	591100	608700	463800	1085700
1-EMF-I	362500	348300	396300	970200	654700	716500	192200	396800	453800	335300	860900	760800
1-EMF-J	240400	353700	704600	543700	939500	762500	305300	415000	427000	925800	1017600	1021600
1-EMF-K	367100	572300	994900	1628600	n/a	1710900	239500	310400	276400	558900	614900	601900
1-IMF-A	n/a	385500	592100	635100	648100	772300	n/a	317300	285000	357100	535000	609700
1-IMF-B1	n/a	350900	408100	767200	823400	748500	n/a	481900	477300	456800	387300	983900
1-IMF-B2	n/a	n/a	n/a	n/a	n/a	n/a	n/a	n/a	n/a	n/a	n/a	n/a
1-IMF-C1	245500	319200	307800	949400	928200	998600	357200	440900	624700	633400	498900	1649700
1-IMF-C2	139700	198800	265000	n/a	n/a	n/a	256500	219900	235600	n/a	n/a	n/a
1-IMF-D1	216300	283200	207100	485800	613700	552300	230700	340000	368400	1041800	694600	714400
1-IMF-D2	440300	339300	271500	452200	430700	321600	2007800	571700	453700	683200	611700	690200
1-IMF-E1	177600	155100	361800	709100	299800	n/a	243100	333700	277000	664100	1526700	892700
1-IMF-E2	202500	277300	498500	695500	562200	n/a	293300	396700	338400	1015300	991200	687500
1-IMF-E2	n/a	n/a	n/a	n/a	n/a	n/a	n/a	n/a	n/a	n/a	n/a	n/a
1-IMF-E3	121700	150700	408200	561100	684600	n/a	110600	289100	n/a	n/a	n/a	n/a
1-IMF-E4	201900	189300	360500	341800	n/a	n/a	149100	144500	201500	n/a	n/a	n/a
1-IMF-F1	235200	322500	379700	695500	596700	667500	397400	471000	699200	693300	1159200	878800
1-IMF-F2	213500	427000	582000	429500	841800	995000	n/a	438800	552400	444800	941900	994200
1-IMF-F3	90800	129800	290100	167400	n/a	n/a	164300	197900	162300	n/a	n/a	n/a
1-IMF-F4	n/a	n/a	n/a	n/a	n/a	n/a	n/a	n/a	n/a	n/a	n/a	n/a
1-IMF-F5	168800	151000	n/a	n/a	n/a	n/a	175000	341200	356700	274200	175000	n/a
1-IMF-G1	170800	191700	222300	n/a	n/a	n/a	215100	295600	472600	422400	909400	894700
1-IMF-G2	178300	319600	586900	598100	841100	793900	203500	304600	509000	640500	580800	563100
1-IMF-G3	88800	162300	157900	n/a	n/a	n/a	160500	148200	252200	n/a	n/a	n/a
1-IMF-G4	94700	127400	81000	n/a	n/a	n/a	186600	215400	304900	252000	n/a	n/a
1-IMF-G5	268500	277100	601000	558400	528500	614700	140600	213600	300300	486800	n/a	n/a
1-IMF-H1	302400	224900	374800	400600	385300	479800	n/a	554200	721100	642200	621500	1087700
1-IMF-H2	Inf	565500	721200	829500	750100	922200	194700	288900	330300	839700	989400	1078800
1-IMF-H3	125300	202800	n/a	n/a	n/a	n/a	136900	82200	179800	n/a	n/a	n/a
1-IMF-H4	112100	155400	231100	n/a	n/a	n/a	99800	172100	n/a	n/a	n/a	n/a
1-IMF-H5	113400	96900	279500	n/a	n/a	n/a	148000	191700	441000	515900	n/a	n/a
1-IMF-H6	n/a	n/a	n/a	n/a	n/a	n/a	n/a	n/a	n/a	n/a	n/a	n/a
1-IMF-I1	138100	88200	284900	239300	n/a	n/a	228500	200900	368400	503600	449700	402900
1-IMF-I2	422300	546800	559700	1039500	851800	933900	220000	372300	342100	327200	n/a	955100
1-IMF-I3	148900	158900	228400	n/a	n/a	n/a	147500	202300	n/a	n/a	n/a	n/a
1-IMF-I4	147600	242500	376400	440200	536600	n/a	31600	n/a	n/a	n/a	n/a	n/a
1-IMF-I5	124300	167400	329800	n/a	n/a	n/a	n/a	238500	260600	357100	584600	n/a
1-IMF-I6	209700	344000	491500	847800	877300	943600	205700	280800	246000	737800	839300	757100
1-IMF-J1	340800	266500	494300	443900	417000	n/a	180700	75700	299400	309200	n/a	n/a
1-IMF-J2	120100	165700	170000	n/a	n/a	n/a	124900	279500	249700	n/a	n/a	n/a

Appendix: Physical property data collected from *Ziphius cavirostris* specimen

Sample #	Elastic Modulus at 5 kPa AP	Elastic Modulus at 10 kPa AP	Elastic Modulus at 20 kPa AP	Elastic Modulus at 30 kPa AP	Elastic Modulus at 40 kPa AP	Elastic Modulus at 50 kPa AP	Elastic Modulus at 5 kPa DV	Elastic Modulus at 10 kPa DV	Elastic Modulus at 2 0kPa DV	Elastic Modulus at 30 kPa DV	Elastic Modulus at 40 kPa DV	Elastic Modulus at 50 kPa DV
1-IMF-J3	113900	130500	215700	n/a	n/a	n/a	148800	190800	303100	272800	n/a	n/a
1-IMF-J4	84100	87900	221800	302100	n/a	n/a	n/a	216200	297500	245400	n/a	n/a
1-IMF-J5	196200	207500	255300	414700	569800	471000	89300	103400	323200	n/a	n/a	n/a
1-IMF-K1	n/a	185600	284400	616100	610900	880200	n/a	n/a	n/a	n/a	n/a	n/a
1-IMF-K2	76800	99100	n/a	n/a	n/a	n/a	133600	198200	399900	323900	316000	n/a
1-IMF-K3	123800	193800	531100	677500	649700	595100	151500	302300	281200	652500	783200	790300
1-IMF-K4	118900	150000	372100	403700	599700	n/a	181600	133900	329500	257700	n/a	n/a
1-IMF-K5	n/a	n/a	n/a	n/a	n/a	n/a	n/a	n/a	n/a	n/a	n/a	n/a
1-IMF-K6	n/a	n/a	n/a	n/a	n/a	n/a	n/a	n/a	n/a	n/a	n/a	n/a
1-IMF-K7	n/a	n/a	n/a	n/a	n/a	n/a	n/a	n/a	n/a	n/a	n/a	n/a
1-LNP-1	51500	136400	227300	n/a	n/a	n/a	64000	227600	358200	498400	822700	973900
1-LNP-1	51200	n/a	n/a	n/a	n/a	n/a	43900	145500	237100	237100	n/a	n/a
1-RNP-2	115700	35000	535800	834000	1190700	954300	130600	242300	903400	970000	1025500	n/a
1-Thyroid-1	n/a	n/a	n/a	n/a	n/a	n/a	n/a	n/a	n/a	n/a	n/a	n/a
1-Thyroid-2	n/a	n/a	n/a	n/a	n/a	n/a	n/a	n/a	n/a	n/a	n/a	n/a
1-Thyroid-3	n/a	n/a	n/a	n/a	n/a	n/a	n/a	n/a	n/a	n/a	n/a	n/a
1-Tongue-1A	202900	174800	308400	476400	357900	429800	194500	195900	324200	393900	601100	384200
1-Tongue-2P	294800	210600	374800	499400	402400	783300	177700	228500	380900	399000	761700	n/a
1-VCB-1	207200	397700	464800	749900	1174300	1087600	186500	338800	606000	773400	610500	720500
1-Hyoid-1	n/a	n/a	n/a	n/a	n/a	n/a	n/a	n/a	n/a	n/a	n/a	n/a
1-Hyoid-2	n/a	n/a	n/a	n/a	n/a	n/a	n/a	n/a	n/a	n/a	n/a	n/a
1-Hyoid-3	n/a	n/a	n/a	n/a	n/a	n/a	n/a	n/a	n/a	n/a	n/a	n/a
1-Hyoid-4	n/a	n/a	n/a	n/a	n/a	n/a	n/a	n/a	n/a	n/a	n/a	n/a
1-Hyoid-5	n/a	n/a	n/a	n/a	n/a	n/a	n/a	n/a	n/a	n/a	n/a	n/a
1-Hyoid-6	n/a	n/a	n/a	n/a	n/a	n/a	n/a	n/a	n/a	n/a	n/a	n/a
1-F-A1	401450	440550	693410	1135900	1366900	1824800	293760	485970	813720	1022300	1727300	1753800
1-F-A2	185900	329780	746850	1399500	1801300	2203900	84992	253340	294200	686470	n/a	n/a
1-F-A3	200090	504630	1262400	1750800	n/a	2509000	120240	362120	464720	591460	n/a	n/a
1-F-B1	122680	480060	1202400	1304200	1543300	2080300	176330	418820	1241000	1015500	1257500	1461400
1-F-B2	124040	235160	516190	904390	1065400	1247800	219650	402950	666530	1127000	1348200	1367900
1-F-B3	74483	289660	480000	937950	n/a	n/a	94853	257460	418130	338760	n/a	n/a
1-F-B4	104690	366420	945210	982680	1569800	n/a	352740	574330	805660	776020	1914900	2007900
1-F-B5	389030	530150	619400	805520	1043500	1954300	185390	310040	717460	1058900	1061000	1278900
1-F-B6	176530	394000	1002900	1225800	1508900	1764100	159560	216300	611660	670160	992830	1657700
1-F-C1	272550	481530	443120	1251000	1004200	1441900	235040	485300	750470	1241600	1499900	1484400
1-F-C2	367350	632380	1335200	1919800	3603100	1764200	233660	368020	615870	1316900	1034000	1199500
1-F-C3	103860	264010	766030	1190000	1920100	1879600	265170	366940	684070	1364500	1508200	1959300
1-F-C4	283200	640100	847540	819160	n/a	n/a	173110	352520	572480	1545400	1276600	1872600
1-F-C5	124920	389450	509470	578050	940570	813200	212780	352550	655940	883300	947230	1003400
1-F-C6	217200	290330	573660	630240	739830	1012200	86809	252930	325800	563290	n/a	n/a
1-F-C7	295500	400580	624290	953460	n/a	n/a	253220	385900	600120	1215400	1481300	1412900
1-F-C8	205480	402670	1184700	1401100	1450200	1506100	88884	299340	584910	804250	1211100	1072300
1-F-C9	59559	270720	779670	933990	1510600	1830100	154230	292580	622970	792320	1149900	1329800
1-F-D1	279390	555600	873090	1131700	1658900	1053500	388870	701150	1004600	1320500	1555500	1382700
1-F-D2	126520	349200	673090	1210400	1176900	2225900	259490	390030	572070	1032700	1009700	1550200
1-F-D3	109060	233690	1051600	817910	1064600	1239900	96673	217080	528410	n/a	n/a	n/a
1-F-D4	147490	490040	615130	1044600	1403800	1383100	176010	378200	694580	896040	1215100	1360100
1-F-D5	126450	300690	841940	1127600	1308000	n/a	247780	692340	835950	n/a	1570900	n/a
1-F-D6	106300	273580	353290	641520	898450	911160	106050	282800	362340	433040	537320	n/a
1-F-D7	94540	182410	312130	568530	313520	n/a	143900	308260	373390	526790	n/a	n/a
1-F-D8	114250	146240	436290	624580	639820	621530	76040	255490	374720	n/a	n/a	n/a
1-F-D9	184410	465490	653720	720170	2327400	1709300	146560	177830	616280	663320	1021500	1016200
1-F-D10	94654	276680	352530	413400	n/a	n/a	78655	196320	393720	468150	n/a	n/a
1-F-D11	144940	305720	942080	1316700	985840	1273400	144870	485480	808470	687990	1093800	1268200
1-F-E1	238940	450260	694430	957630	1058400	n/a	179840	439440	761690	1368700	1184800	1317100
1-F-E2	149870	319210	1034700	1116100	1603900	1198700	141330	245840	565300	723260	659520	681690
1-F-E3	149960	243060	943940	847980	870300	1198300	296890	362870	635020	633580	645100	673910
1-F-E4	239620	333070	421050	1098300	1063900	1086300	245430	403450	998550	980390	1062400	1022100

Appendix: Physical property data collected from *Ziphius cavirostris* specimen

Sample #	Elastic Modulus at 5 kPa AP	Elastic Modulus at 10 kPa AP	Elastic Modulus at 20 kPa AP	Elastic Modulus at 30 kPa AP	Elastic Modulus at 40 kPa AP	Elastic Modulus at 50 kPa AP	Elastic Modulus at 5 kPa DV	Elastic Modulus at 10 kPa DV	Elastic Modulus at 2 0kPa DV	Elastic Modulus at 30 kPa DV	Elastic Modulus at 40 kPa DV	Elastic Modulus at 50 kPa DV
1-F-E5	268630	419650	821930	1343200	1571700	1098600	275690	429070	780590	833970	1775500	1853300
1-F-E6	277450	424200	699410	479160	1747200	1868500	199530	342060	697040	1170600	991020	1401200
1-F-E7	141120	211690	488900	819870	584660	1139100	64782	214900	320350	n/a	n/a	n/a
1-F-E8	188540	222210	630190	592560	780680	696030	198120	269140	493420	794960	601360	853210
1-F-E9	176220	173870	512990	765280	822350	669630	146560	173700	352830	411760	n/a	n/a
1-F-E10	431050	490260	665850	826780	n/a	2036800	283540	495160	842320	1093900	1207100	1377600
1-F-E11	100820	179300	596080	720060	724830	877430	148320	287510	793490	1201400	1097500	1364500
1-F-E12	162360	228530	392630	417830	443420	n/a	177750	219250	735540	819820	851320	1187600
1-F-E13	126910	234980	800880	717450	1023500	1182400	72616	311590	761660	1307100	2207500	2033300
1-F-F1	267390	336930	646910	565440	1380100	1437600	187200	472540	1004600	1255800	1325000	1594300
1-F-F2	305160	485520	693140	1092200	1193200	1307500	164820	335470	596550	600610	1003200	594110
1-F-F3	190650	346350	346950	912860	842960	1198300	93535	160510	319620	n/a	n/a	n/a
1-F-F4	239970	316140	762950	983730	868590	770780	145140	271860	351620	558660	n/a	n/a
1-F-F5	221590	484390	673480	1200300	1691600	1937600	249210	406000	441870	1053500	1104700	1233300
1-F-F6	142670	396860	541370	747450	1178800	1113700	256310	524250	863710	303940	2234500	1707000
1-F-F7	266370	333910	541210	1062800	1158700	1293600	243440	267130	316370	725290	679950	1171000
1-F-F8	150230	198800	641030	650690	737670	737670	133370	31716	224130	n/a	n/a	n/a
1-F-F9	175370	209790	669350	652720	576500	565420	135090	153920	414030	442100	278360	n/a
1-F-F10	295330	479370	400360	1288300	1137600	1064900	195250	255330	610170	857720	886770	1529500
1-F-F11	93305	439310	618920	1190700	1594000	1621200	130270	521090	718470	1018500	1070800	1724300
1-F-F12	117470	241670	791850	1150100	879830	1058900	132010	274800	499760	n/a	n/a	n/a
1-F-F13	12916	135620	n/a	n/a	n/a	n/a	127660	149460	496410	546450	728600	890510
1-F-F14	159480	166420	696110	626710	686810	667070	73798	304720	354110	424940	n/a	n/a
1-F-F15	243060	311930	540130	491520	571190	613730	18625	71707	n/a	n/a	n/a	n/a
1-F-F16	41585	90102	n/a	n/a	n/a	n/a	170340	251360	411310	483120	280730	n/a
1-F-F17	92811	311950	739910	860050	1470200	1448300	106260	715820	n/a	n/a	n/a	n/a
1-F-G1	265900	279130	725170	1216900	1298200	1560600	299640	449460	682890	1024300	1274300	1449400
1-F-G2	106810	107640	326140	419790	415750	458540	157150	208960	395120	493900	533420	n/a
1-F-G3	139550	360160	444640	437020	675850	n/a	103690	138250	n/a	n/a	n/a	n/a
1-F-G4	132340	280120	813900	989250	1041100	1085200	186530	375050	726610	1199600	976530	822920
1-F-G5	132220	281780	1252800	2057400	n/a	1596900	219550	379220	1011900	1103900	1481800	2357400
1-F-G6	244720	399820	547400	569940	1807800	1499100	100660	186230	352320	327150	n/a	n/a
1-F-G7	82859	402790	498690	524150	922310	926420	116520	269170	277090	n/a	n/a	n/a
1-F-G8	110720	204410	n/a	n/a	n/a	n/a	85654	187370	203430	n/a	n/a	n/a
1-F-G9	365680	394110	501590	844790	1061200	1028900	125820	327470	352180	n/a	n/a	n/a
1-F-G10	134220	272570	107380	1291900	1208000	n/a	228390	387840	413700	1022700	1325100	1292800
1-F-G11	187830	99150	605920	775570	1357200	1267200	130300	304310	880540	1385600	2092400	2117200
1-F-G12	41504	147710	n/a	n/a	n/a	n/a	133680	335620	346990	n/a	n/a	n/a
1-F-G13	173350	133350	404490	480050	210020	n/a	67857	158330	n/a	n/a	n/a	n/a
1-F-G14	60375	147580	211310	n/a	n/a	n/a	171670	176440	384220	392400	n/a	n/a
1-F-G15	80667	272020	322050	402000	759770	n/a	182510	71106	355530	186650	n/a	n/a
1-F-G16	58036	193450	n/a	n/a	n/a	n/a	70706	14590	n/a	n/a	n/a	n/a
1-F-G17	156370	241080	767080	1048300	1269900	1323200	180030	281530	690530	1395900	1273600	1908800
1-F-H1	207350	463810	613600	1051100	1458100	n/a	281530	754210	843780	1126100	667330	2210500
1-F-H2	231910	531170	436670	1053900	1231800	1252100	200050	325090	793590	684590	713910	911520
1-F-H3	194190	279010	293270	931840	784700	1242500	158230	171060	443200	555950	769770	818650
1-F-H4	275880	334860	961410	1017400	1360400	1327700	118860	188070	442210	623500	460850	n/a
1-F-H5	304630	387680	659760	752610	1769500	2011400	324550	452190	878410	950700	1638300	1574700
1-F-H6	132830	633140	634350	1319400	1917800	1974700	143990	101110	818270	913600	667320	n/a
1-F-H7	320380	137780	715810	898030	1941000	1548500	n/a	n/a	n/a	n/a	n/a	n/a
1-F-H8	178600	317520	363310	687960	1083000	678330	183870	124170	376490	105070	n/a	n/a
1-F-H9	256750	270320	684520	693230	865770	809020	168330	167040	336660	382910	n/a	n/a
1-F-H10	315260	288160	387380	1154400	1200800	1210100	120690	114410	302360	451080	n/a	n/a
1-F-H11	403580	601420	791340	1343700	1727100	1698700	81054	209790	257860	n/a	n/a	n/a
1-F-H12	n/a	n/a	n/a	n/a	n/a	n/a	100410	468430	524410	1142900	1071400	1431600
1-F-H13	66589	258850	341460	732480	n/a	n/a	93906	181940	510620	n/a	n/a	n/a
1-F-H14	n/a	n/a	n/a	n/a	n/a	n/a	63910	105820	n/a	n/a	n/a	n/a
1-F-H15	210130	310620	609060	502480	409290	n/a	96266	138560	262060	424500	485790	n/a

Appendix: Physical property data collected from *Ziphius cavirostris* specimen

Sample #	Elastic Modulus at 5 kPa AP	Elastic Modulus at 10 kPa AP	Elastic Modulus at 20 kPa AP	Elastic Modulus at 30 kPa AP	Elastic Modulus at 40 kPa AP	Elastic Modulus at 50 kPa AP	Elastic Modulus at 5 kPa DV	Elastic Modulus at 10 kPa DV	Elastic Modulus at 2 0kPa DV	Elastic Modulus at 30 kPa DV	Elastic Modulus at 40 kPa DV	Elastic Modulus at 50 kPa DV
1-F-H16	87157	217890	377680	n/a	n/a	n/a	117520	204770	200310	n/a	n/a	n/a
1-F-H17	201950	309520	315390	716110	710320	732260	151340	231220	246630	n/a	n/a	n/a
1-F-H18	137890	107570	253040	298270	n/a	n/a	105760	191930	222090	n/a	n/a	n/a
1-F-H19	54579	168420	360140	316070	n/a	n/a	83405	125110	338640	n/a	n/a	n/a
1-F-H20	126460	82873	538670	749210	1078300	1109200	88020	324570	572130	655260	1214700	1179500
1-F-I1	194800	355370	280610	n/a	1300400	n/a	183790	376180	962480	1679000	1710900	2128100
1-F-I2	207520	408880	743840	970230	2384000	2146600	307800	564290	699570	1122400	1187300	1319300
1-F-I3	148160	323100	735740	859830	957340	988370	105520	278320	392500	513820	337190	n/a
1-F-I4	329490	577220	914730	959800	1641100	n/a	118860	413420	458210	511610	198950	n/a
1-F-I5	122020	347300	826010	1109500	1727100	n/a	138050	644230	763870	1089100	1390700	1616300
1-F-I6	112660	323550	860860	1031300	1590800	1612000	70602	405960	711900	1317900	1388500	1553200
1-F-I7	193580	247600	643760	702280	799820	1170500	80532	317390	431080	522270	549510	671500
1-F-I8	70788	213020	297010	n/a	n/a	n/a	96385	112450	n/a	n/a	n/a	n/a
1-F-I9	141000	163120	421490	543600	641800	905710	119040	213280	223200	n/a	n/a	n/a
1-F-I10	78626	207920	277230	381600	n/a	n/a	174510	207630	480880	593340	713560	525200
1-F-I11	246960	358290	842080	896060	791880	971630	103130	292830	486200	442010	430950	n/a
1-F-I12	147120	244360	754030	961930	1229600	1671300	139810	349110	713000	1280100	1634700	1934000
1-F-I13	115880	227460	531110	726160	1081600	n/a	98718	344020	638180	1088100	1403800	1334900
1-F-I14	156560	176320	390570	480520	542030	588710	92234	159870	n/a	n/a	n/a	n/a
1-F-I15	101250	215020	314940	453170	n/a	n/a	115730	175480	217840	n/a	n/a	n/a
1-F-I16	98208	290610	473180	693700	343730	n/a	62015	177820	128030	n/a	n/a	n/a
1-F-I17	121880	182300	452100	427790	1104700	514080	157940	170740	445150	435390	163630	n/a
1-F-I18	84456	162100	228850	n/a	n/a	n/a	71224	174450	n/a	n/a	n/a	n/a
1-F-I19	408960	693770	917540	904070	2348300	n/a	45255	n/a	n/a	n/a	n/a	n/a
1-F-I20	92350	215480	n/a	n/a	n/a	n/a	141610	154490	544990	822090	844850	951060
1-F-I21	96435	376100	275150	671600	443250	n/a	336470	373590	133250	774540	804290	585370
1-F-I22	87829	163730	347500	n/a	n/a	n/a	86857	209000	314130	n/a	n/a	n/a
1-F-I23	73138	300680	292560	n/a	n/a	n/a	120740	508000	819200	884740	1786300	n/a
1-F-J1	174090	305840	795170	1073800	1137700	1913700	99628	193720	714000	759670	n/a	n/a
1-F-J2	188240	385260	544810	2235800	n/a	1659600	132280	258270	793700	1052000	1063200	1229100
1-F-J3	176570	261600	250290	889920	1052800	991630	119010	30855	459400	1100500	811050	730240
1-F-J4	95914	360920	641630	866530	1023200	1476400	119010	171400	244290	n/a	n/a	n/a
1-F-J5	149550	341160	537440	635580	n/a	n/a	174300	357470	1026700	1160400	1555400	1992000
1-F-J6	433360	443210	714180	652660	1726100	1802700	256950	419070	587300	738720	1293300	2232200
1-F-J7	108690	205630	370140	n/a	n/a	n/a	213600	149680	406570	740330	n/a	n/a
1-F-J8	241520	207020	504220	697310	633980	1115400	189720	133510	333770	474300	n/a	n/a
1-F-J9	54329	113510	n/a	n/a	n/a	n/a	152370	146080	110820	n/a	n/a	n/a
1-F-J10	n/a	544320	675010	834740	806640	1923700	271590	263360	256500	502440	547700	1071300
1-F-J11	172960	199570	213830	908060	997870	1345300	69666	171110	597140	708120	1017500	1292500
1-F-J12	159410	247220	581690	1030100	967970	1430000	117510	270410	685040	n/a	n/a	n/a
1-F-J13	115710	166930	552810	580460	685730	690470	275540	370920	594710	571490	675080	787590
1-F-J14	154730	202340	630830	790020	1127300	1219100	147320	139780	385420	575560	n/a	n/a
1-F-J15	197400	138800	485790	666220	570330	971570	212620	379780	489030	497540	708030	312550
1-F-J16	198550	420850	652710	1170800	1918000	1807000	106000	355530	506960	n/a	n/a	n/a
1-F-K1	n/a	286130	352860	1035000	1627400	1986900	139920	186310	553590	819740	1052400	1161900
1-F-K2	146140	292290	947400	1375200	1268700	1534500	n/a	143930	323840	719650	969530	1175400
1-F-K3	263760	372360	429650	124120	1459900	1386000	n/a	52347	n/a	n/a	n/a	n/a
1-F-K4	96520	132610	275770	n/a	n/a	n/a	256800	209780	261930	n/a	n/a	n/a
1-F-K5	101550	123320	587940	681130	975520	936920	331450	347240	613810	621990	969810	871600
1-F-K6	393220	403550	518910	524290	1603900	n/a	391700	323500	465820	1329000	1110700	1433900
1-F-K7	275870	304910	422180	1293000	1603600	2090800	94550	229100	575300	956010	1137000	1425500
1-F-K8	247200	251680	212770	904820	928760	1086700	137730	282710	1052300	1235600	n/a	1855300
1-F-K9	226190	245330	398100	1143900	1156800	1092200	136190	215630	n/a	n/a	n/a	n/a
1-F-K10	165870	262690	461030	783170	495170	607120	238740	188640	353690	n/a	n/a	n/a
1-F-K11	n/a	n/a	n/a	n/a	n/a	n/a	n/a	n/a	n/a	n/a	n/a	n/a
1-F-K12	230790	435200	1023100	1548800	1096200	2107800	348900	381990	624700	848200	880680	1899400
1-F-K13	57549	106160	n/a	n/a	n/a	n/a	315330	324980	401670	986520	1193700	1306300
1-F-K14	284050	258030	537430	712370	847630	897220	148440	207340	n/a	n/a	n/a	n/a

Appendix: Physical property data collected from *Ziphius cavirostris* specimen

Sample #	Elastic Modulus at 5 kPa AP	Elastic Modulus at 10 kPa AP	Elastic Modulus at 20 kPa AP	Elastic Modulus at 30 kPa AP	Elastic Modulus at 40 kPa AP	Elastic Modulus at 50 kPa AP	Elastic Modulus at 5 kPa DV	Elastic Modulus at 10 kPa DV	Elastic Modulus at 2 0kPa DV	Elastic Modulus at 30 kPa DV	Elastic Modulus at 40 kPa DV	Elastic Modulus at 50 kPa DV
1-F-K15	308280	435220	598430	764220	1262100	1142500	142940	215510	963810	869060	1322200	1743800
1-F-K16	176270	259230	402800	813970	842480	1022100	n/a	569810	1042900	n/a	1578700	1118500
1-F-K17	257570	272020	435040	439200	555320	1512500	167220	255950	389050	1218300	1110800	1261300
1-F-K18	153590	121520	351060	526590	607040	800850	159850	139870	399620	479540	619410	531490
1-F-K19	254830	240670	130250	515950	601680	703820	157340	150190	438300	598450	531020	616250
1-F-K20	218750	188370	602790	802100	831800	1166700	155510	202220	818350	671860	919930	985680
1-F-K21	178310	287040	461000	930710	1067900	1164600	139080	241200	604450	590550	1126900	1162500
1-F-K22	119230	169310	463050	711810	1071000	915690	130170	163540	564060	677950	1106400	949140
1-F-K23	127960	192510	240260	n/a	n/a	n/a	44328	n/a	n/a	n/a	n/a	n/a
1-F-K24	238050	324390	429600	1068300	1117000	1432000	183630	234960	662790	767990	1106100	1142200
1-F-K25	361880	444810	546580	650870	870760	490040	227950	406090	554220	759820	1051200	n/a
1-F-K26	373940	768240	1285600	2047400	2004500	n/a	n/a	528270	1079200	1305600	1304800	2477200
1-F-K27	108920	158850	536110	628330	734220	1025700	117910	141490	411900	605270	866920	871410
1-F-K28	221670	394320	542000	671410	1851300	1586800	184690	304430	360440	809600	716320	604710
1-F-K29	232170	514340	821510	1004900	1089600	975090	156000	229550	690350	771210	1044900	932910
1-F-K30	n/a	n/a	n/a	n/a	n/a	n/a	242810	312180	439370	1474200	1295000	1769000
1-F-K31	201710	266050	632700	813800	1314600	n/a	259770	474590	779320	887560	779320	1659700
1-F-L1	335430	504850	784790	1032100	1097900	1856800	329360	441300	668160	981620	613510	2026200
1-F-L2	287920	349190	983560	1124400	1435200	1301300	327170	360180	869550	785200	1177800	1590000
1-F-L3	114090	260570	344080	n/a	n/a	n/a	200730	200110	438080	295070	n/a	n/a
1-F-L4	257580	346740	613030	881490	798490	1205500	187640	210230	516020	647080	1254200	817030
1-F-L5	382190	580860	608900	816650	2081900	1791400	506830	495090	494760	440270	1095000	941980
1-F-L6	133870	236980	774730	971370	995510	1113800	270410	563640	750170	1308400	969990	788550
1-F-L7	164930	261140	568090	581830	645970	804030	222090	303140	337440	709950	1111800	1865600
1-F-L8	n/a	363400	552570	885300	1244800	1164900	n/a	498440	898650	1152600	824060	1686200
1-F-L9	304420	311480	433800	1121600	1265500	1070800	138240	164070	469040	581190	661590	n/a
1-F-L10	182790	428830	714510	523900	1001500	1047800	305530	584190	706970	1175000	1164400	1234400
1-F-L11	183870	288170	473030	1055300	n/a	n/a	n/a	734670	1021300	1119500	1165000	1795900
1-F-L12	162680	190240	619020	712650	827090	716700	173480	186820	364300	456380	760630	655540
1-F-L13	99635	256740	419220	571630	614590	748810	106440	177400	n/a	n/a	n/a	n/a
1-F-L14	132430	195870	634120	831200	912130	971170	284640	233520	434290	853930	618080	1089800
1-F-L15	91617	127610	n/a	n/a	n/a	n/a	184850	238760	n/a	n/a	n/a	n/a
1-F-L16	455790	512770	955410	1115400	1170300	1172700	315160	419200	623750	1369400	1130800	1047200
1-F-L17	231140	208420	839840	1057800	932390	1410300	235630	181460	325000	557150	477350	771890
1-F-L18	172340	323750	530930	853750	863490	977100	230810	356940	493700	994820	998190	957720
1-F-L19	89177	199880	473050	524690	n/a	n/a	212230	277190	646790	642290	848900	779600
1-F-L20	333130	285540	645450	758810	1106500	1171200	135820	168470	354170	830590	713050	1167500
1-F-M1	97042	149590	n/a	n/a	n/a	n/a	82356	168300	263760	n/a	n/a	n/a
1-F-M2	76278	175710	n/a	n/a	n/a	n/a	60521	99909	n/a	n/a	n/a	n/a
1-F-M3	137480	94200	423580	630120	443420	n/a	176070	186030	450660	450660	n/a	n/a
1-F-M4	201880	293170	471050	576140	720170	1014600	118720	175440	675460	677210	656160	481420
1-F-M5	117940	211380	329040	n/a	n/a	n/a	123150	228710	490100	n/a	n/a	n/a
1-F-M6	173780	220680	312100	n/a	n/a	n/a	115910	199120	336260	361100	n/a	n/a
1-F-M7	165670	269040	613610	791550	925010	797690	253430	349560	474090	1048700	675680	1140400
1-F-M8	193510	234980	516040	681330	655800	757930	191630	292800	537400	916500	877340	1113700
1-F-M9	185390	278580	513440	851480	910770	1142500	107910	95364	403610	755880	791040	900730
1-F-M10	169080	193560	n/a	n/a	n/a	n/a	98112	205350	n/a	n/a	n/a	n/a
1-F-M11	132440	264880	614910	851410	948710	977090	191600	274580	753650	592010	1019200	1076100
1-F-M12	184810	302540	693670	1117900	1433300	1348700	142430	194900	501690	860820	596890	n/a
1-F-M13	282350	449940	798130	1177100	1243700	1348100	261290	467710	806730	1554700	1930300	2003200
1-F-M14	68326	133100	n/a	n/a	n/a	n/a	63693	169110	n/a	n/a	n/a	n/a
1-F-M15	225530	419430	316560	797860	786320	730940	997440	703260	1396900	1537000	1846900	1710700
1-F-O1	67275	163980	n/a	n/a	n/a	n/a	118760	375250	560810	696070	669670	n/a
1-F-O2	345470	552850	783410	1741600	1255700	1355300	215210	427870	329110	1172700	1741100	1830900
1-F-O3	285050	492740	663440	1405700	1717500	2054400	230290	376590	668890	864570	1067400	1145700
2-DLB-A1												
2-DLB-B1												
2-DLB-C1												

Appendix: Physical property data collected from *Ziphius cavirostris* specimen

Sample #	Elastic Modulus at 5 kPa LR	Elastic Modulus at 10 kPa LR	Elastic Modulus at 20 kPa LR	Elastic Modulus at 30 kPa LR	Elastic Modulus at 40 kPa LR	Elastic Modulus at 50 kPa LR
1-DLB-A	1578600	658700	812400	961300	759700	1816400
1-DLB-B	256000	370500	993200	1095700	1036000	763700
1-EMB-A	170900	330000	860600	1218300	1150600	1253100
1-EMB-B	229600	485000	853600	1629600	1716900	1857600
1-EMB-C	197000	391100	792200	1260500	n/a	2626100
1-EMB-D	302200	487100	829000	1119300	1098700	1970000
1-EMB-E	277600	458700	576000	494600	1061600	1188800
1-EMB-F	168400	296200	420200	614000	587600	845100
1-EMB-G	176300	353500	598700	1148600	1129600	1539500
1-EMB-H	159000	484300	425000	775800	546500	n/a
1-EMB-I	147600	282500	510900	863600	697100	817400
1-EMF-A	264600	516200	635000	755000	666200	1476500
1-EMF-B	n/a	558200	798900	n/a	1410900	1595600
1-EMF-C	184100	225400	416300	488100	524000	473300
1-EMF-D	248600	287500	469500	1080200	985200	1388900
1-EMF-E	306100	382800	554000	583900	1340700	1052300
1-EMF-F	n/a	549400	595600	951300	1544000	1266800
1-EMF-G	310400	485900	553400	506700	1085800	1067800
1-EMF-H	293800	469300	470100	520800	986300	1021300
1-EMF-I	243100	276500	290700	488000	408000	523600
1-EMF-J	n/a	n/a	350400	365000	275800	1080500
1-EMF-K	1360000	838700	934600	923900	941200	936900
1-IMF-A	n/a	528700	545000	584800	420200	1402900
1-IMF-B1	n/a	700600	925200	983600	n/a	982300
1-IMF-B2	n/a	n/a	n/a	n/a	n/a	n/a
1-IMF-C1	176000	291800	226600	444700	483600	550300
1-IMF-C2	2000	163600	139700	212700	259400	396700
1-IMF-D1	203900	312600	436900	923800	967500	1017400
1-IMF-D2	115600	82000	246900	319200	399300	479600
1-IMF-E1	230800	267700	582000	677400	784600	985900
1-IMF-E2	148800	248900	287500	n/a	n/a	n/a
1-IMF-E2	n/a	n/a	n/a	n/a	n/a	n/a
1-IMF-E3	154500	200200	304300	401700	n/a	n/a
1-IMF-E4	146600	223700	n/a	n/a	n/a	n/a
1-IMF-F1	n/a	386100	521400	602300	976300	1242700
1-IMF-F2	n/a	378800	477800	210400	767600	940600
1-IMF-F3	191000	287300	261900	600200	525100	n/a
1-IMF-F4	n/a	n/a	n/a	n/a	n/a	n/a
1-IMF-F5	n/a	966800	1169000	1318300	1224900	1025700
1-IMF-G1	180800	195400	364100	397800	n/a	n/a
1-IMF-G2	159300	211800	405600	516500	173800	n/a
1-IMF-G3	120800	121100	260000	167700	n/a	n/a
1-IMF-G4	173000	172100	377800	462300	594000	n/a
1-IMF-G5	191500	212000	526800	780000	499700	n/a
1-IMF-H1	223400	259200	463400	429800	569200	537300
1-IMF-H2	n/a	436400	542100	613100	1410300	1232600
1-IMF-H3	179000	163500	285200	n/a	n/a	n/a
1-IMF-H4	157800	48400	318300	n/a	n/a	n/a
1-IMF-H5	223100	270900	557700	733000	613500	994600
1-IMF-H6	n/a	n/a	n/a	n/a	n/a	n/a
1-IMF-I1	301700	324600	627000	505900	587800	429700
1-IMF-I2	246600	271000	391400	432800	n/a	n/a
1-IMF-I3	176700	258000	511800	499700	546700	834800
1-IMF-I4	n/a	329400	351200	496300	565900	352900
1-IMF-I5	92900	223900	244600	n/a	n/a	n/a
1-IMF-I6	350200	429800	458600	1177800	1065500	1037700
1-IMF-J1	212800	204600	318300	344900	n/a	n/a
1-IMF-J2	165000	118800	400800	316900	n/a	n/a

Appendix: Physical property data collected from *Ziphius cavirostris* specimen

Sample #	Elastic Modulus at 5 kPa LR	Elastic Modulus at 10 kPa LR	Elastic Modulus at 20 kPa LR	Elastic Modulus at 30 kPa LR	Elastic Modulus at 40 kPa LR	Elastic Modulus at 50 kPa LR
1-IMF-J3	161300	144700	293300	249300	n/a	n/a
1-IMF-J4	228700	213600	410500	355400	196100	n/a
1-IMF-J5	n/a	269900	296000	508700	440200	n/a
1-IMF-K1	287700	552400	796000	974400	1319100	1815800
1-IMF-K2	n/a	169400	146900	n/a	n/a	n/a
1-IMF-K3	347300	266200	421700	775600	1074900	882600
1-IMF-K4	136400	161200	272900	n/a	n/a	n/a
1-IMF-K5	n/a	n/a	n/a	n/a	n/a	n/a
1-IMF-K6	n/a	n/a	n/a	n/a	n/a	n/a
1-IMF-K7	n/a	n/a	n/a	n/a	n/a	n/a
1-LNP-1	104500	156800	n/a	n/a	n/a	n/a
1-LNP-1	129400	92400	517600	649100	599800	1170800
1-RNP-2	52300	95000	n/a	n/a	n/a	n/a
1-Thyroid-1	n/a	n/a	n/a	n/a	n/a	n/a
1-Thyroid-2	n/a	n/a	n/a	n/a	n/a	n/a
1-Thyroid-3	n/a	n/a	n/a	n/a	n/a	n/a
1-Tongue-1A	n/a	345900	301600	444700	n/a	n/a
1-Tongue-2P	179300	153300	268700	419200	585300	684100
1-VCB-1	363400	635600	774100	1119200	1234500	1462400
1-Hyoid-1	n/a	n/a	n/a	n/a	n/a	n/a
1-Hyoid-2	n/a	n/a	n/a	n/a	n/a	n/a
1-Hyoid-3	n/a	n/a	n/a	n/a	n/a	n/a
1-Hyoid-4	n/a	n/a	n/a	n/a	n/a	n/a
1-Hyoid-5	n/a	n/a	n/a	n/a	n/a	n/a
1-Hyoid-6	n/a	n/a	n/a	n/a	n/a	n/a
1-F-A1	262010	383500	526270	982560	1059900	1174900
1-F-A2	155630	293180	558080	690790	490020	n/a
1-F-A3	79337	357190	558110	631330	765720	n/a
1-F-B1	108590	262010	628450	610550	675240	905710
1-F-B2	276370	379580	501470	1153400	1060900	1183500
1-F-B3	101230	189810	n/a	n/a	n/a	n/a
1-F-B4	111040	227120	503370	614410	621810	637070
1-F-B5	51244	376650	497710	554010	956550	854920
1-F-B6	120070	396760	540040	698910	720440	1114600
1-F-C1	217920	389840	559940	1053300	1148600	1312100
1-F-C2	236240	401160	292200	841330	742900	967890
1-F-C3	226580	449570	580990	539490	1201300	1447600
1-F-C4	241740	338070	267180	954230	1204400	1221400
1-F-C5	40622	182800	n/a	n/a	n/a	n/a
1-F-C6	172080	107270	333240	483470	n/a	n/a
1-F-C7	121640	281510	784570	988930	1354200	n/a
1-F-C8	235180	335100	828330	1136200	1095500	1168800
1-F-C9	134440	447090	757000	914500	1085800	1219300
1-F-D1	133410	248080	501400	618130	1299800	1446500
1-F-D2	153520	402980	503730	646970	712760	882730
1-F-D3	75668	255380	n/a	n/a	n/a	n/a
1-F-D4	240390	339900	808740	835200	1002500	1127900
1-F-D5	91434	153570	626030	799020	1004900	1264900
1-F-D6	126830	251100	353490	381440	n/a	n/a
1-F-D7	54048	135120	n/a	n/a	n/a	n/a
1-F-D8	77170	192430	n/a	n/a	n/a	n/a
1-F-D9	229830	455450	284200	1052600	1053000	1125900
1-F-D10	108150	310180	467240	1097700	908450	n/a
1-F-D11	187420	429970	1051000	1825700	1361600	2668000
1-F-E1	233050	394950	626040	868230	858080	749420
1-F-E2	101060	199120	268550	n/a	n/a	n/a
1-F-E3	116040	225810	332440	n/a	n/a	n/a
1-F-E4	200420	321190	747400	749720	843440	515900

Appendix: Physical property data collected from *Ziphius cavirostris* specimen

Sample #	Elastic Modulus at 5 kPa LR	Elastic Modulus at 10 kPa LR	Elastic Modulus at 20 kPa LR	Elastic Modulus at 30 kPa LR	Elastic Modulus at 40 kPa LR	Elastic Modulus at 50 kPa LR
1-F-E5	269820	463320	869650	849070	1012900	2774100
1-F-E6	297700	401770	426370	1395400	1111700	1301500
1-F-E7	137550	327100	619990	590460	462970	n/a
1-F-E8	88374	189370	257550	n/a	n/a	n/a
1-F-E9	161620	197670	486560	378440	682970	n/a
1-F-E10	166110	317400	809810	729720	1094600	1364500
1-F-E11	204110	241800	190510	798310	824620	865440
1-F-E12	199340	167870	439340	457140	681950	n/a
1-F-E13	108610	368510	678840	918050	1280100	1137900
1-F-F1	161520	258610	764340	1083400	1124600	1170300
1-F-F2	173580	261750	490440	547990	708500	588940
1-F-F3	49184	133460	n/a	n/a	n/a	n/a
1-F-F4	134920	330950	351950	368290	n/a	n/a
1-F-F5	158130	306530	638610	884930	814980	995700
1-F-F6	106760	455380	793670	998470	2033200	1715000
1-F-F7	236600	306710	832500	881180	1151700	1040600
1-F-F8	101440	171790	n/a	n/a	n/a	n/a
1-F-F9	171700	273400	422380	662260	603390	559250
1-F-F10	139960	294390	384900	438600	680290	n/a
1-F-F11	136610	305640	806800	804930	1366100	1725300
1-F-F12	103100	198970	766940	1128700	1340300	2228500
1-F-F13	229170	255880	1033800	840290	1174400	1592100
1-F-F14	157640	183910	434490	441390	n/a	n/a
1-F-F15	283830	215110	443880	358510	n/a	n/a
1-F-F16	171920	157290	312950	465590	418460	n/a
1-F-F17	75022	315200	452740	816080	n/a	n/a
1-F-G1	130150	430290	576380	660050	886260	644560
1-F-G2	195370	191880	499280	493310	614020	605650
1-F-G3	125820	185870	260680	n/a	n/a	n/a
1-F-G4	172790	196860	552710	668650	823390	1181100
1-F-G5	121740	493540	817080	1085800	1425800	2213900
1-F-G6	171220	264820	743600	833280	847230	1239300
1-F-G7	152060	178610	313780	282400	n/a	n/a
1-F-G8	100690	205570	208830	n/a	n/a	n/a
1-F-G9	87380	227670	398060	402110	n/a	n/a
1-F-G10	210350	312530	927810	1427000	1782400	1709100
1-F-G11	98010	330140	750550	928510	1207100	n/a
1-F-G12	156960	147260	533660	621560	244860	n/a
1-F-G13	164550	139380	580770	655440	508170	659580
1-F-G14	179220	202270	367410	425010	292730	n/a
1-F-G15	147690	154720	384470	511640	471200	n/a
1-F-G16	119920	77512	259500	347960	n/a	n/a
1-F-G17	123990	461100	701770	1054800	1327100	1898600
1-F-H1	265340	513430	711550	1466700	1818800	1611900
1-F-H2	142700	203250	381840	581130	564410	646630
1-F-H3	174860	253790	374010	391820	623350	427440
1-F-H4	146340	169320	365030	435290	514690	361370
1-F-H5	275670	356300	648590	1158800	820120	998150
1-F-H6	191600	284490	912700	1658200	1804500	2480300
1-F-H7	148470	270070	518200	539740	766380	898320
1-F-H8	207190	294960	296760	798550	746130	801630
1-F-H9	81141	117730	95460	n/a	n/a	n/a
1-F-H10	134730	205370	229410	n/a	n/a	n/a
1-F-H11	120500	347550	474460	801310	660730	n/a
1-F-H12	140560	456410	949670	1036300	1559200	1785900
1-F-H13	80545	288850	611040	593870	1077600	1510900
1-F-H14	111350	241690	407850	455750	n/a	n/a
1-F-H15	163930	140510	360650	523670	704290	1214300

Appendix: Physical property data collected from *Ziphius cavirostris* specimen

Sample #	Elastic Modulus at 5 kPa LR	Elastic Modulus at 10 kPa LR	Elastic Modulus at 20 kPa LR	Elastic Modulus at 30 kPa LR	Elastic Modulus at 40 kPa LR	Elastic Modulus at 50 kPa LR
1-F-H16	57310	89149	n/a	n/a	n/a	n/a
1-F-H17	120310	300770	403900	375960	n/a	n/a
1-F-H18	95756	220580	293130	n/a	n/a	n/a
1-F-H19	126690	161210	518470	749930	797310	1125900
1-F-H20	339120	467530	796670	832830	1633700	n/a
1-F-I1	309030	461260	915210	1060100	1095800	1856200
1-F-I2	139290	257130	583960	639800	746930	790690
1-F-I3	144580	184200	424090	407560	n/a	n/a
1-F-I4	102940	274820	376100	507500	402170	n/a
1-F-I5	103270	284170	593280	955630	785940	n/a
1-F-I6	87627	578340	1042800	1238500	1674600	2453600
1-F-I7	123090	307730	423130	n/a	n/a	n/a
1-F-I8	70298	112980	n/a	n/a	n/a	n/a
1-F-I9	123060	168770	295340	n/a	n/a	n/a
1-F-I10	158260	123090	304650	400680	n/a	n/a
1-F-I11	273490	506810	537710	339930	1042500	1027200
1-F-I12	275820	490130	661350	1110000	2295700	n/a
1-F-I13	83474	230650	632640	1031800	1434000	1571100
1-F-I14	139430	175320	389590	458930	429210	668580
1-F-I15	73666	106730	n/a	n/a	n/a	n/a
1-F-I16	81145	82412	n/a	n/a	n/a	n/a
1-F-I17	78185	215010	262480	n/a	n/a	n/a
1-F-I18	209610	213490	491020	507620	718730	742940
1-F-I19	48113	493150	1390800	n/a	2285300	3643500
1-F-I20	110700	295210	565820	928690	1071500	1588500
1-F-I21	110060	121130	n/a	n/a	n/a	n/a
1-F-I22	116370	166130	n/a	n/a	n/a	n/a
1-F-I23	183620	244970	1490900	1453700	n/a	n/a
1-F-J1	83627	454890	561030	1415200	n/a	n/a
1-F-J2	197360	253020	959370	984340	1111000	964850
1-F-J3	127820	227840	379420	385370	n/a	n/a
1-F-J4	119900	395440	731700	710180	645620	n/a
1-F-J5	52637	252330	501800	393460	n/a	n/a
1-F-J6	138250	336630	1278000	1122300	1349000	1048400
1-F-J7	118430	197320	419040	656520	857020	904400
1-F-J8	74020	132730	n/a	n/a	n/a	n/a
1-F-J9	170500	130780	195370	362320	n/a	n/a
1-F-J10	n/a	363740	467670	401460	n/a	1622400
1-F-J11	93484	244220	959440	2046800	1975700	n/a
1-F-J12	85378	260790	584360	1048900	1063000	1502600
1-F-J13	185090	197380	463360	965930	814820	1093200
1-F-J14	175280	157090	338980	444110	959090	n/a
1-F-J15	167890	109200	584990	696140	993040	n/a
1-F-J16	182950	216220	919910	1884200	2005400	2264900
1-F-K1	169580	231620	525750	606630	1042300	864450
1-F-K2	n/a	n/a	n/a	n/a	n/a	n/a
1-F-K3	24055	n/a	n/a	n/a	n/a	n/a
1-F-K4	149730	154560	n/a	n/a	n/a	n/a
1-F-K5	195500	205250	432430	407370	497090	557720
1-F-K6	351440	369740	557910	1093400	1246500	1411200
1-F-K7	231730	250270	286770	908400	830460	1020100
1-F-K8	232030	363040	589280	n/a	n/a	2110300
1-F-K9	279240	466530	653140	1242400	1006800	1211600
1-F-K10	223630	296030	279430	724510	830380	878050
1-F-K11	n/a	n/a	n/a	n/a	n/a	n/a
1-F-K12	148230	236070	503980	375510	n/a	n/a
1-F-K13	584940	408790	466120	1542300	1401400	1617700
1-F-K14	304030	443370	758120	709400	770630	n/a

Appendix: Physical property data collected from *Ziphius cavirostris* specimen

Sample #	Elastic Modulus at 5 kPa LR	Elastic Modulus at 10 kPa LR	Elastic Modulus at 20 kPa LR	Elastic Modulus at 30 kPa LR	Elastic Modulus at 40 kPa LR	Elastic Modulus at 50 kPa LR
1-F-K15	260410	490000	921450	1041600	1287000	1337100
1-F-K16	n/a	n/a	n/a	n/a	n/a	n/a
1-F-K17	245890	470080	491780	527380	n/a	2063500
1-F-K18	194060	215950	254210	254210	n/a	n/a
1-F-K19	393670	461150	562380	498110	421790	n/a
1-F-K20	112080	269240	343900	532140	n/a	n/a
1-F-K21	171680	259330	556020	662210	561880	567730
1-F-K22	n/a	544380	841270	912250	1269800	2870700
1-F-K23	209370	158350	258630	540530	n/a	n/a
1-F-K24	352970	426310	684160	1072700	2750400	2217500
1-F-K25	n/a	651730	964360	1189700	1309700	1309700
1-F-K26	484440	764480	1188300	2155600	1427300	1622400
1-F-K27	293420	315990	814230	788960	909590	838330
1-F-K28	764850	611880	1116700	n/a	n/a	2379500
1-F-K29	308710	320740	425230	935500	892980	1298000
1-F-K30	105120	134660	853330	1163300	n/a	n/a
1-F-K31	213330	269010	283080	563920	689240	656410
1-F-L1	781540	357770	617220	1279400	1156700	1094200
1-F-L2	171670	420530	499640	726130	n/a	n/a
1-F-L3	336270	286530	459860	679930	n/a	n/a
1-F-L4	240170	213780	422230	411730	n/a	n/a
1-F-L5	178950	238410	479740	670120	1047100	837640
1-F-L6	222550	518710	582460	973670	1060600	956280
1-F-L7	258640	302980	378020	796460	951440	1011500
1-F-L8	153280	94208	360490	392540	n/a	n/a
1-F-L9	n/a	358580	331660	1045900	1215500	1486000
1-F-L10	160850	283220	867920	945960	1269900	1056400
1-F-L11	n/a	1049800	1720900	1587900	n/a	1992700
1-F-L12	132410	141870	436780	437290	641050	744830
1-F-L13	280640	265160	486490	637530	n/a	n/a
1-F-L14	293650	266240	755100	880960	756150	1468300
1-F-L15	120030	125740	n/a	n/a	n/a	n/a
1-F-L16	205850	401320	465250	916450	809890	881940
1-F-L17	213930	233380	800160	732550	1141900	998340
1-F-L18	105100	289830	n/a	n/a	n/a	n/a
1-F-L19	176250	220030	420770	660700	n/a	n/a
1-F-L20	225600	291890	821050	1156700	1260700	1198300
1-F-M1	155780	386640	623940	1220800	1017300	838580
1-F-M2	83582	161940	n/a	n/a	n/a	n/a
1-F-M3	101730	250810	n/a	n/a	n/a	n/a
1-F-M4	55230	121570	n/a	n/a	n/a	n/a
1-F-M5	254140	392580	817010	1416600	1001500	1251900
1-F-M6	105500	178270	366870	n/a	n/a	n/a
1-F-M7	149310	158850	401080	535540	587730	n/a
1-F-M8	147140	143760	398670	n/a	n/a	n/a
1-F-M9	105590	220610	277810	n/a	n/a	n/a
1-F-M10	148340	232180	494470	601960	1047600	657850
1-F-M11	179370	292010	562940	608480	722990	n/a
1-F-M12	100810	296430	480530	n/a	n/a	n/a
1-F-M13	371840	649250	820500	1007400	864030	1458000
1-F-M14	55372	149170	n/a	n/a	n/a	n/a
1-F-M15	243720	348180	1001000	971080	933000	936810
1-F-O1	100890	212020	213850	n/a	n/a	n/a
1-F-O2	283930	415160	920460	988750	1256800	1373700
1-F-O3	287510	554780	857660	792690	1301100	1125700
2-DLB-A1						
2-DLB-B1						
2-DLB-C1						